



## **Terms and Conditions of Use of Digitised Theses from Trinity College Library Dublin**

### **Copyright statement**

All material supplied by Trinity College Library is protected by copyright (under the Copyright and Related Rights Act, 2000 as amended) and other relevant Intellectual Property Rights. By accessing and using a Digitised Thesis from Trinity College Library you acknowledge that all Intellectual Property Rights in any Works supplied are the sole and exclusive property of the copyright and/or other IPR holder. Specific copyright holders may not be explicitly identified. Use of materials from other sources within a thesis should not be construed as a claim over them.

A non-exclusive, non-transferable licence is hereby granted to those using or reproducing, in whole or in part, the material for valid purposes, providing the copyright owners are acknowledged using the normal conventions. Where specific permission to use material is required, this is identified and such permission must be sought from the copyright holder or agency cited.

### **Liability statement**

By using a Digitised Thesis, I accept that Trinity College Dublin bears no legal responsibility for the accuracy, legality or comprehensiveness of materials contained within the thesis, and that Trinity College Dublin accepts no liability for indirect, consequential, or incidental, damages or losses arising from use of the thesis for whatever reason. Information located in a thesis may be subject to specific use constraints, details of which may not be explicitly described. It is the responsibility of potential and actual users to be aware of such constraints and to abide by them. By making use of material from a digitised thesis, you accept these copyright and disclaimer provisions. Where it is brought to the attention of Trinity College Library that there may be a breach of copyright or other restraint, it is the policy to withdraw or take down access to a thesis while the issue is being resolved.

### **Access Agreement**

By using a Digitised Thesis from Trinity College Library you are bound by the following Terms & Conditions. Please read them carefully.

I have read and I understand the following statement: All material supplied via a Digitised Thesis from Trinity College Library is protected by copyright and other intellectual property rights, and duplication or sale of all or part of any of a thesis is not permitted, except that material may be duplicated by you for your research use or for educational purposes in electronic or print form providing the copyright owners are acknowledged using the normal conventions. You must obtain permission for any other use. Electronic or print copies may not be offered, whether for sale or otherwise to anyone. This copy has been supplied on the understanding that it is copyright material and that no quotation from the thesis may be published without proper acknowledgement.

**The Synthesis and  
The Synthesis and Photochemistry  
of Some 3-Phenylenones**

by

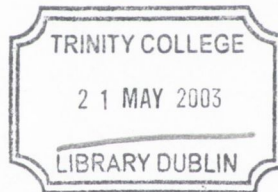
Michael Seery

A thesis submitted to the University of Dublin for the degree of Doctor of Philosophy

Trinity College  
Dublin

December 2002



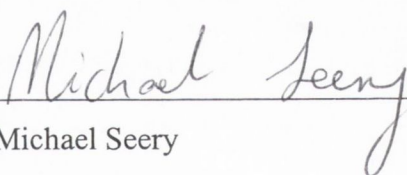


T4681S  
~~7354~~  
7414

## DECLARATION

This thesis has not been submitted as an exercise for a degree at any other university. Except where otherwise stated, the work described herein has been carried out by the author alone.

I give permission for the Library to lend or copy this thesis upon request.

  
Michael Seery

December 2002

## SUMMARY

The excited triplet state of 3-phenylcyclohexenone has been studied by laser flash photolysis and time-resolved infrared spectroscopy. Laser flash photolysis has been used to determine rate constants of decay of excited state and quenching by ground state. The excited state absorption spectrum was obtained, giving a broad maximum similar to that found for other enones. Time-resolved infrared spectroscopy has been used to obtain an infrared spectrum of the excited state, showing a reduction in frequency of the carbonyl bond strength. In addition, the shift of the carbonyl from ground to excited state indicates the excited state is  $\pi,\pi^*$  in character, a result previously determined by phosphorescence. In addition to studying 3-phenylcyclohexenone, the enone was examined in the presence of E-1-phenylpropene quencher. Laser flash photolysis was used to calculate rate constants for quenching by the alkene. Time resolved infrared spectroscopy was used to obtain a spectrum of the excited state and investigate the presence of any other intermediates in the enone-alkene cycloaddition reaction.

A new group of enones was also synthesised – all having the 3-phenylenone backbone. Various methods of synthesising these molecules were attempted, and the most useful routes are described. These molecules are designed so that they are synthetic precursors to the photo-therapeutic drug psoralen. They have an active site for [2+2] addition to simple alkenes or to thymine in DNA. Some crystal structures were obtained showing an essentially planar molecule with the phenyl substituent at an angle to the plane. This indicates that these molecules may be useful as photoactive intercalators, in a manner similar to psoralen.

The reaction of 6-methoxy-3-phenylindenone with E-1-phenylpropene was examined in both deuterio acetonitrile and benzene. The reactions were followed by NMR. It was found that dimerisation of the enone is overwhelmingly favourable, a fact attributed to efficient  $\pi$ -stacking of the enone molecules in solution. Some adduct formation with the

alkene was observed in benzene, but sufficient quantities could not be formed for further analysis. Computer modelling of the molecule shows that  $\pi$ -stacking can be a favourable process, as the barrier for rotation of the phenyl group is relatively small.



## **ACKNOWLEDGEMENTS**

I would like to thank Prof. John Kelly for taking me on and giving me an interesting and wide-ranging project to work on and to Prof. Brian McMurry for useful discussions. I would also like to thank Dr. Michael George, University of Nottingham for allowing me work with his equipment.

Financial support from Enterprise Ireland, Wicklow County Council, Trinity College Dublin, The British Council and Trinity Trust was gratefully received.

Many thanks to Dr. John O'Brien for running NMR samples and to Drs. Sylvia Draper and Tom McCabe for running X-ray crystal structures.

Thanks to Dr. Chris Colley and Jixin Yang, University of Nottingham, who made me very welcome and who spent many long hours in the lab with me.

To my family – many thanks for the support (emotional and financial) through the long four years and for not asking too often when I was finishing and getting a real job.

I have been very fortunate in my time at Trinity to have made many friends. On starting my Ph.D., I was welcomed to “Hotel California” by Ruth and Emmanuel, who made me feel very welcome even if they did continually slag me. Thanks to the other members of the Kelly Group – my predecessor Dan, Sarah (really quickly), Áine, Yvonne and Conor. Special mention goes to Carlos, for all his help and support and knowing everything about everything and teaching me some of it, and of course Karen for living through it all with me – we got there eventually, and Sharon who lived through half of it with me and then got sense.

In the Elan lab days, the first year was spent with the original Gunlaugsson gang, Mark and Claire'n'Caroline who were always available for a chat and a pint in the Pav. That

torch was carried on by Rowan, Eoin and Úna, who listened to me moaning with absolutely no grace. To all other postgrads, it was a please knowing you and working with you. Special mention to Dr. Dorothy Donnelly for her advice, tips, dry ether and explaining the workings of Mr Crozier.

To the technical staff, thanks for all your help and advice. Thanks to Fred and Eddie in the stores, who were always very helpful and friendly. When things needed fixing, two men could be called upon. Paul Byrne – whose Skills I envied greatly and Brendan “I’ll get right down to that for you” Mulvaney who was always about when I needed a hand. Thanks to John Kelly for his work on the vacuum lines. Special thanks go to Martin and Patsy for helping me with demonstrating, for always being on hand with advice and encouragement and in general for keeping it real. I hope all that gardening waste isn’t wasted! Thanks also to the secretarial staff Corinne, Helen and Tess.

The last year has been a bit of a crazy time for me and I really appreciate the friendship of Zeb – cheers mate! Thanks to Angela for your friendship and constant questions on affairs of state, Simplex clues, spellings and much more... you kept the brain ticking over! Thanks to Mark and Pádraic for having no interest whatsoever in this thesis and allowing me a means of escape, Benji for shortening my life by about five years and all the rest.... You know who you are.

Finally, after submitting this thesis, I was ‘rewarded’ with a very nice surprise. I look forward to spending many happy years with him.

An overwhelming longing to rest and remain at Bilbo's side in Rivendell filled all his heart. At last, with effort he spoke, and wondered to hear his own words, as if some other will was using his small voice.

"I will take the Ring," he said, "though I do not know the way."

Elrond raised his eyes and looked at him, and Frodo felt his heart pierced by the sudden keenness of the glance. "If I understand aright what I have heard," he said, "I think that the task is appointed to you, Frodo; and that if you do not find a way, no one will..."

..."But you won't send him off alone surely Master?" cried Sam, unable to contain himself any longer, and jumping up from the corner where he had been quietly sitting on the floor. "No indeed!" said Elrond, turning towards him with a smile. "You at least should go with him. It is hardly possible to separate you from him, even when he is summoned to a secret council and you are not."

Sam sat down, blushing and muttering. "A nice pickle we have landed ourselves in, Mr. Frodo!" he said, shaking his head.

The Council of Elrond  
The Lord of the Rings: The Fellowship of the Ring  
By J. R. R. Tolkien



## TABLE OF CONTENTS

List of Abbreviations

List of Figures and Tables

### Chapter 1 Introduction

1.1 The Photochemistry of 3-Phenyl Cyclic Enones	2
1.1.1 Photophysics	2
1.1.2 Dimerisation	3
1.1.3 Adduct Formation	3
1.2 Psoralen	4
1.2.1 Introduction	4
1.2.2 Interaction of Psoralen with DNA	5
1.3 Photochemical Activation	6
1.3.1 The Absorption of Light - The Born-Oppenheimer Approximation	7
1.3.2 Vibrational Wavefunctions - The Franck-Condon Principle	8
1.3.3 Spin Wavefunctions	9
1.3.4 Electronic Wavefunctions	9
1.3.5 Forbidden Transitions	9
1.3.6 UV-visible Absorption Spectra	10
1.3.7 Fate of the Excited State	10
1.4 Enone Photochemistry - A Review	15
1.4.1 Molecular Orbital Diagrams for Enones	15
1.4.2 Lowest Triplet State of Enones	16
1.4.3 Enones in Photochemical Synthesis	17
1.4.3.1 Photodimerisation	18
1.4.3.2 Photocycloaddition to alkenes	19
1.4.4 Photocycloaddition Mechanism	21
1.4.4.1 Corey Mechanism	21
1.4.4.2 Corey-de Mayo Mechanism	22



1.4.4.3 Alternative Mechanism	23
1.4.4.4 Bauslaugh's Biradical Proposal	24
1.4.4.5 Trapping of biradical Intermediates	25
1.4.4.6 Bauslaugh-Schuster-Weedon Mechanism	29
1.4.4.7 Mechanistic Conclusions	30
1.5 Current Study	31
1.6 References Cited	33
<b>Chapter 2 A Study of 3-Phenylcyclohexenone and its Interaction with 1-phenylpropene using Laser Flash Photolysis and Time-resolved Infrared Spectroscopy</b>	
2.1 Introduction	37
2.1.1 The Enone-Alkene Cycloaddition Reaction	37
2.1.2 Aims	38
2.1.3 Time-Resolved Infrared Spectroscopy	38
2.1.3.1 Infrared Spectroscopy	39
2.1.3.2 Time-Resolved Infrared Spectroscopy	42
2.1.3.3 Development of Technique	44
2.1.3.4 The TRIR Experiment	45
2.1.3.5 Excited-State Infrared Spectra	46
2.1.3.6 Interpreting the Excited-State IR Spectra of Organic Ketones	46
2.1.4 Current Study	48
2.2 Results	50
2.2.1 Design of Experiment	50
2.2.1.1 Solvent	50
2.2.1.2 Sample Concentration	50
2.2.1.3 Excitation Wavelength	51
2.2.2 The Photophysical Properties of 3-Phenylcyclohexenone	51
2.2.2.1 UV/vis Absorption Spectrum	51

2.2.2.2 Laser Flash Photolysis	52
2.2.3 Infrared Spectroscopy	56
2.2.3.1 Ground-State Infrared Absorption Spectrum	56
2.2.3.2 Excited-State Infrared Absorption Spectrum	58
2.2.3.3 Number of Scans	59
2.2.3.4 Varying Resolution	61
2.2.3.5 Decay Profile Kinetics	62
2.2.3.6 Dimerisation	62
2.2.4 The Photolysis of PCH and <i>trans</i> -1-phenylpropene	64
2.2.4.1 Laser Flash Photolysis	64
2.2.4.2 Time-Resolved Infrared Spectroscopy	65
2.2.4.3 Decay Profile Kinetics	69
2.3 Discussion	71
2.3.1 General Comments	71
2.3.2 The Step-Scan -TRIR Experiment	71
2.3.2.1 Experimental Design	71
2.3.3 TRIR Spectrum of the Excited State of PCH	72
2.3.3.1 Excited State Spectrum	72
2.3.3.2 Kinetics	73
2.3.4 TRIR Study of PCH and 1PP	74
2.3.4.1 TRIR Spectrum and Kinetics	74
2.3.4.2 Evidence for Intermediates	74
2.3.5 Conclusions	75
2.4 References Cited	76

## Chapter 3 The Synthesis of 3-Phenylindenones

3.1 Introduction	79
3.1.1 Synthesis of Indanones	80
3.1.1.1 Friedel-Crafts Acylation	80
3.1.1.2 Friedel-Crafts Alkylation	82
3.1.1.3 Acylation vs Alkylation	83
3.1.1.4 Newer Method	84
3.1.2 Indenones from Indanones	85
3.1.2.1 Bromination-Dehydrobromination	85
3.1.2.2 Oxidation	86
3.1.3 Indenones from Propanedione Derivatives	86
3.1.4 Routes Devised for Synthesis of 3-Phenylindenones	87
3.2 Results	89
3.2.1 6-Methoxy-3-Phenylindenone	89
3.2.1.1 Chalcone Synthesis	89
3.2.1.2 Friedel-Crafts Alkylation of Chalcone	89
3.2.2 Bromination of Indanones	91
3.2.2.1 Bromine	91
3.2.2.2 N-bromosuccinimide	
3.2.3 Dehydrobromination	93
3.2.3.1 Lithium Chloride/DMF	93
3.2.3.2 Sodium Ethoxide/ethanol	93
3.2.4 Oxidation of Indanones to Indenones	94
3.2.5 Modified Anstead Method	95
3.2.5.1 Attempts to Synthesise 6-Methoxy-3-Phenylindenone	95
3.2.5.2 Synthesis of 2-carbethoxy-6-Methoxy-3-Phenylindenone	96
3.2.6 Spectroscopic Analysis of Products	97
3.2.6.1 NMR	97
3.2.6.2 Infrared Spectroscopy	99
3.2.6.3 X-ray Crystallography	99



3.3 Discussion	103
3.3.1 6-Methoxy-3-Phenylindanone	103
3.3.2 Dehydrogenation of Indanones	104
3.3.2.1 Methoxy-derivative	104
3.3.2.2 Parent Compound	106
3.3.3 Anstead Method	106
3.4 Experimental	108
3.5 References Cited	111

## **Chapter 4 The Photo-interaction of 6-Methoxy-3-Phenylindenone with 1-Phenylpropene**

4.1 Introduction	115
4.2 Results	118
4.2.1 6-Methoxy-3-Phenylindenone	
4.2.1.1 UV/vis Absorption Spectrum	118
4.2.1.2 Flash Photolysis	118
4.2.1.3 NMR Spectrum	119
4.2.2 Irradiation of 6-Methoxy-3-Phenylindenone in the Absence and Presence of 1-Phenylindenone	120
4.2.2.1 6-Methoxy-3-Phenylindenone (acetonitrile)	120
4.2.2.2 6-Methoxy-3-Phenylindenone in the Presence of 1-Phenylpropene (acetonitrile)	122
4.2.2.3 Irradiation of 6-Methoxy-3-Phenylindenone (benzene)	126
4.2.2.4 6-Methoxy-3-Phenylindenone in the Presence of 1-Phenylpropene (benzene)	127
4.3 Discussion	129
4.3.1 Experimental Procedure	129
4.3.2 6-Methoxy-3-Phenylindenone	129
4.3.3 Irradiation of 6-Methoxy-3-Phenylindenone in the Presence of 1-Phenylpropene	132



4.3.4 <i>Cis-Trans</i> Isomerisation	132
4.4 Conclusions	134
4.5 References Cited	135

## **Chapter 5 Materials and Methods**

5.1 Materials	137
5.1.1 Reagents	137
5.1.2 Solvents	137
5.2 Methods	137
5.2.1 NMR Spectroscopy	137
5.2.2 UV/vis Spectroscopy	138
5.2.3 Infrared Absorption Spectroscopy	138
5.2.4 Electrospray Mass Spectrometry	138
5.2.5 Chromatography	138
5.2.6 Laser Flash Photolysis	138
5.2.7 Step-Scan Fourier Transform Time-Resolved Infrared Spectroscopy	140
5.3 References Cited	143
Future Work	144

Appendix I X-ray Crystal Structure Data for 2-bromo-6-methoxy-3-Phenylindanone

Appendix II X-ray Crystal Structure Data for 2-bromo-6-methoxy-3-Phenylindenone

## List Of Abbreviations

A	Absorbance, alkene.
c	Concentration.
DME	Dimethylethylene
DNA	Deoxyribonucleic acid.
$\Delta$ OD	Change in optical density.
E	Enone.
$\epsilon$	Extinction coefficient.
( <i>E</i> )-1-PP	( <i>E</i> )-1-Phenylpropene.
$\phi$	Quantum yield.
FTIR	Fourier transform infrared.
H-H	Head-to-head adducts
H-T	Head-to-tail adducts
HOMO	Highest occupied molecular orbital.
HSOMO	Highest singly occupied molecular orbital.
k	Rate constant.
l, P/L	Path length.
$\lambda$	Wavelength.
LUMO	Lowest unoccupied molecular orbital.
MO	Molecular orbital.
NMR	Nuclear magnetic resonance.
$\nu$ (CO)	Frequency of the carbonyl stretching vibration.
S <sup>2</sup>	Step-scan
$\tau$	Lifetime.
TRIR	Time resolved infrared.
UV/Vis	Ultra-violet/Visible.

## List of Figures, Tables and Schemes

Fig. 1.1: Dimers formed on irradiation of PCP and PCH

Fig. 1.2: Adducts formed on irradiation of PCP and PCH with either cis- or trans-1-phenylpropene

Fig. 1.3: Psoralen and some derivatives.

Fig. 1.4: Intercalation of a psoralen (e.g. 8-methoxypsoralen) (--) between two base pairs; and cycloaddition to form mono adducts(--) and diadducts(--).

Fig. 1.5: Thymine monoadducts formed by cycloaddition of a psoralen

Fig 1.6: Excitation of an electron from the ground vibrational, electronic state to an vibrationally excited upper excited state. The vertical arrow indicates that the nuclear geometry is unchanged

Fig. 1.7: Jablonski diagram for organic compounds

Fig. 1.8: Energy level diagram for triplet-triplet energy transfer between benzophenone and naphthalene (Energy differences in  $\text{kJ mol}^{-1}$ )

Fig. 1.9: MO description of quenching of a triplet organic by molecular oxygen. An electron exchange mechanism is assumed

Fig. 1.10: Energy level diagrams for alkenes (left), ketones (right), and enones (centre)

Fig. 1.11: Xanthone forms either  $n,\pi^*$  or  $\pi,\pi^*$  depending on solvent

Fig. 1.12: Thermal [2+2] addition is forbidden

Fig. 1.13: Photochemical [2+2] cycloaddition is allowed via a suprafacial pathway

Fig. 1.14: Dimerisation of cyclopentenone on irradiation forming two adducts – “head to head” 112 and “head to tail” 113

Fig. 1.15: Top: Photocycloaddition of dimethylethylene to cyclohexenone as a key step in the synthesis of carophyllene Bottom: Cyclobutane adducts of 3-phenylcyclopentenone to thymine (left) and of 3-methylcyclohexenone to buckminsterfullerene (right)

Fig. 1.16: Corey's original mechanism for [2+2] cycloadditions

Fig. 1.17: Corey – de Mayo mechanism which considers reversion of all intermediates



Fig. 1.18: Products obtained on photolysis of 4,4-dimethylcyclohexenone in the presence of tetramethylethylene

Fig. 1.19: Possible biradical intermediates on irradiation of cyclohexenone in the presence of 2-methylpropene

Fig. 1.20: Irradiation of cyclopentenone and cyclopentene: adducts formed and compounds formed as a result of trapping with  $H_2Se$ .

Fig. 1.21: Products and trapped intermediates after irradiation of cyclopentenone in presence of ethyl vinyl ether

Fig. 1.22: Bauslaugh-Schuster-Weedon Mechanism for [2+2] cycloaddition

Fig. 1.23: 3-phenylindenone backbone (left) and a furanoindenone which has analogies with psoralen (right)

Fig. 2.1: Photocycloaddition reaction between 3-phenylcyclohexenone and trans-1-phenylpropene giving rise to one adduct

Fig. 2.2: Light of various frequencies incident on a molecule. Frequencies absorbed by the molecule will not be transmitted through the molecule resulting in a reduction in transmittance at that frequency

Fig. 2.3: The Dispersive Infrared Spectrometer

Fig. 2.4: The Fourier - Transform Interferometer

Fig. 2.5: Schematic of data collection in a step-scan interferometer. (Top) The mirror moves a discrete distance, stops, the photochemical process is triggered and the temporal change in intensity is recorded over time. (Bottom) The interferogram at any time  $t$ . Fourier transformation gives the IR spectrum.

Fig. 2.6: Schematic of the TRIR apparatus at Nottingham

Fig. 2.7: Schematic of a transient infrared spectrum showing depletion of ground state peaks (bleaching) and formation of excited state peaks

Fig. 2.8: Schematic transient infrared spectrum with the difference between ground state carbonyl and excited state carbonyl,  $\Delta$  marked

Fig. 2.9: Observed shifts in C=O frequency of model systems as measured by TRIR



Fig. 2.10: IR absorbance spectrum of deuterioacetonitrile

Fig. 2.11: (Left) UV/vis absorption Spectrum of PCH (0.1mM) in cyclohexane (red) and ethanol (blue); (Right) of PCH (1mM)

Fig. 2.12: Transient Absorption Spectrum of PCH(10mM) immediately after laser flash

Fig. 2.13: Decay profile of transient observed at 370 nm after photolysis of PCH (10mM)

Fig. 2.14: Decay rate of transient PCH as a function of [PCH]

Fig. 2.15: Plot of Absorbance at 355nm as a function of [PCH]

Fig. 2.16: NMR of high (10mM), medium (2mM) and low (0.5mM) [PCH]

Fig. 2.17: Infrared absorption spectrum of PCH (10mM)

Fig. 2.18: Ground state (bottom) and excited state (top) infrared absorption spectra of PCH (10mM) Bleaching peaks in the excited state spectrum are marked with the corresponding peaks in the ground state spectrum

Fig. 2.19: Effect on spectral resolution of varying number of scans: Top 44 scans; centre 12 scans and bottom 32 scans

Fig. 2.20: Effect of resolution on spectral quality - top  $16\text{cm}^{-1}$  and bottom  $4\text{cm}^{-1}$  resolution

Fig. 2.21: Decay profiles, best fits and residuals for parent bleach( $\blacktriangle$ ) and excited state( $\bullet$ ) at different resolutions From top:  $16\text{cm}^{-1}$ ,  $8\text{cm}^{-1}$  and  $4\text{cm}^{-1}$ .

Fig. 2.22: Transient absorption spectrum of PCH (10mM) in the presence of 1PP (10mM) immediately after laser flash.

Fig. 2.23: Effect on decay rate of PCH (10mM) on increasing alkene concentration

Fig. 2.24: Ground state absorption spectrum of PCH (10mM) and 1PP (10mM) (bottom), transient infrared spectrum of PCH (10mM) (centre) and transient infrared spectrum of PCH (10mM) in the presence of 1PP (10mM). All spectra at  $8\text{cm}^{-1}$  resolution

Fig. 2.25: Transient infrared spectrum of PCH (10mM) in the presence of 1PP (10mM) 250ns (top) and  $3\mu\text{s}$  (bottom) after laser flash. Spectral resolution is  $16\text{cm}^{-1}$ .

Fig. 2.26: Transient infrared spectra of PCH (10mM) and 1PP (10mM, red) (30mM, blue) 250ns after laser flash.

Fig. 2.27: Decay profiles, best fits and residuals for parent bleach ( $1666\text{cm}^{-1}$ , top), excited state ( $1488\text{cm}^{-1}$ , centre) and peak at  $1548\text{cm}^{-1}$  (bottom).

Fig.3.1: General literature procedures for synthesis of 3-phenylindenone derivatives

Fig. 3.2: Intermediate in propionic acid ring-closure

Fig. 3.3: Retrosynthetic analysis showing possible routes to indenones (X=H, OMe)

Fig. 3.5: Keto-enol tautomers of propanedione derivatives

Fig. 3.6: X-Ray crystal structure of 2-bromo-6-methoxy-3-phenylindanone

Fig. 3.7: X-ray crystal structure of 2-bromo-6-methoxy-3-phenylindenone

Fig 3.8: C-H COSY showing the  $^1\text{H}$  peaks of the  $\alpha$ - and  $\beta$ - hydrogens are on different carbon atoms

Fig. 4.1: Irradiation of cyclobutene 400 in the presence of the substituted cyclopentenone 401 gives adduct 402 only

Fig. 4.2: Irradiation of enone 403 gives quantitative cycloaddition yielding adduct 404

Fig. 4.3: Irradiation of naphthyl-substituted cyclopentenone 405 gives adduct 406

Fig. 4.4: 6-methoxy-3-phenylindenone 407

Fig. 4.5: UV spectrum of 407

Fig. 4.6: Proposed Charge-Transfer mechanism for 407

Fig. 4.7:  $^1\text{H}$  NMR spectrum of 407

Fig. 4.8: Irradiation of 407 leading to dimer 408

Fig. 4.9 (a) NMR spectra recorded on irradiation of 407 in  $\text{CD}_3\text{CN}$ ; (b) Region of interest expanded (time = 0 - 60 mins)

Fig. 4.10: Relative amounts of methoxy singlet of 407 (at 3.87 ppm), methoxy singlet of 408 (at 3.78 ppm) and  $\alpha$ -H (at 3.70 ppm) after irradiation in  $\text{CD}_3\text{CN}$

Fig. 4.11: Relative amounts of methoxy singlet of 407 (at 3.87 ppm), methoxy singlet of 408 (at 3.78 ppm) and  $\alpha$ -H (at 3.70 ppm) after irradiation in the presence of 1-phenyl propene in  $\text{CD}_3\text{CN}$  (E:A = 1:5)



Fig. 4.12: Expected adduct to be formed on irradiation of 407 in the presence of 1-phenylpropene

Fig. 4.12: Relative amounts of methoxy singlet of 407 (at 3.87 ppm), methoxy singlet of 408 (at 3.78 ppm) and  $\alpha$ -H (at 3.70 ppm) after irradiation the presence of 1-phenylpropene in  $\text{CD}_3\text{CN}$  (E:A = 1:10)

Fig. 4.13: Formation of cis-isomer on irradiation of solution containing trans isomer – Top spectrum: no irradiation, bottom spectrum after 60 minutes irradiation

Fig. 4.13: Ratio of trans: cis isomers of 1-phenylpropene after irradiation time t

Fig. 4.14: Adduct that may be formed on irradiation of 407 in the presence of 1-phenylpropene

Fig. 4.15: NMR spectra of 407 after irradiation in the presence of 1-phenylpropene after 0, 30 and 90 minutes.

Fig. 4.16 – Models of  $\pi$ -stacking of indenones – a process that may enhance dimerisation

Fig. 4.17: Variation in energy of molecule on rotation of phenyl substituent

Fig. 5.1: Schematic of laser flash photolysis apparatus (PM = photomultiplier)

Table 2.1: Rate Constants for Quenching ( $k$ , in  $\text{dm}^3\text{mol}^{-1}\text{s}^{-1}$ ) of 3-Phenylcyclohexenone by itself and E-1-Phenylpropene in various solvents at room temperature<sup>5</sup>

Table 2.2: Quenching rate constants, limiting lifetimes and quantum yields of adduct formation with E-1-phenylpropene for PCP and PCH in acetonitrile

Table 2.3: Extinction coefficients at wavelengths of interest for PCH in acetonitrile

Table 2.4: Assignments of bands appearing in IR absorption spectrum (Fig. 2.17)

Table 2.5: First order decay constants for PCH (10mM)

of parent bleach ( $1666\text{cm}^{-1}$ ) and excited state peak ( $1488\text{cm}^{-1}$ )

Table 2.6: First order decay constants for PCH (10mM) in the presence of 1PP (10mM) of parent bleach ( $1666\text{cm}^{-1}$ ), excited state peak ( $1488\text{cm}^{-1}$ ) and peak at  $1548\text{cm}^{-1}$

Table 2.7: Comparison of expected and experimental results for decay rate of PCH (10mM)



Table 2.8: Comparison of expected and experimental results for decay rate of 10mM PCH + 10mM 1PP

Table 3.1: NMR Data for the  $\alpha$ - and  $\beta$ - hydrogens in the reaction scheme from chalcone to indenone

Table 3.2: Observed aromatic proton shifts 3'-methoxychalcone

Table 3.3: Observed aromatic proton shifts 3-phenylindanone

Table 3.4: Observed aromatic proton shifts 2-carbethoxy-6-methoxy-3-phenylindanone

Table 3.5: Change in carbonyl frequency through reaction sequence

Table 3.6: Important parameters derived from X-ray crystal structure data

Scheme 3.1: Synthesis of indanone from 3-phenylpropionic acid chloride

Scheme 3.2: Synthesis of 3-arylindanones

Scheme 3.3: Ring-closure of chalcone

Scheme 3.4: Alternative route to 3-arylindanones as described by Sommer et al<sup>15</sup>

Scheme 3.5: Two methods for creating  $\alpha,\beta$ -unsaturation

Scheme 3.6: Example of Anstead synthesis (a) and modified method to synthesis 3-substituted indenones(b)

Scheme 3.7: Modified Anstead method for synthesis of 3-phenylindenones

Scheme 3.7: Synthesis of 6-methoxy-3-phenylindanone

Scheme 3.8: Synthesis of indenone via bromo intermediate

Scheme 3.9: Synthesis of indenone by direct oxidation

Scheme 3.10: Proposed two-step synthesis following method of Anstead et al<sup>8</sup>

Scheme 3.11: Synthesis of ester derivative

Scheme 3.12: Mechanism for ring-closure of chalcone

*Chapter One*

*Introduction*

## INTRODUCTION

For chemical reactions to proceed, the reactant molecules involved must overcome an energy barrier to form products. The energy source can be provided by either heat or light. On heating a molecule, the internal energy is increased – *i.e.* the molecule's translational, rotational and vibrational energy increases. If the molecule collides with another, and their energy exceeds the energy barrier, products may be formed.

When a molecule is irradiated with UV/visible light, an electronically excited state may be formed. This is a *different chemical species* to the corresponding ground state – also called an *electronic isomer*, and therefore will react differently. In addition, excited states are highly energetic, as in this case an higher electronic excited state is occupied, whereas in the case of thermal activation, only higher vibrational, rotational and translational states are readily accessible. This is the beauty of photochemistry – it allows access to highly reactive electronic excited states not readily obtainable by thermal means.

This thesis is primarily concerned with the photochemistry of enones – and the interaction of enone excited states with alkenes. This interaction – which may lead to a [2+2] cycloaddition between the enone and alkene – is a very convenient method for forming cyclobutane adducts, and is widely used in organic synthesis.

### 1.1 THE PHOTOCHEMISTRY OF 3-PHENYL CYCLIC ENONES

#### 1.1.1 Photophysics

Workers in this laboratory have studied the properties of 3-phenylcyclic enones – mainly 3-phenylcyclopentenone (PCP, **100**), 3-phenylcyclohexenone (PCH, **101**) and their derivatives.<sup>1</sup> These compounds are of interest as the 3-phenyl substituent prolongs the triplet lifetime, which is attributed to the fact that the phenyl group may conjugate



with the enone excited species, in turn inhibiting twisting about the C=C bond (a means of energy dissipation). Triplet lifetimes are of the order of  $10^{-6}$  s.

### 1.1.2 Dimerisation

Both PCP<sup>2</sup> and PCH<sup>3</sup> dimerise on irradiation. In both cases, only the HH dimer is formed, which is attributed to the fact that the biradical intermediate precursor to the HH dimer is highly stabilised due to delocalisation of the biradical in the phenyl substituent. (Fig.1.1)

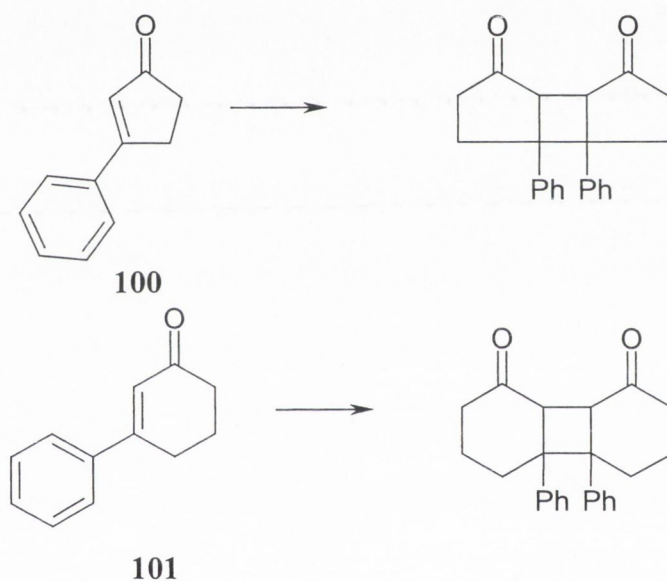


Fig. 1.1: Dimers formed on irradiation of PCP and PCH

### 1.1.3 Adduct Formation

Work on the addition of PCH and PCP to alkenes – namely (*Z*)- and (*E*)-1-phenylpropene (1-PP) showed that PCP formed two adducts – 7-*endo*- and 7-*exo*-methyl-5,6-*endo*-diphenylbicycloheptan-2-one (102 and 103). PCH gives only one isomer – 8-*exo*-methyl-6,7-*endo*-diphenylbicyclooctan-2-one (104). (Fig. 1.2)<sup>4</sup>

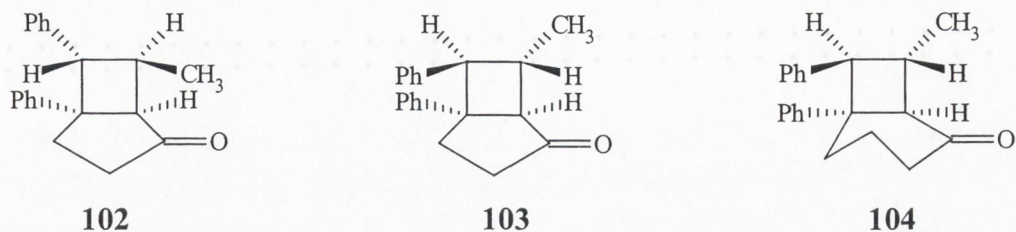


Fig. 1.2: Adducts formed on irradiation of PCP and PCH with either *cis-* or *trans-*1-phenylpropene

The regiochemistry of all isomers is the same and the methyl and phenyl groups of the original alkenes are *trans* to each other. The reactions were followed by  $^1\text{H}$  NMR time studies.<sup>1</sup> (More details in Chapter 2)

## 1.2 PSORALEN

### 1.2.1 Introduction

Psoralen **105** belongs to a family of heterocyclic compounds known as furocoumarins. These compounds are naturally occurring and some examples are shown in Fig 1.3.

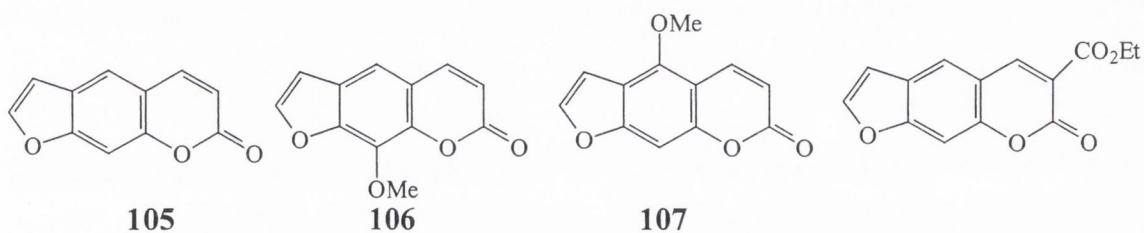


Fig. 1.3: Psoralen and some derivatives.

It was found in pre-Christian times that extracts from plants such as *Dorstenia* applied to the skin, followed by exposure to sunlight gave relief to skin ailments. Modern phytochemical experiments found that the active compound to be psoralen and its derivatives, and today psoralens are used in phototherapy to treat successfully diseases such as psoriasis, vitiligo and atopic eczema.<sup>5</sup> The method of treatment involves the

drug (usually 8-MOP **106**, sometimes 5-MOP **107**) being applied topically or orally. After a period of two hours, the affected area is irradiated with UVA light (320 – 400 nm) to initiate the interaction with DNA. The therapy is called PUVA therapy (psoralen +UVA).

### 1.2.2 Interaction of Psoralen with DNA

Different steps have been identified in the interaction of psoralens with DNA<sup>6</sup> (Fig. 1.4). The first is intercalation, a non-covalent interaction, which occurs in the dark. Psoralens have two photochemical reaction sites – the 3,4-pyrone double bond and the 4'5'-furan double bond. On irradiation, therefore, either one of these sites can undergo cycloaddition to a pyrimidine base (usually thymine).

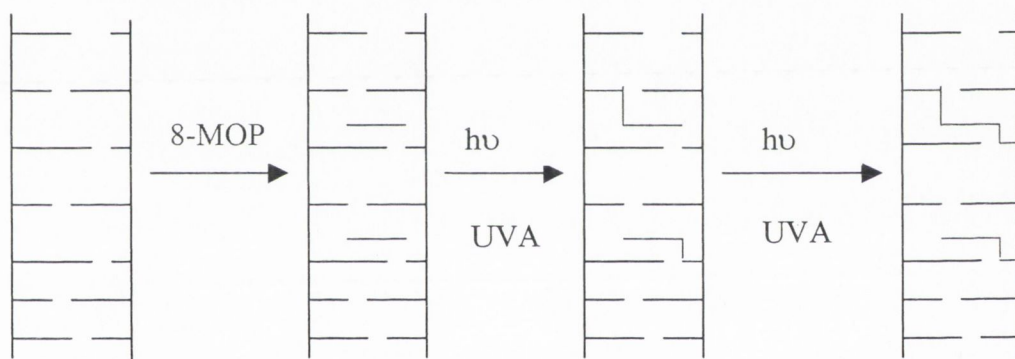


Fig. 1.4: Intercalation of a psoralen (e.g. 8-methoxypsoralen) (--) between two base pairs; and cycloaddition to form mono adducts(--) and diadducts(--).

Absorption of a second photon causes a second cycloaddition between the remaining double bond and another DNA base. This yields an interstrand crosslink provided the geometry is favourable. One difference between the two types of monoadducts (shown in Fig. 1.5) is that the 3,4 pyrone adduct **109** does not absorb UVA radiation, whereas the 4',5' furan adduct **108** does.<sup>7,8</sup>



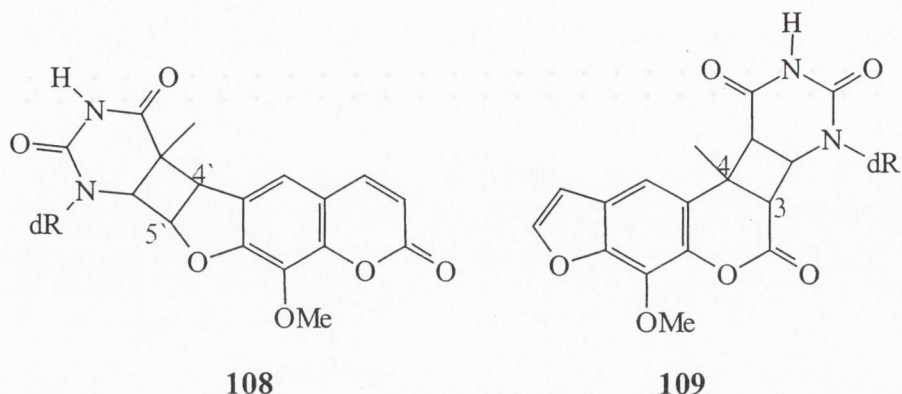


Fig. 1.5: Thymine monoadducts formed by cycloaddition of a psoralen

Crosslinks are only formed when the first photon absorbed forms a 4',5' monoadduct rather than a 3,4 monoadduct. It is this crosslink which is thought to prevent the formation of further psoriasis (for example) DNA. There are however long-term side effects related to this treatment, most notably, the carcinogenic nature of these mono- and diadducts. As a result, at the molecular level, current work with psoralens is aiming to design new psoralens and psoralen analogues with higher therapeutic activity but lower carcinogenic risks.<sup>9</sup>

### 1.3 PHOTOCHEMICAL ACTIVATION<sup>10</sup>

Light is described as packets of energy travelling in a wave. Each packet of energy is termed a photon; and each photon has a discrete energy. Light of frequency  $\nu$  has an energy  $E$  given by Eqn. 1.1, where  $h$  is Planck's constant.

$$E = h\nu \quad \text{Eqn. 1.1}$$

Energies required to excite an electron to an higher excited state usually involve wavelengths in the UV/visible region of the electromagnetic spectrum (200-800nm). These electrons are outer atomic electrons – shorter wavelengths (*i.e.* X-rays) promote inner electrons. Longer wavelengths (*i.e.* infrared and radio waves) excite higher

vibrational and rotational states of the same electronic state. Therefore, on UV/visible irradiation, the electron is promoted from its highest occupied molecular orbital (HOMO) to some upper excited state – depending on the energy of the incident light. This species is now highly energetic and highly reactive. But the question arises – why does a molecule absorb light? From the point of view of an organic photochemist, it is pointless in trying a photochemical reaction if the molecule does not absorb light at that radiation. Below, the factors governing the absorption of light by a molecule and the fate of the excited state are discussed.

### 1.3.1 The Absorption of Light – The Born-Oppenheimer Approximation

The promotion of an electron from a ground to an excited state is either *allowed* or *forbidden* in the language of quantum chemistry. A series of conditions must be met for a transition to be allowed. The probability of absorption,  $\rho$ , of incident light is proportional to the square of the *transition dipole moment* (Eqn. 1.2).

$$\rho \propto \left| \int \Psi_{gs} M \Psi_{es} d\tau \right|^2 \quad \text{Eqn. 1.2}$$

Eqn 1.2 governs how the ground and excited state wavefunctions ( $\Psi_{gs}$  and  $\Psi_{es}$  respectively) interact, and uses  $M$ , the dipole moment operator as a method for describing the interaction. These total wavefunctions include terms for vibrational, rotational electronic and other wavefunctions. To simplify matters, the Born-Oppenheimer Approximation is used. As the motions of electrons in orbitals are much more rapid than nuclear motions, electronic and nuclear motions can be treated separately in terms of an approximate wavefunction. Furthermore, spin wavefunctions may be treated separately as it is due to a magnetic interaction. which interact weakly with electronic interactions for most organic molecules,

It is found that the absorption of light is therefore dependent on the interactions of three variables: vibrational wavefunctions; spin wavefunctions and electronic wavefunctions. If any one of these terms give a value of zero the transition is forbidden.

### 1.3.2 Vibrational Wavefunctions - The Franck-Condon Principle

The interaction of ground and excited state vibrational wavefunctions describes how well the ground and excited state vibrational levels interact. The ground and excited states must have similar nuclear geometry, according to the Franck-Condon principle which states that electronic excitation occurs on a much faster timescale than nuclear motion, and the nuclear geometry of the excited state will therefore be very similar to that of the ground state (*Fig. 1.6*). These 'vertical transitions' indicate that the most intense absorption band is that lying directly above the ground state, where the overlap of vibrational wavefunctions is maximum. Other transitions will occur, but their probabilities, and hence their intensities are lower.

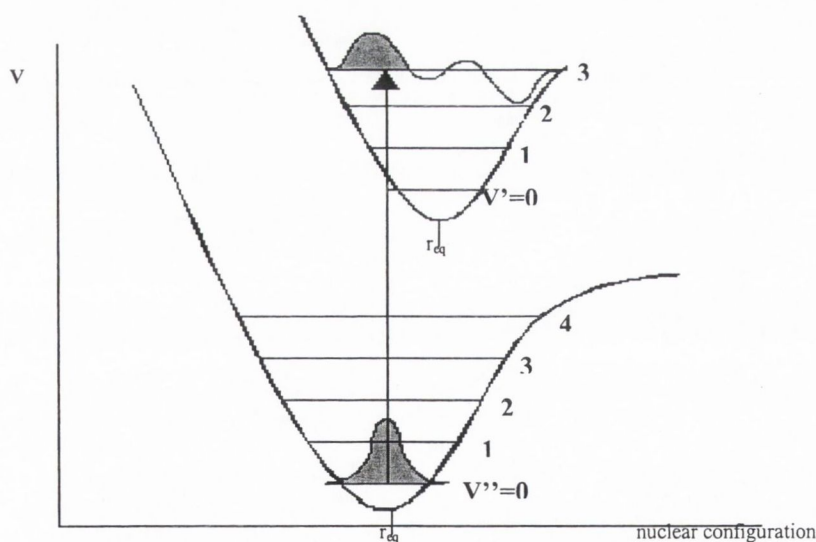


*Fig 1.6: Excitation of an electron from the ground vibrational, electronic state to an vibrationally excited upper excited state for a diatomic molecule. The vertical arrow indicates that the nuclear geometry is unchanged.*



### 1.3.3 Spin Wavefunctions

The spin of the excited state must be the same as that of the ground state for a transition to occur. Hence, singlet – singlet transitions are allowed, singlet – triplet transitions are forbidden.

### 1.3.4 Electronic Wavefunctions

The interaction of electronic wavefunctions depends on the symmetry (point group) of the ground state, excited state and the incident light. The symmetry of the product of the ground and excited state must be the same as that of the dipole moment operator (which represents the incident light) for that point group. Therefore, if the ground state electronic wavefunction has point group  $A_1$ , the excited state point group  $A_2$  (as is the case for the ground and first electronic states of formaldehyde), and the molecule has  $C_{2v}$  symmetry, then the product of  $A_1 \times A_2 \times$  symmetry of the incident light must yield  $A_1$  (*i.e.* be symmetric). In the case of  $C_{2v}$ , the symmetry of  $x$ ,  $y$  and  $z$  polarized light are  $B_1$ ,  $B_2$  and  $A_1$  respectively, and so in all cases the transition is forbidden. Transitions to higher states may be allowed – in the case of formaldehyde, the second electronic excited state has symmetry  $A_1$ , and the transition is allowed with  $z$ -polarised light.

### 1.3.5 Forbidden Transitions

There is a clear set of rules governing whether a transition is allowed, and how intense it will be. However, these rules are not always obeyed. Spin-forbidden transitions can occur, for example, if there is mixing of the theoretically ‘pure’ singlet and triplet excited states of an organic molecule (termed ‘spin-orbit coupling’). These transitions will be weak, but measurable. The presence of a heavy atom in a molecule may also cause a breakdown in the quantum mechanical rules, as it will distort the symmetry of the molecule (termed ‘the heavy-atom effect’).

### 1.3.6 UV-visible Absorption Spectra

UV-vis absorption spectra show the wavelength at which a molecule absorbs radiation in the electromagnetic spectrum. The absorption at any wavelength is given by *Eqn. 1.3* – the Beer-Lambert law, where  $c$  is the sample concentration,  $l$  is the cell path length and  $\epsilon$  is the molar extinction coefficient.

$$A = \epsilon cl \quad \text{Eqn. 1.3}$$

$\epsilon$  can be considered as a measure of how efficiently a molecule absorbs light at any particular wavelength. It is proportional to the area under the absorption band. Values in the range  $10^4 - 10^5$  indicate the transition is fully allowed; values in the range  $10^1 - 10^2$  symmetry forbidden and values less than 10 are spin and symmetry forbidden. Each absorption band in the spectrum corresponds to a different transition from a HOMO or lower molecular orbital to the lowest unoccupied molecular orbital (LUMO) or higher orbital. Each band will have its own probability of absorption, intensity and extinction coefficient and produces an excited state with its own electron distribution, reactivity and lifetime.

### 1.3.7 Fate of the Excited State

After excitation of an electron to a higher energy level, the molecule is highly unstable, very reactive and generally very short-lived. Several processes can occur for the molecule to dissipate this energy: chemical reaction or molecule fragmentation; a radiative transition (defined as transfer of an electron from one energy level to another resulting in the emission of a photon); a non-radiative transition (change of energy level without the emission of a photon) and the molecule can transfer its energy (“sensitise”) another molecule.

Absorption by an organic molecule of a photon at 300nm takes *ca.*  $10^{-15}$  s. The excited singlet state is generally very short-lived ( $\mu\text{s} - \text{ns}$ ), and hence rate constants of emission

and reaction must be very fast to compete with non-radiative transitions. The first process that occurs is internal conversion from the upper excited singlet states to the first excited singlet state,  $S_1$  (Fig. 1.7). This occurs on a timescale of  $10^{-11} - 10^{-14}$  sec. An exception to this rule is that of thiones – where the  $S_2 - S_1$  energy gap is large enough to minimise their interaction and hence dissuade internal conversion. Vibrational relaxation occurs (on a timescale of  $10^{-13}$  sec), and the electron now occupies the lowest vibrational energy level in the first excited state. It is from this position that all reactions /photo-processes occur. (Kasha's rule)<sup>11</sup>

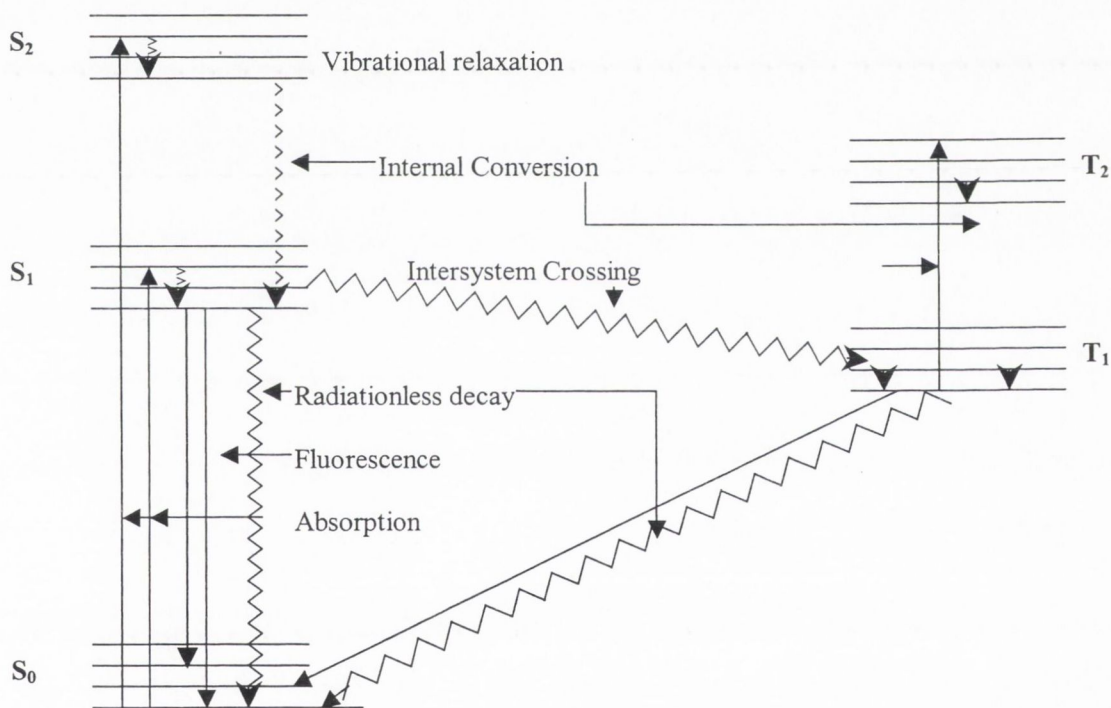


Fig. 1.7: Jablonski diagram for organic compounds

The lifetime of this  $S_1$  state is now determined by the rate constants of fluorescence, internal conversion – both leading to  $S_0$  ground state, the rate constant of reaction, if a reaction occurs from the singlet state and finally the rate constant of intersystem-



crossing to the triplet state. The radiative lifetime of the singlet state  $\tau_0$  can be approximated by the expression<sup>10</sup>

$$\tau_0 = \frac{5 \times 10^{-4}}{\epsilon_{\max}}$$

where  $\epsilon_{\max}$  is the molar extinction coefficient at the wavelength of maximum absorption. The greater this value, the shorter the lifetime. The logic to this is that if a transition is highly allowed in one direction, the reverse process is allowed and hence its rate-constant will be high, indicating its lifetime is short. Fluorescence from a  $^1(\pi, \pi^*)$  excited state is allowed (orbitals have the same symmetry), whereas that from a  $^1(n, \pi^*)$  is symmetry forbidden, as the orbitals are orthogonal and overlap is minimised. Nevertheless, fluorescence rate constants are of the order of  $10^7 - 10^{10} \text{ s}^{-1}$ , depending on whether process is allowed or not. Rate constants for intersystem crossing and reaction require similarly high rate constants in order to be competitive with this process.

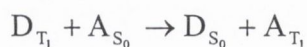
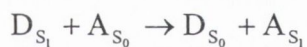
Rate constants for intersystem crossing for organic compounds are of the order  $10^7 - 10^8 \text{ sec}^{-1}$  for aromatic hydrocarbons and alkyl ketones and  $10^8 - 10^{11} \text{ s}^{-1}$  for aromatic ketones. This process is spin-forbidden, but can compete favourably with other processes, as S-T state mixing may be effective. This process is governed by the El-Sayed rules, which state that there must be a change of symmetry.<sup>12</sup> The reason is that the process is spin forbidden, and hence there must be spin-orbit interactions for the process to occur. The possibilities for organic carbonyl compounds are shown below. Both (a) and (d) are permitted by El-Sayed rules



After intersystem crossing, the electron is in an upper excited triplet state, and after internal conversion and vibrational relaxation, the excited state now is now localised in the lowest triplet state,  $T_1$ . It can now phosphoresce (return to ground state with

emission of a photon), undergo a radiationless transition to the ground state or react. In this case, reaction rate constants are much more competitive, as these other processes require a change of spin, and hence are much slower. Rate constants for phosphorescence are of the order  $10^{-1} - 10^4 \text{ sec}^{-1}$ . The rate depends on whether the lowest lying triplet state is  $n,\pi^*$  or  $\pi,\pi^*$ . The singlet-triplet energy gap for  $^3(n,\pi^*)$  is smaller than that for  $^3(\pi,\pi^*)$ . Thus, rate constants for phosphorescence from an  $n,\pi^*$  triplet are faster than that from a  $\pi,\pi^*$  triplet. Rate constants for radiationless transitions to the ground state are of a similar order. Hence, for organic compounds, most reactions occur from the triplet state and therefore depend on the quantum yield of intersystem crossing.

The excited state can dissipate its excess energy by sensitisation or energy transfer. In this case, a second molecule – an ‘acceptor’ A, with an available energy level lower than that of the excited state can accept the excited state energy from the ‘donor’ D and itself become excited. This acceptor can itself release energy by all the means described above. Energy transfer can occur in one of the following modes:



In the first case, energy transfer from the donor singlet creates an excited acceptor singlet state. In the second case, the excited acceptor triplet state is directly formed. This occurs when the  $S_1$  state of the donor is lower than  $S_1$  state of the acceptor, but higher than the  $T_1$  state of the acceptor (*Fig. 1.8*). An example of this is the sensitisation of naphthalene by benzophenone.

The corollary of sensitisation is quenching, whereby a molecule's excited state energy is quenched by another molecule before it has time to react. One of the most efficient quenchers is  $^3\text{O}_2$ , which forms  $^1\text{O}_2$  on quenching of an excited triplet state (*Fig. 1.9*).

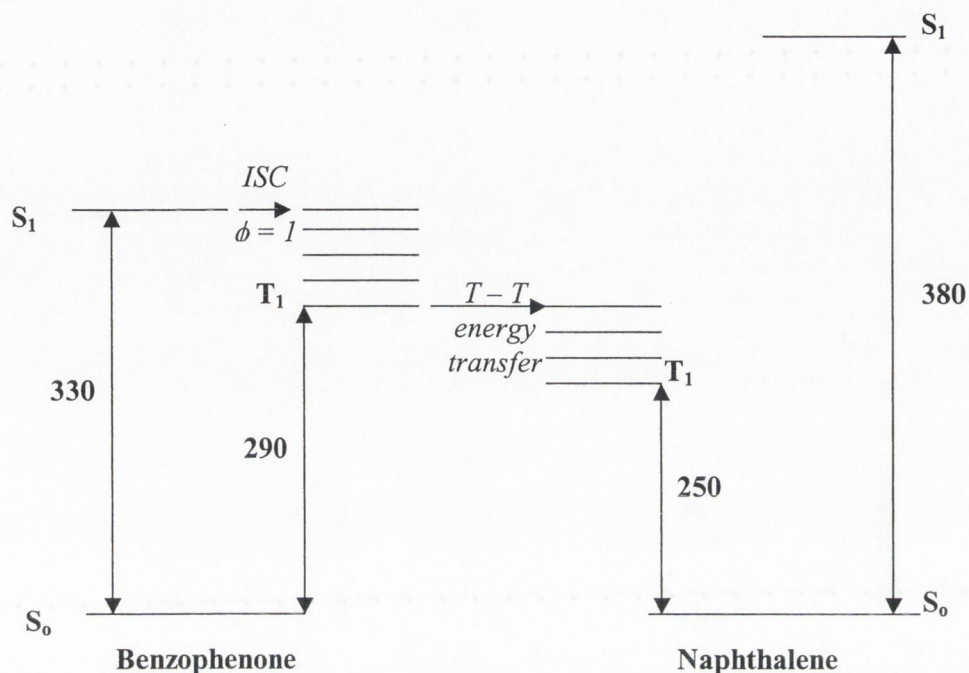


Fig. 1.8: Energy level diagram for triplet-triplet energy transfer between benzophenone and naphthalene (Energy differences in  $\text{kJ mol}^{-1}$ )

Oxygen is an efficient quencher of organic molecules, with a rate constant of the order of  $10^{10} \text{ dm}^3 \text{ mol}^{-1} \text{ sec}^{-1}$  (depending on solvent), and hence must be excluded from organic photoreactions.

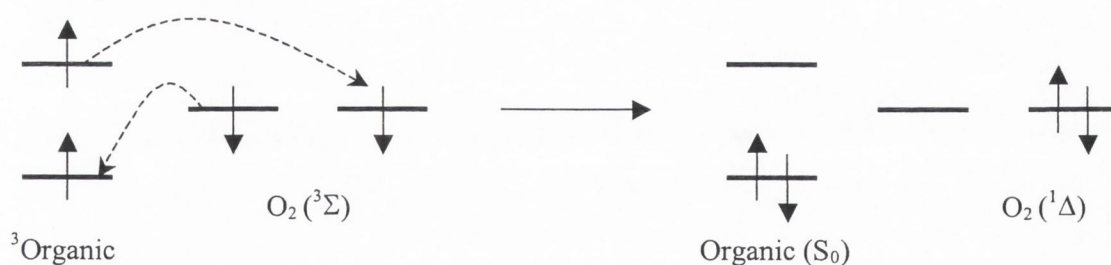


Fig. 1.9: MO description of quenching of a triplet organic by molecular oxygen. An electron exchange mechanism is assumed

A further method of dissipating excess energy is that of photoelectron transfer (PET). Certain molecules after photoexcitation become powerful electron donors or acceptors. In these cases an electron migrates between a photoexcited and ground-state species.



## 1.4 ENONE PHOTOCHEMISTRY – A REVIEW<sup>13</sup>

This thesis is primarily concerned with the photochemistry of enones – compounds that contain an  $\alpha,\beta$ -unsaturated carbonyl moiety. These compounds have an alkene and a carbonyl system that are in conjugation, and hence have different photophysical properties to those of simple ketones.

### 1.4.1 Molecular Orbital Diagrams for Enones

In the case of simple ketones, the lowest energy transition is that from the n-orbital of the oxygen to an anti-bonding  $\pi$  orbital of the C-O double bond to create an  $n,\pi^*$  state. (*Fig. 1.10*) This transition is forbidden as these orbitals are orthogonal, although distortions in symmetry mean that they are observed, with extinction coefficients in the range 10-100, and is generally observed in the range 290 – 330nm.<sup>10</sup> The next highest transition is from a bonding carbonyl  $\pi$  orbital to an anti-bonding carbonyl  $\pi$  orbital, to create a  $\pi,\pi^*$  state. This is a symmetry allowed transition, and the extinction coefficient is of the order of  $10^4$ , occurring in the range 180 – 220nm. Close to this is the excitation of the n electron to a  $\sigma$ -orbital. In the case of alkenes, the lowest energy transition is from a bonding  $\pi$  orbital to an anti-bonding  $\pi$ -orbital to give a  $\pi,\pi^*$  state, in the range 170 – 210 nm.

The MO diagram for an enone is shown below (*Fig. 1.10*).<sup>14</sup> The result is that both the  $\pi,\pi^*$  and  $n,\pi^*$  energies are lowered, as would be expected with conjugation, and hence their position in the UV spectrum is shifted to longer wavelengths. For enones,  $\pi,\pi^*$  bands appear in the region 220 – 250nm and  $n,\pi^*$  in the region 300 – 350nm. It is found that  $\pi,\pi^*$  bands shift to the red on increasing solvent polarity, whereas  $n,\pi^*$  bands shift to the blue. This can be rationalised by the fact that a  $\pi,\pi^*$  state can interact more favourably with polar solvents, as the molecule has become more polarised. In the case on  $n,\pi^*$  states, electron density has been removed from the oxygen and placed in the anti-bonding carbonyl bond, reducing the polarity.

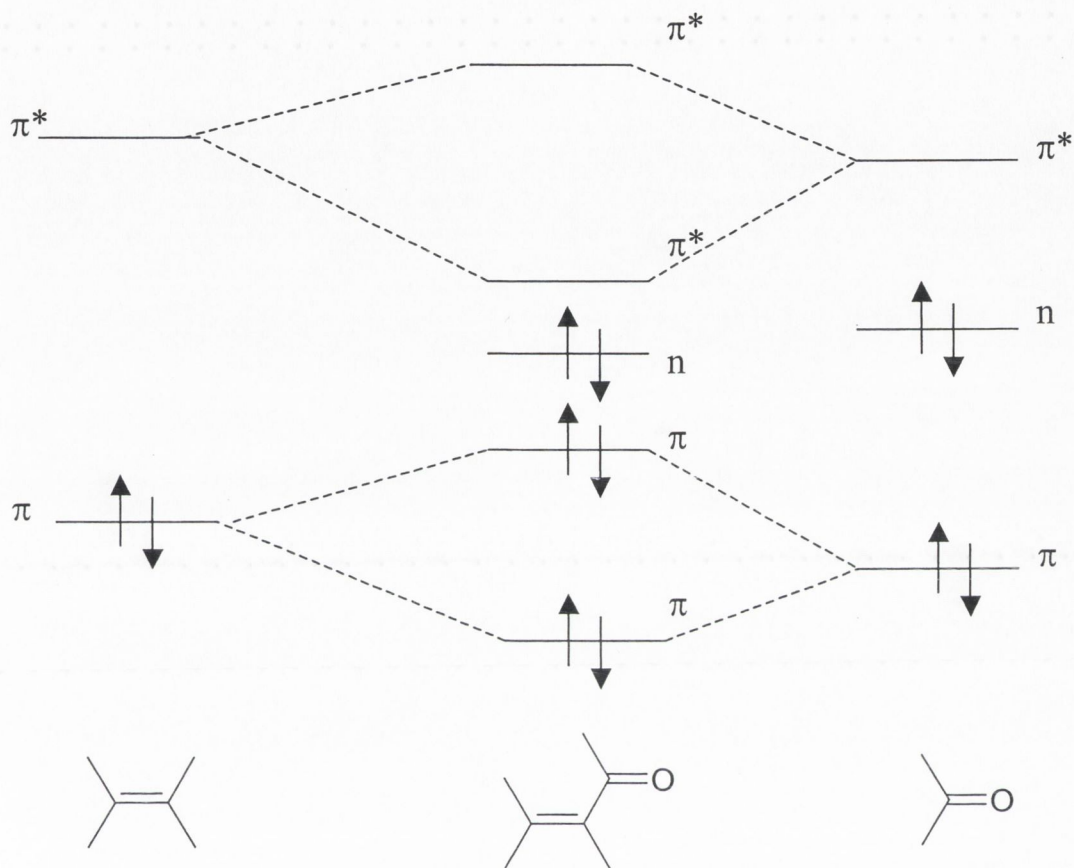


Fig. 1.10: Energy level diagrams for alkenes (left), ketones (right), and enones (centre)<sup>14</sup>

### 1.4.2 Lowest Triplet State of Enones

In the case of enones, the lowest excited singlet state may be either  $n,\pi^*$  or  $\pi,\pi^*$ , as these energy levels lie much closer in energy than in the case of simple ketones. This has implications on what the lowest energy level of the triplet state of enones is – and the energies of  $^3n,\pi^*$  and  $^3\pi,\pi^*$  states are sometimes so close that choice of solvent may

decide which is the lowest state. A classic example of this is xanthone, where state inversion is observed on changing solvent polarity. (Fig. 1.11)

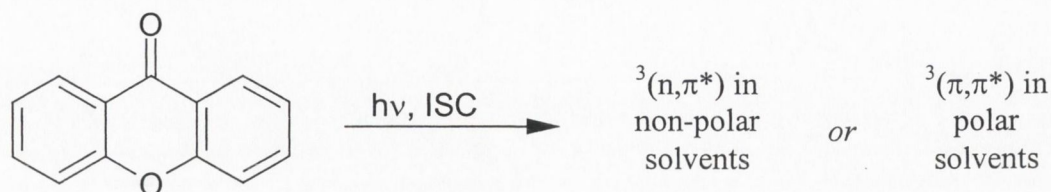


Fig. 1.11: Xanthone forms either  $n, \pi^*$  or  $\pi, \pi^*$  depending on solvent<sup>10</sup>

The nature of the triplet-excited state is of great importance to the synthetic photochemist. Most reactions of enones occur from this state, as intersystem crossing is usually efficient, and as described above, reaction rate constants can compete favourably with deactivation by other means. In general,  ${}^3n, \pi^*$  states are more suited to reactions involving H-abstraction, as this state has a radical like oxygen centre. In  $\pi, \pi^*$  excited states, the excited state is localised on a  $\pi$ -system in the molecule – and if it lies on the double bond of the alkene, reactions involving this alkene bond (e.g. [2+2] cycloaddition to another double bond) are favourable.

### 1.4.3 Enones in Photochemical Synthesis

Both acyclic and cyclic enones are widely used in chemical synthesis. Two types of reactions will be discussed here: photodimerisation of cyclic enones and photocycloaddition to alkenes. In both cases, a highly strained cyclobutanes adduct is formed.

$[\pi_2 + \pi_2]$  reactions of this type do not occur thermally. This can be explained by orbital symmetry arguments - orbital geometry of the HOMO of one molecule and the LUMO of another shows that the antarafacial transition state is very difficult to achieve (Fig. 1.12).



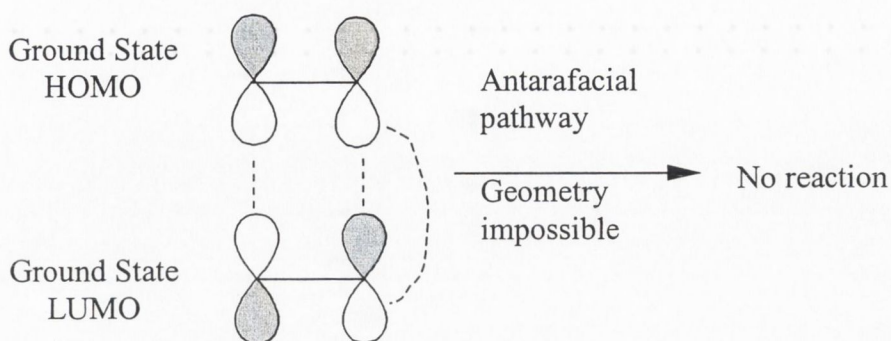


Fig. 1.12: Thermal [2+2] addition is forbidden

However the reaction does occur photochemically. This can be explained by the fact that irradiation of one molecule excites one electron from the HOMO to the LUMO, creating a highest singly-occupied molecular orbital (HSOMO). Orbital overlap between this orbital and the ground state LUMO of the second molecule is now favourable, and the reaction proceeds successfully via a suprafacial pathway (Fig. 1.13).

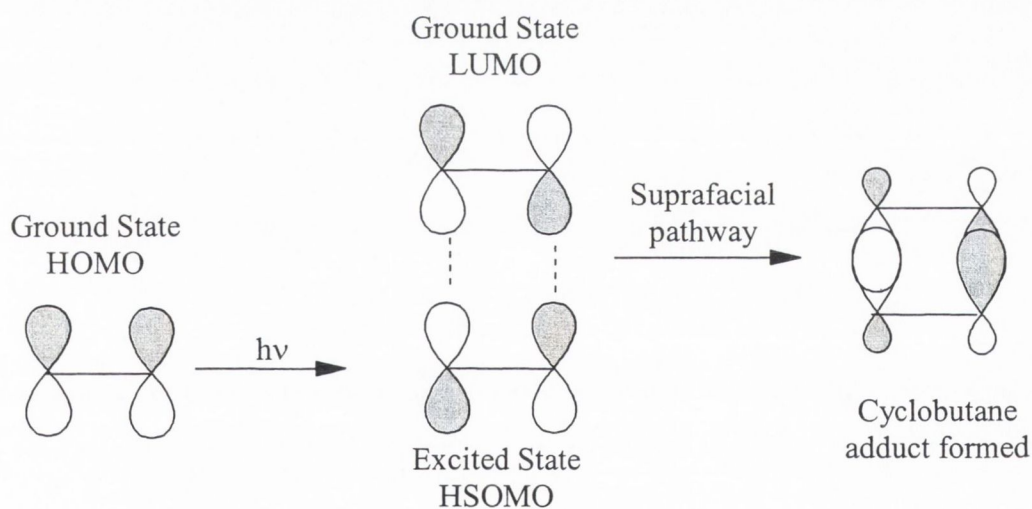


Fig. 1.13: Photochemical [2+2] cycloaddition is allowed via a suprafacial pathway

**1.4.3.1 Photodimerisation** The photodimerisation reaction of cyclic enones was first discovered by Eaton, who observed the photocycloaddition of cyclopentenone **110** to itself after UV irradiation.<sup>15</sup> Two adducts are formed – head to head (H-H) and head to

tail (H-T) (Fig. 1.14). The reaction proceeds via a  $^3(\pi,\pi^*)$  excited state and is relatively inefficient – the quantum efficiency in acetonitrile is 0.34. Quenching studies have shown that the triplet is formed with 100% efficiency, and hence the inefficiency is due to decay of subsequent intermediates to the ground state.

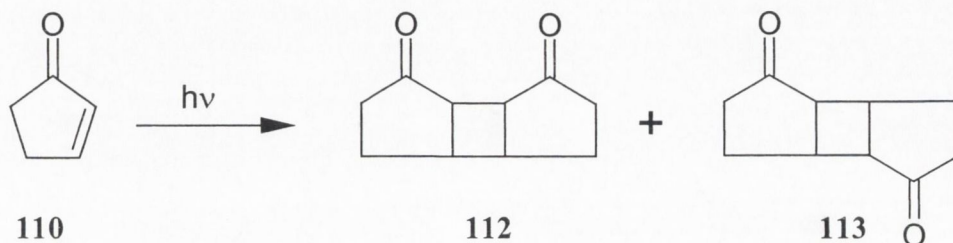


Fig. 1.14: Dimerisation of cyclopentenone on irradiation forming two adducts – “head to head” 112 and “head to tail” 113

It is found that the ratio of H-H : H-T dimers is strongly solvent dependent. Polar solvents favour the formation of H-H dimers.<sup>16</sup> A similar result is found for the dimerisation of cyclohexenone. The quantum efficiency is low, and polar solvents favour H-H dimers. The explanations for these observations are discussed later.

**1.4.3.2 Photocycloaddition to alkenes** Eaton, shortly after discovering the photodimerisation reaction observed that cyclopentenone undergoes [2+2] addition to cyclopentene to yield a cyclobutane adduct.<sup>17</sup> This [2+2] addition reaction to alkenes became one of the most important reactions in terms of use in synthesis. This was first exploited by Corey who used the reaction in a key step of his synthesis of carophyllene 114.<sup>18</sup>

Since then, cyclic enones – mainly cyclopentenone and cyclohexenone have been used in a wide variety of synthetic applications to a wide variety of alkenes.<sup>19</sup> Some examples are shown below. Recent, more exotic, examples include the addition of 3-phenylcyclopentenone to thymine<sup>20</sup> indicating the use of enones as DNA probes and

even the cycloaddition of 3-substituted cyclohexenones to buckminsterfullerene, as completed by Schuster (Fig. 1.15).<sup>21</sup>

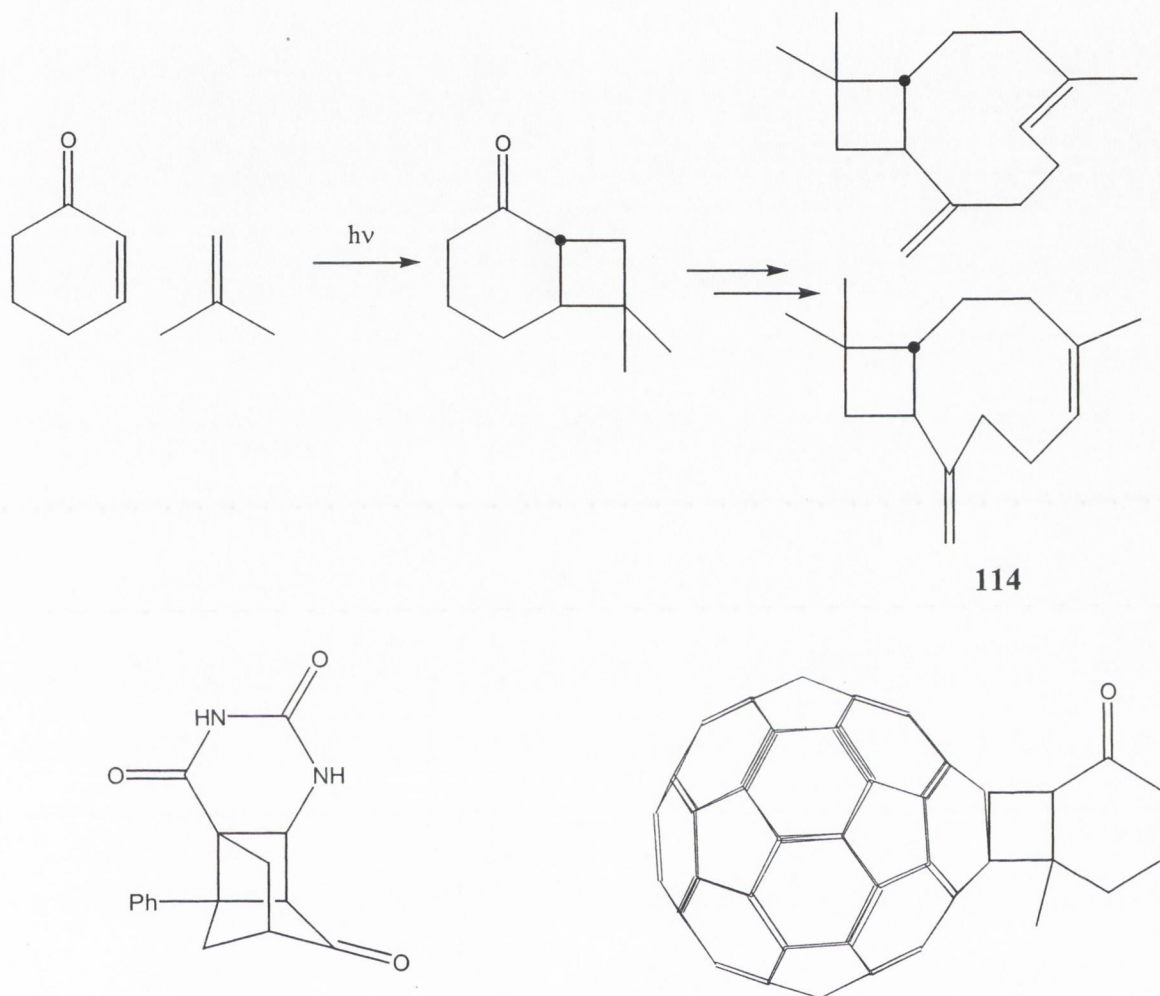


Fig. 1.15: Top: Photocycloaddition of dimethylethylene to cyclohexenone as a key step in the synthesis of carophyllene<sup>18</sup> Bottom: Intramolecular cyclobutane adducts of 3-phenylcyclopentenone to thymine<sup>20</sup> (left) and of 3-methylcyclohexenone to buckminsterfullerene<sup>21</sup> (right)



In general, the major adduct in these systems has a *trans* fusion of the four- and six-membered ring. Corey, in his pioneering work, recognised this fact and immediately realised its potential in the synthesis of complex ring systems. A mixture of identical cycloadducts was obtained on addition of cyclohexenone to either *cis*- or *trans*-2-butene, indicating that the stereochemistry of the alkene is lost in the course of the reaction.

#### 1.4.4 Photocycloaddition Mechanism

Observations about low quantum efficiency, stereo- and regio-chemistry of products, and work done on comparing rates of reaction with various alkenes led to the development of some theories on the mechanism of [2+2] addition. The first proposal was suggested in 1964, and still today, almost 40 years later the mechanism of this reaction is not fully understood.

**1.4.4.1 Corey Mechanism<sup>18</sup>** Corey, in 1964, suggested that enone-alkene cycloaddition proceeded via an excited state complex (exciplex) which subsequently collapsed to a biradical to give products. His basis for this mechanism was the observation that cyclohexenones react with alkenes, giving predictable products. An alkene with an electron withdrawing substituent Z gives H-H adducts, whereas one with an electron-donating group X gives H-T adducts. Corey assumed that the excited enone state was triplet  $n,\pi^*$  (it was not until 1968 that it was established as  $\pi,\pi^*$ )<sup>22</sup> and therefore the charge polarisation of the enone aligned with the alkene depending on the alkene's substituent. Corey argued that all reactions would lead to H-H adducts in the absence of an exciplex, and that the concept of biradicals were necessary to account for disproportionation products. Corey's mechanism is shown below.

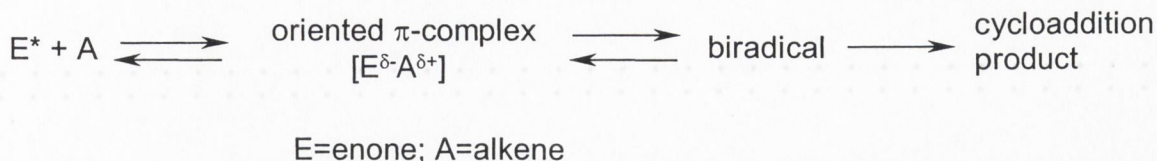


Fig. 1.16: Corey's original mechanism for [2+2] cycloadditions

Given the information that was available to Corey at the time, this model was a fair one, but with hindsight it is subject to criticism. The enone excited state is triplet  $\pi, \pi^*$ . Corey did endeavour to look for phosphorescence from cyclohexenones to identify the lowest triplet state but was unsuccessful. It was not until 1968 that phosphorescence from steroidal enones showed the lowest triplet state to be  $\pi, \pi^*$ .<sup>22</sup> Therefore the charge distribution is not that proposed in Corey's complex. In addition, any or all of Corey's intermediates can revert to ground state in competition with the forward reaction. These reversion reactions are of significance. McCullough showed that irradiation of 3-phenylcyclohexenone and *cis*-2-butene gave a much higher yield of *trans*-2-butene than of addition products,<sup>23</sup> indicating that reversion is a more favourable process to the biradical than cyclisation.

**1.4.4.2 Corey-de Mayo Mechanism** Corey's model has been successful in correlating regiochemical results for a large number of examples. In 1971 however, de Mayo reviewed the mechanism and pointed out the kinetic deficiencies of Corey's model.<sup>24</sup> He studied a number of alkenes and their reaction to cyclopentenone and found that none had a quantum yield greater than 0.5. He devised a model which explicitly considered reversion of *all* possible intermediates to ground state enone and alkene. (Fig. 1.17) The fundamental features are: (i) the triplet exciplex is formed irreversibly and is short lived; (ii) this exciplex collapses to biradical which goes on to form products or reverts directly to starting materials; (iii) this biradical reversion is the main source of inefficiency in the reaction and (iv) it is unclear whether the first bond is formed to the  $\alpha$ - or  $\beta$  carbon.

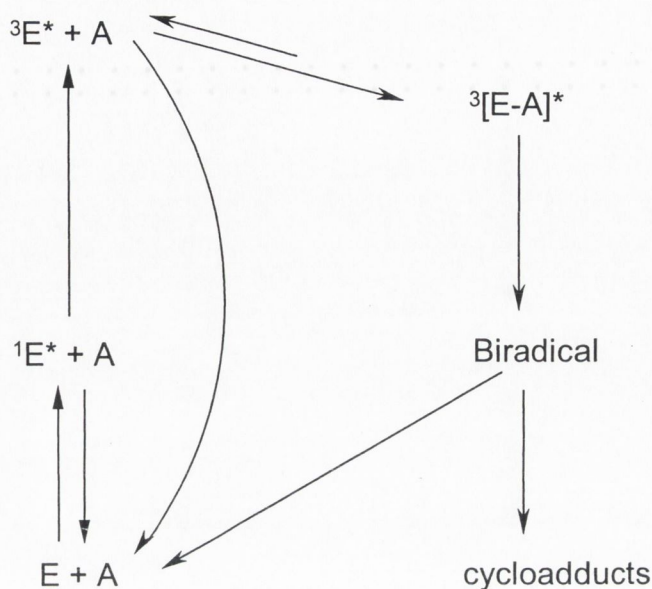
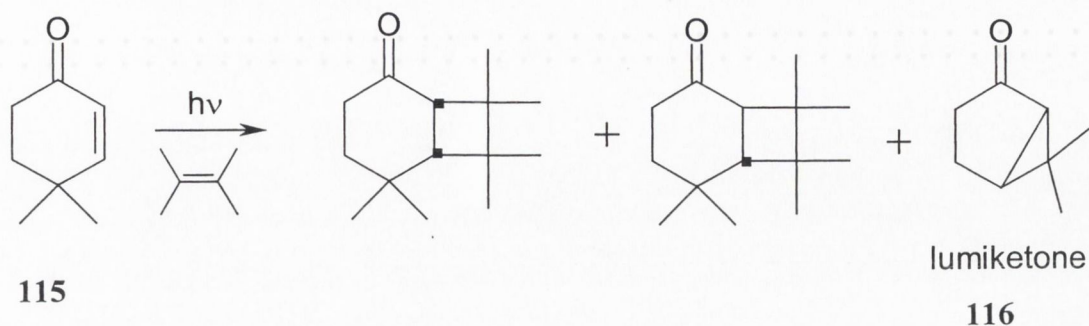


Fig. 1.17: Corey – de Mayo mechanism which considers reversion of all intermediates

**1.4.4.3 Alternative Mechanism** The Corey-de Mayo mechanism does not answer all observations on this reaction. For example, on irradiation, 4,4-dimethylcyclohexenone **115** forms an adduct with tetramethylethylene. It also forms the lumiketone **116**, via photo-rearrangement<sup>25</sup> (Fig. 1.18). Increasing alkene concentration favours the formation of the *cis*- and *trans*- adducts at the expense of the lumiketone photo-rearrangement. It is known that photo-rearrangements to lumiketones take place via the  $\pi, \pi^*$  state,<sup>21, 31, 26, 27</sup> and therefore [2+2] addition reactions take place from this state also (based on naphthalene quenching data).<sup>13</sup>





*Fig. 1.18: Products obtained on photolysis of 4,4-dimethylcyclohexenone in the presence of tetramethylethylene*

However, Schuster observed that although a variety of alkenes quenched this enone triplet state giving lumiketones as products, the derived Stern-Volmer constants *bore no relationship with the ionisation potential of the alkenes*.<sup>13</sup> Therefore, the idea of a 'donor-acceptor' mechanism is *not* borne out by these results. Furthermore, subsequent flash-photolysis work showed that (i) the same triplet state was responsible for both adduct formation and rearrangement and (ii) alkenes which form photo-adducts with reasonable efficiency ( $\phi \sim 0.4$ ) do not appear to *directly* quench this enone triplet.<sup>28</sup> These results led to the development of an alternative mechanism for cycloaddition.

**1.4.4.4 Bauslaugh's biradical proposal** In 1970, Bauslaugh proposed that the enone alkene cycloaddition reaction did not need to proceed via an exciplex intermediate.<sup>29</sup> He suggested that biradicals were directly formed and the regiochemistry could be explained by the fact that the most stable biradical intermediate leads to favoured product. In addition, *cis-trans* isomerisation of the alkene could be explained by the fact that reversion of the biradical intermediate to ground state enone and alkene can lead to alkene isomerisation.

Examining the addition of dimethylethylene (DME) to cyclohexenone, Bauslaugh proposes four intermediate biradicals. He suggests that the most stable of these

biradicals **117** – **120** would give rise to most reversion to ground state enone and alkene. **120** is considered highly unstable and probably plays little role in the reaction. **117** is considered highly stable, and would therefore would show most reversion to ground state products. Therefore, the predominant products would be those arising from intermediates **118** and **119**, giving predominantly H-T adducts.

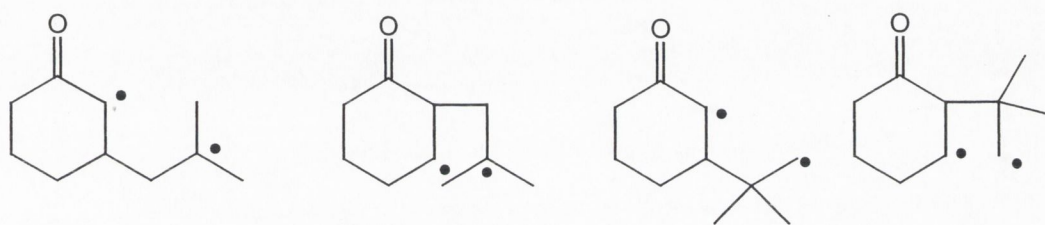


Fig. 1.19: Possible biradical intermediates on irradiation of cyclohexenone in the presence of 2-methylpropene

In addition, Bauslaugh considered the formation of *trans*-fused products from cyclohexenones. Using simple stereochemical arguments, he proposes three staggered conformations of biradical **118** which is most likely to be the predominant, if not the only, source of H-T adduct. These three conformations lead to *trans*-adduct, *cis*-adduct, and one unable to give either adduct. According to Bauslaugh, examination of models suggests that reaction of the biradical leading to *trans* adduct is conformationally more stable, and also that the intermediate leading to *cis*-adduct suffers more severe steric problems when it forms the cyclobutane adduct.

**1.4.4.5 Trapping of biradical intermediates** Bauslaugh's proposals, while rationalising experimental results nicely, lack any firm kinetic analysis. A lot of questions on the enone-alkene cycloaddition mechanism could be answered if the following were known:

- (i) the quantum efficiency for the formation of the several possible triplet biradicals;
- (ii) the lifetime and energy of each biradical and

- (iii) the extent of reversion to starting material and conversion to products for each biradical.

Weedon used a biradical trapping agent  $H_2Se$  to isolate the biradical intermediates.<sup>30, 31, 32, 33</sup> Examining the addition of cyclopentene to cyclopentenone, he isolated the  $\beta$ -bonded compound **122**, and the  $\alpha$ -bonded compounds **123** and **124**.<sup>33</sup> The ratio of these is almost 1:1, suggesting that in the absence of constraints, there is virtually no difference in reactivity between the  $\alpha$ - and  $\beta$ - carbons of the enone triplet. This pioneering work resolved a long-standing controversy in this field.

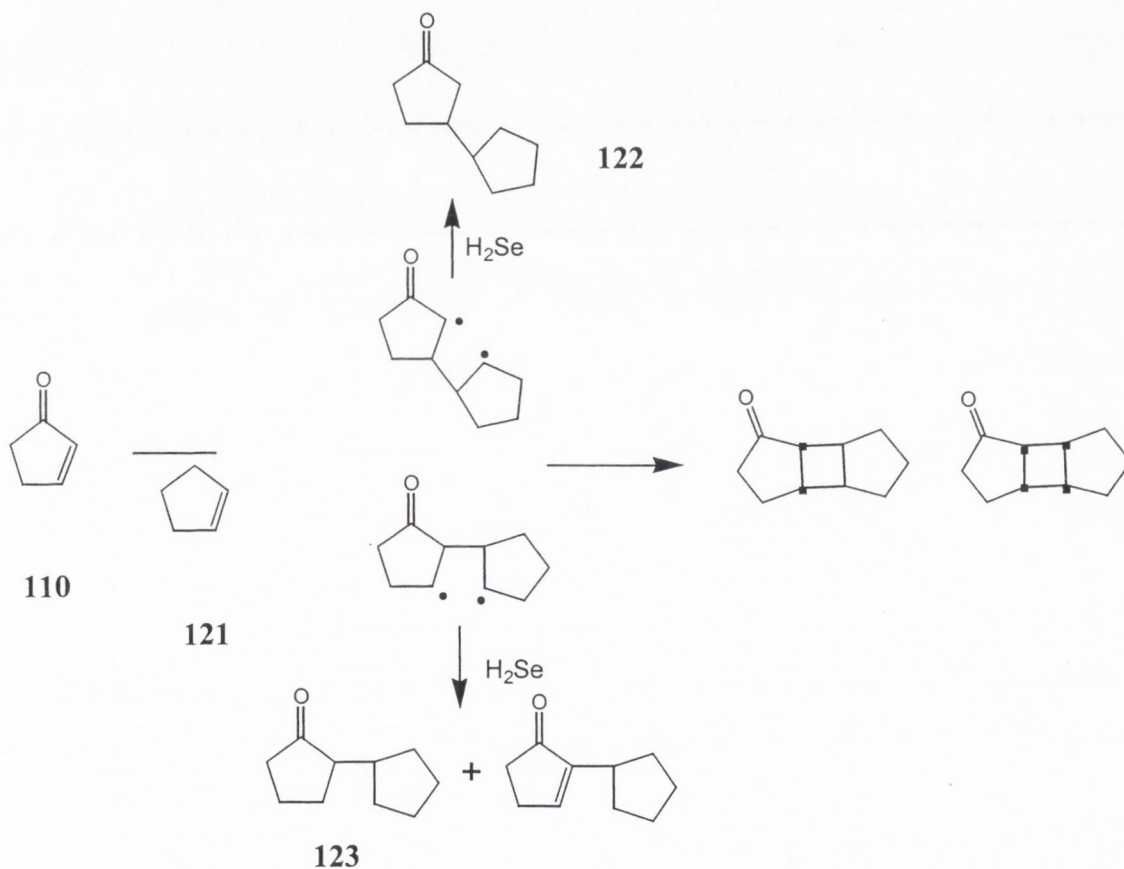


Fig. 1.20: Irradiation of cyclopentenone and cyclopentene: adducts formed and compounds formed as a result of trapping with  $H_2Se$ .



Following on from this, Weedon studied the addition of ethyl vinyl ether (EVE) to cyclopentenone.<sup>32, 33</sup> This reaction gives a ratio of HT : HH of 3.1 : 1. In the presence of H<sub>2</sub>Se, adduct formation is prevented and compounds **125** to **128** are isolated. **125** and **126** would result in HH adducts, whereas **127** and **128** would result in HT adducts. Products derived from the trapping the radicals **130** and **131** were not isolated. These radicals have primary radical centres and are either too unstable to be formed or revert faster than they can be trapped. The former is more likely as no adducts are formed in the presence of H<sub>2</sub>Se, and this shows that the excited enone becomes attached exclusively to the more substituted carbon of the alkene, giving more stable biradical intermediates.

The ratio of trapped intermediates derived from **129** and **132** is essentially 1:1, showing again that no significant difference in initial bond formation between  $\alpha$ -carbon and  $\beta$ -carbon of the enone triplet. What is most interesting however, is that although the HT : HH biradicals are formed in a 1 : 1 ratio, the adducts formed in reaction are 3 : 1. Hence reversion is favoured for HH, whereas conversion is preferential for HT, by a factor of 2.6. Similar results are found for cyclopentenone/ dimethylethylene (DME). It is still unclear why HT adducts preferentially form adducts.

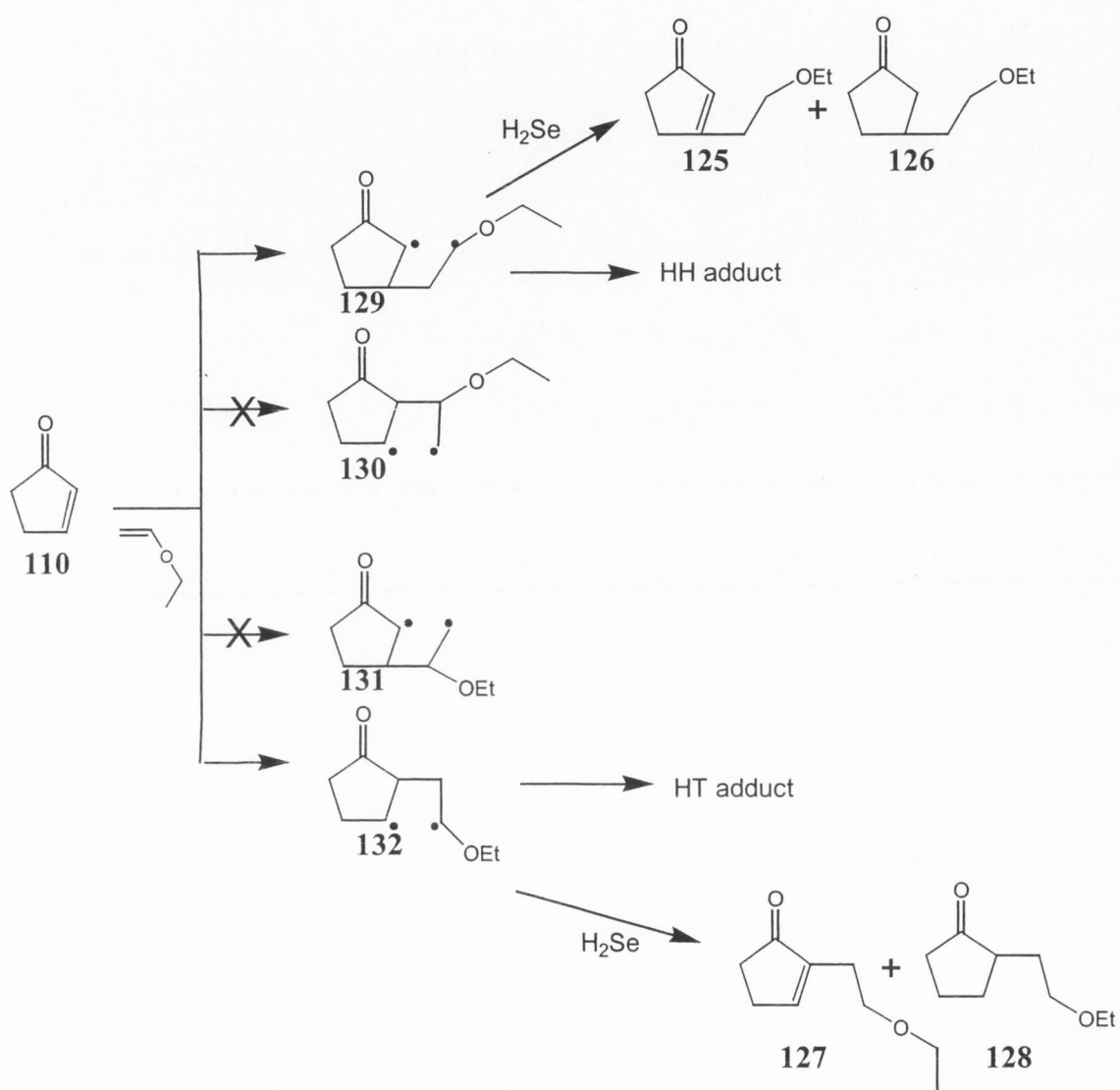


Fig. 1.21: Products and trapped intermediates after irradiation of cyclopentenone in presence of ethyl vinyl ether

**1.4.4.6 Bauslaugh-Schuster-Weedon Mechanism**<sup>13</sup> The Corey – de Mayo mechanism, while accounting for a large number of experimental observations, has a number of faults. These include the fact that the enone excited state is  $\pi,\pi^*$ , as opposed to  $n,\pi^*$  originally proposed and the fact that reactivity of electron deficient alkenes with enone triplets is found to be larger than the reactivity of electron rich alkenes, which is contrary to the exciplex hypothesis. There appeared to be little evidence to support the hypothesis that there is a preferred orientation of the enone triplet and the alkene in a polarised donor acceptor complex. In addition, solvent polarity did not appear to affect the rate constants of interaction of a large number of alkenes with enones. Finally, there is no actual requirement for an exciplex intermediate, and so taking into account the work by Bauslaugh, Weedon and Schuster (who detected the presence of triplet 1,4-biradicals following laser flash photolysis of cyclopentenone in acetonitrile<sup>34</sup>) an alternative mechanism to that of Corey-de Mayo's was developed. This is essentially Bauslaugh's proposed mechanism and accounts for deactivation of the enone triplet and biradical reversion.



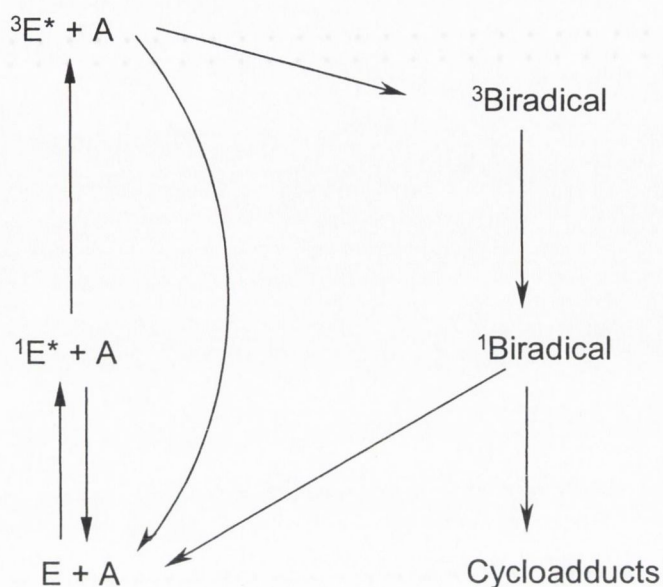


Fig. 1.22: Bauslaugh-Schuster-Weedon Mechanism for [2+2] cycloaddition<sup>13</sup>

**1.4.4.7 Mechanistic Conclusions** The following conclusions may be drawn on the [2+2] cycloaddition mechanism. The reactive enone triplet state is  $\pi,\pi^*$ . Initial bond formation may be from either the  $\alpha$ - or  $\beta$ - carbon of the enone, barring steric constraints. The presence of a biradical has been detected, and these are the direct precursors to cycloadducts. Biradical reversion is the main source of inefficiency, and also accounts for alkene isomerisation. What is not clear, and is still unresolved is whether there is an exciplex precursor to the triplet 1,4-biradical. Schuster argues that there is no evidence and simply no need to include this intermediate. However, Caldwell observed a transient with a 50ns lifetime, which he ascribes to an exciplex intermediate,<sup>35</sup> and Kelly *et al* observed an intermediate on irradiation of 3-phenylcyclopentenone in the presence of 1-phenylpropene in cyclohexane which is independent of enone concentration.<sup>1</sup> It is unclear whether this intermediate is an exciplex or a biradical. In conclusion, it seems that Schuster's observation is a fair one: "The exciplex hypothesis should be regarded with scepticism, at least until compelling

*experimental evidence supporting its validity is presented.*"<sup>36</sup> To date no such evidence has been reported.

## 1.5 CURRENT STUDY

The aims of this work are to investigate several of the topics described above.

Firstly, in Chapter 2, the interaction of 3-phenylcyclohexenone **101** and 1-phenylpropene is studied by Fourier Transform time-resolved infrared spectroscopy, in an attempt to investigate any intermediates using IR spectroscopy. IR spectroscopy, by its nature is a very informative tool, as it provides sharp bands in characteristic regions of the spectrum, unlike UV spectroscopy, where bands are generally broad and featureless. Laser flash photolysis is used to complement this work.

In Chapter 3, some new bicyclic enones **133** are synthesised. The design of these enones based on two factors – they contain the 3-phenylcyclopentenone back-bone much studied in this laboratory, and they are a synthetic precursor to furanoindenones **134**, which have analogies with the phototherapeutic drug psoralen, in that they have two potential binding sites for addition to bases in DNA.

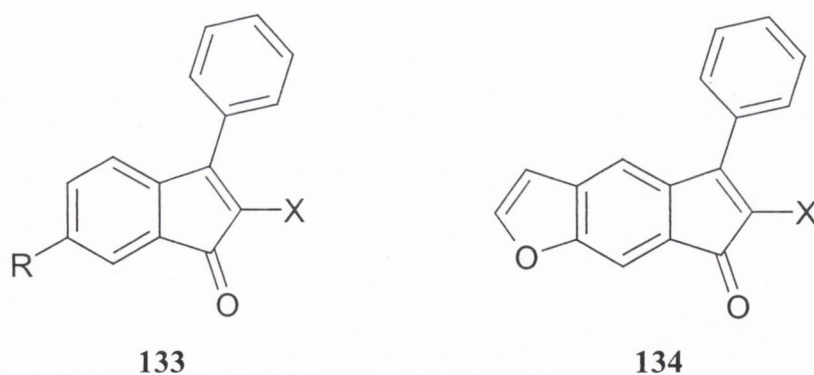


*Fig. 1.23: 3-phenylindenone backbone 133 and a furanoindenone 134 which has analogies with psoralen*

Finally, in Chapter 4, the interaction of these indenones with 1-phenylpropene is studied, again to compare them with PCP, and to identify the preferred regiochemistry of addition.



## 1.6 REFERENCES CITED

---

- 1 J. F. D. Kelly, T. B. H. McMurry and J. M. Kelly, *J. Chem. Soc. Perkin Trans 2*, 1999, 1933.
- 2 M. Magnifico, E. J. O'Connell, A. V. Fratini and C. M. Shaw, *J. Chem. Soc., Chem. Commun.*, 1972, 1095.
- 3 P. Yeats, S. N. Ege, G. Buchi and D. Knutson, *Can. J. Chem.*, 1967, **45**, 2927.
- 4 T. B. H. McMurry, A. G. Murphy, D. N. Work, A. G. Avent and J. P. James, *J. Chem. Soc. Perkin Trans. 2*, submitted.
- 5 G. Rodighiero and F. Dall'Acqua, *Photochem. Photobiol.*, 1976, **24**, 647.
- 6 G. S. Han, D. J. Yook, S. K. Kim, S. C. Shim and H. K. Kang, *Photochem. Photobiol.*, 1996, **64(3)**, 525.
- 7 L. Musajo, F. Bordin, G. Caporale, S. Marciani and G. Rigatti, *Photochem. Photobiol.*, 1967, **6**, 711.
- 8 L. Musajo, F. Bordin, and R. Bevilacqua, *Photochem. Photobiol.*, 1967, **6**, 927.
- 9 R. V. Bennasson, E. J. Land and T. G. Truscott, *Excited States and Free Radicals in Biology and Medicine*, Oxford University Press, 1993.
- 10 (i) A. Gilbert and J. Baggott, *Essentials of Molecular Photochemistry*, Blackwell Science Ltd., 1991; (ii) N. J. Turro, *Modern Molecular Photochemistry*, Benjamin/Cummings Publishing company, Inc., 1978; (iii) P. W. Atkins, *Molecular Quantum Mechanics*, Oxford University Press, 1983.
- 11 M. Kasha, *Disc. Faraday Soc.*, 1950, **9**, 14.
- 12 M. A. El-Sayed, *J. Chem. Phys.*, 1963, **38**, 2834; 1962, **36**, 573; 1964, **41**, 2462.
- 13 D. I. Schuster, G. Lem and N. A. Kaprinidis, *Chem. Rev.*, 1993, **93**, 3; D. I. Schuster, *The Chemistry of Enones*, Vol. 2, S Patai and Z Rappoport, Eds. Wiley, New York 1989, pp623-756,
- 14 H. H. Jaffe and M. Orchin, *Theory and Applications of Ultraviolet Spectroscopy*, Wiley, New York, 1962, p. 205.
- 15 P. E. Eaton and W. S. Hurt, *J. Am. Chem. Soc.*, 1966, **88**, 5038.
- 16 D. J. Treacker, *Org. Photochem.*, 1969, **2**, 63.

- 
- 17 P. E. Eaton, *J. Am. Chem. Soc.*, 1962, **84**, 2454.
- 18 E. J. Corey, R. B. Mitra, H. Uda; *J. Am. Chem. Soc.*, (1964), **86**, 485.
- 19 A. C. Weedon, *Synthetic Organic Chemistry*, W. M. Horspool, Ed., Plenum Press, New York, 1984, pp 61-144; H. A. J. Carless, *Photochemistry in Organic Synthesis*, J. D. Coyle, Ed., Royal Soc. Chem., London, 1986, pp 95-117.
- 20 P. V. Kavanagh, J. M. Kelly, T. B. H. McMurry and J. P. James, *J. Chem. Soc., Chem. Commun.*, 1993, 231.
- 21 D. I. Schuster, J. R. Cao, N Kaprinidis, Y. H. Yu, A. W. Jensen, Q. Y. Lu, H Wang and S. R. Wilson, *J. Am. Chem. Soc.*, 1996 **118**, 5639.
- 22 D. R. Kearns, G. Marsh and K. Schaffner, *J. Chem. Phys.*, 1968, **49**, 3316; . G. Marsh, D. R. Kearns and K. Schaffner, *Helv. Chim. Acta*, 1968, **51**, 1890; *J. Am. Chem. Soc.*, 1971, **93**, 3129.
- 23 J. J. McCullough, B. R. Ramachandran, F. F. Synder and G. N. Taylor, *J. Am. Chem. Soc.*, 1975, **97**, 6767.
- 24 P. de Mayo, *Acc. Chem. Res.*, 1971, **4**, 41.
- 25 D. I. Schuster, M. M. Greenburg, I. M. Nuñez and P. C. Tucker, *J. Org. Chem.*, 1983, **48**, 2615.
- 26 A. C. Chan and D. I. Schuster, *J. Am. Chem. Soc.*, 1986, **108**, 4561.
- 27 W. G. Dauben and W. A. Spitzer, *J. Am. Chem. Soc.*, 1971, **93**, 3674.
- 28 D. I. Schuster, D. A. Dunn and R. Bonneau, *J. Photochem.*, 1985, **28**, 413; D. I Schuster, P. B. Brown, L. Capponi, C. A. Rhodes, J. C. Scaiano and D. Weir, *J. Am. Chem. Soc.*, 1987, **109**, 2533.
- 29 P. G. Bauslaugh, *Synthesis*, 1970, 287.
- 30 A. Rudolph and A. C. Weedon, *Can. J. Chem.*, 1990, **68**, 1590.
- 31 D. Andrew and A. C. Weedon, *J. Am. Chem. Soc.*, 1995, **117**, 5647
- 32 D. Andrew, D. J. Hastings, D. L. Oldroyd, A. Rudolph, A. C. Weedon, A. C. Wong and B. Zhang, *Pure Appl. Chem.*, 1992, **64**, 1327.
- 33 D. J. Hastings and A. C. Weedon, *J. Am. Chem. Soc.*, 1991, **113**, 8525.

- 
- 34 R. A. Caldwell, W. Tang, D. I. Schuster and G. E. Heibel, *Photochem. Photobiol.*, 1991, **53**, 159.
- 35 R. A. Caldwell, D. C. Hrcir, T. Muñoz Jr. And D. J. Unett, *J. Am. Chem. Soc.*, 1996, **118**, 8741.
- 36 D. I. Schuster, G. E. Heibel and J. Woning, *Angew. Chem. Int. Ed. Engl.*, 1991, **30(10)**. 1345.



## *Chapter Two*

*A Study of 3-Phenylcyclohexenone and its Interaction with  
1-Phenylpropene using Laser Flash Photolysis and Time-  
Resolved Infrared Spectroscopy*

## 2.1 INTRODUCTION

### 2.1.1 The Enone-Alkene Cycloaddition Reaction

The enone-alkene reaction is an important class of reaction in terms of its use in synthetic chemistry<sup>1</sup> and phototherapy.<sup>2</sup> In this laboratory, the interaction of many cyclic enones with alkenes has been studied.<sup>3</sup> 3-phenylcycloalkenones are of interest as they have a relatively long transient lifetime, and they react with alkenes with moderately high quantum efficiency.

The [2+2] cycloaddition reaction between 3-Phenylcyclohexenone (PCH) and 1-phenylpropene (1-PP) has been studied by <sup>1</sup>H NMR and laser flash photolysis.<sup>3</sup> <sup>1</sup>H NMR experiments have shown that only one adduct, 8-*exo*-methyl-6,7-*endo*-diphenylbicyclo[4.2.0]octan-2-one is formed.<sup>4</sup> (Fig. 2.1) Laser flash photolysis of the enone in the presence of the alkene quencher gives a rate constant of quenching of  $5 \times 10^7 \text{ dm}^3 \text{ mol}^{-1} \text{ s}^{-1}$  in cyclohexane, with similar values for benzene and acetonitrile. (Table 2.1)<sup>5</sup>

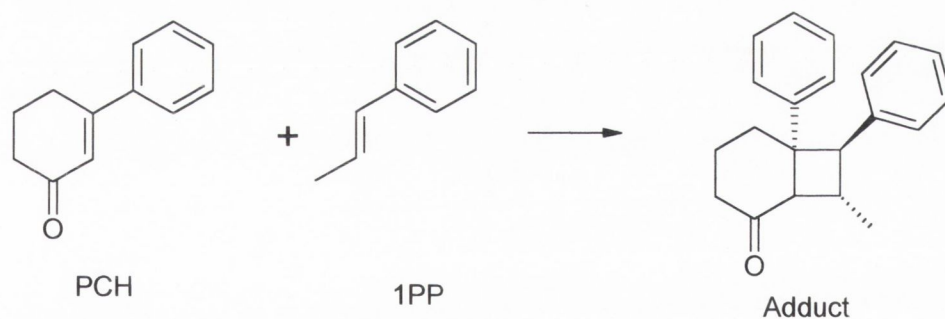


Fig. 2.1: Photocycloaddition reaction between 3-phenylcyclohexenone and *trans*-1-phenylpropene giving rise to one adduct<sup>4</sup>

Table 2.1: Rate Constants for Quenching ( $k$ , in  $\text{dm}^3 \text{mol}^{-1} \text{s}^{-1}$ ) of 3-Phenylcyclohexenone by itself and E-1-Phenylpropene in various solvents at room temperature<sup>5</sup> ( $\pm 10\%$ )

Quencher	Acetonitrile	Benzene	Cyclohexane
PCH	$< 2 \times 10^6$	$< 2 \times 10^6$	$< 2 \times 10^6$
E-1-PP	$3.3 \times 10^7$	$2.4 \times 10^7$	$5.0 \times 10^7$

As described in Chapter 1, the mechanism of the cycloaddition reaction is the subject of debate - namely do the reactants form an enone-alkene excited state complex (exciplex)<sup>6,7</sup> prior to forming biradical intermediates, or are biradicals formed directly on photoexcitation.<sup>8</sup> Evidence for this exciplex is scant,<sup>9</sup> and it was decided to study this reaction further and investigate any intermediates observed.

### 2.1.2 Aims

- To characterise the excited state of PCH using laser flash photolysis and time-resolved infrared spectroscopy;
- To investigate the [2+2] cycloaddition reaction between PCH and 1-phenylpropene (1PP);
- To examine the use of TRIR as a technique for studying the photochemistry of organic compounds.

### 2.1.3 Time-Resolved Infrared Spectroscopy

There is a broad range of spectroscopic tools available to the transient spectroscopist. Given its high sensitivity and the relative experimental ease, UV laser flash photolysis (transient absorption spectroscopy) is most commonly employed to study transient species, obtaining information on the nature and lifetime of transient species. Transient absorption spectroscopy has the downfall that spectra are usually broad and featureless and little *structural* information can be gleaned. Vibrational spectroscopy, of all



spectroscopic techniques probably offers most information on structural changes on photo-excitation.

Time-resolved resonance Raman spectroscopy has been used successfully to study both inorganic and organic transient species, although the range of compounds available for study is limited by the resonance enhancement requirement. Single-frequency IR and Fourier transform IR spectroscopy have been slower to develop, but their potential power in the study of structural changes on electronic excitation is enormous.

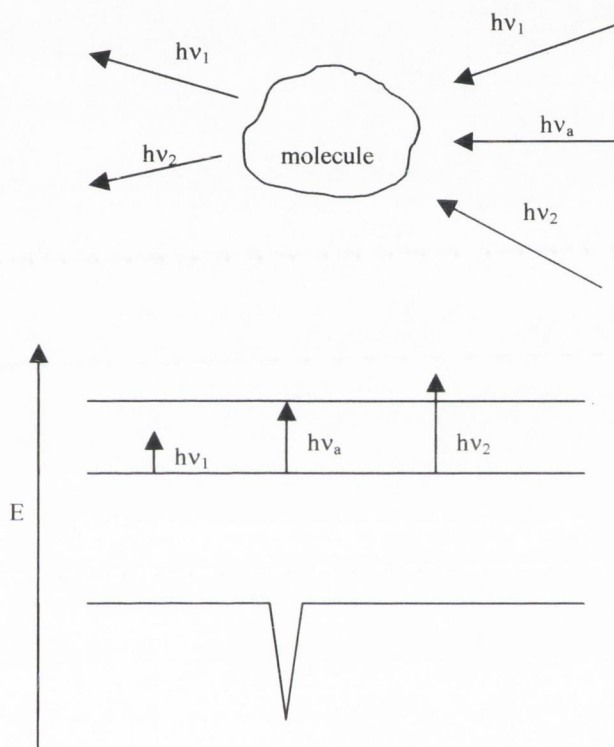


Fig. 2.2: Light of various frequencies incident on a molecule. Frequencies absorbed by the molecule will not be transmitted through the molecule resulting in a reduction in transmittance at that frequency (adapted from Reference 10)

**2.1.3.1 Infrared Spectroscopy** An infrared spectrum reveals information on the vibrational structure of a molecule. IR radiation (*i.e.* heat) is absorbed by different molecules at characteristic frequencies, depending on the vibrational chromophores the

molecule contains. This in turn reveals information of the structure of the molecule. If light quanta  $h\nu_1$ ,  $h\nu_2$  and  $h\nu_a$  are incident on a molecule whose energy difference between its vibrational ground and excited states is proportional to  $h\nu_a$ ,  $h\nu_a$  will be absorbed by the molecule showing a reduction in transmittance at frequency  $\nu_a$  in the spectrum. (Fig. 2.2)

Initially, infrared spectra were obtained using dispersive spectrometers (Fig. 2.3). Light from an IR source is passed through the sample and then through slits, allowing a narrow slice of light to be incident on a diffraction grating. Varying the angle of the grating allowed a range of wavelengths to be examined, and the intensity of incident light on the detector as a function of frequency gives the infrared spectrum.

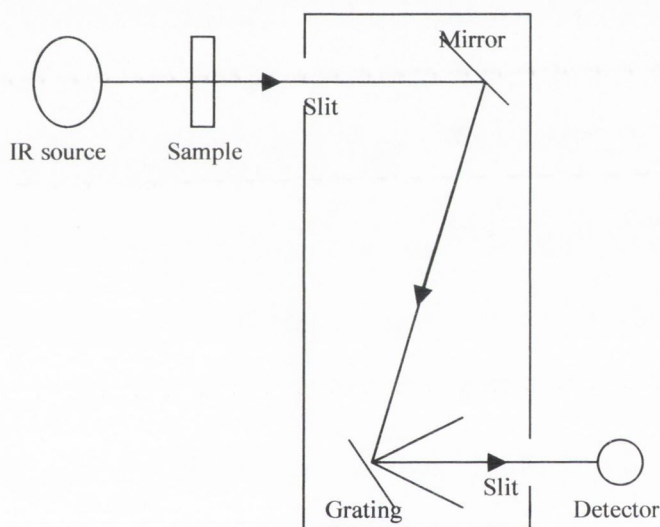


Fig. 2.3: The Dispersive Infrared Spectrometer<sup>10</sup>

When computational capability allowed Fourier transformation to be carried out with relative ease, FT-IR spectrometers soon replaced dispersive instruments. This type of spectrometer, based on the Michelson-Morley interferometer allows the infrared spectrum to be collected quickly (Fig. 2.4).

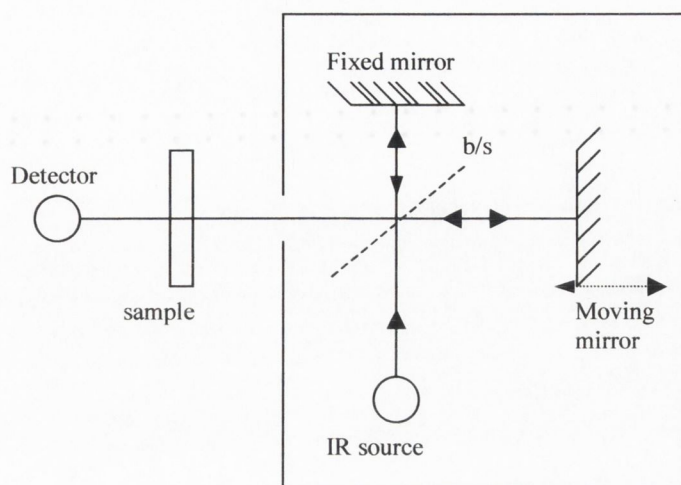


Fig. 2.4: The Fourier - Transform Interferometer<sup>10</sup>

Light, from a broad band infrared source passes through a beamsplitter. About 50% of the light passes through to a stationary mirror and is reflected back to the beamsplitter. The other 50% of the light is refracted at the beamsplitter to a moving mirror and is reflected back to the beamsplitter. The two beams recombine at the beamsplitter, at a frequency dependent on the distance of the moving mirror from the beamsplitter. Hence as the mirror moves from initial to final positions, the range of frequencies pass through the sample and to the detector.

FTIR spectroscopy has well known advantages over dispersive spectrometry - namely:

- Multiplex advantage ( Fellgett<sup>11</sup>): for FTIR, all radiation from source is used for detection, whereas in dispersive instruments radiation passes through input and output slits, reducing its intensity;
- Higher throughput (Jacquinot<sup>12</sup>): FTIR beam has larger cross-section as there is no slit, giving a higher throughput through the sample;
- Wavenumbers accuracy (Connes<sup>13</sup>) advantage: a He-Ne laser, used to calculate accurately the position of the moving mirror, acts as an internal wavelength



calibration standard. This internal calibration is not available in a dispersive spectrometer.

*2.1.3.2 Time-Resolved Infrared Spectroscopy* There are two techniques for nanosecond and longer time-resolved infrared spectroscopy. The first - a conventional pump-probe experiment - excites the sample with a UV source (nanosecond laser), and changes are monitored with either a tunable diode laser or a broad-band IR source.<sup>14</sup> The former has higher photon flux, but only offers a limited frequency range (100-150cm<sup>-1</sup>). The latter offers a broad frequency range but is lower in intensity, giving rise to signal:noise problems. This problem has been somewhat overcome by using a MoSi<sub>2</sub> source, which has a high photon flux and is used by Hamaguchi<sup>15</sup> and Toscano.<sup>16</sup> IR spectra are recorded, one frequency at a time, using a dispersive spectrometer.

The second technique - Fourier transform time-resolved infrared spectroscopy - again uses a nanosecond laser to excite the sample. In this case a FT-IR spectrometer is used to record spectra.<sup>17-19</sup> As described above, the spectrum is acquired while the moving mirror in the interferometer displaces a certain distance. The spectrometer can be rapid-scan or step-scan. Here we discuss step-scan.

In the step-scan technique,<sup>20</sup> the mirror steps a discrete distance, the UV pulse pumps the sample, and the infrared detector records the temporal change in signal. The mirror moves to the next step and the process is repeated. Thus, a series of interferograms are collected, and are Fourier-transformed to give a series of time-dependent infrared spectra, each corresponding to incremental time delays from the trigger signal. (*Fig. 2.5*)

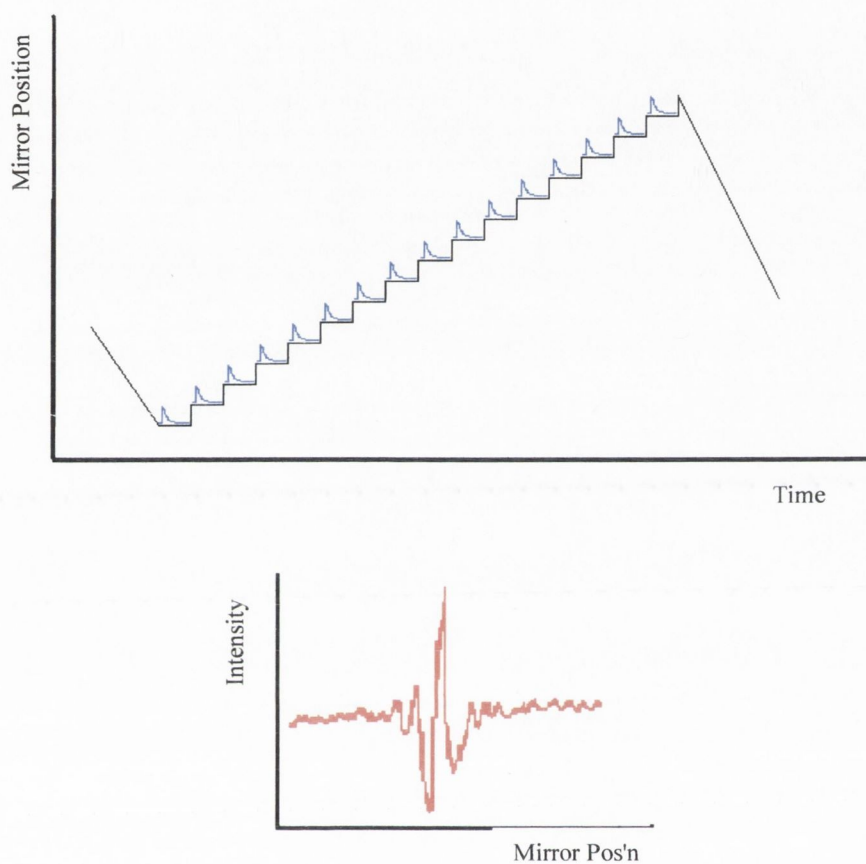


*Fig. 2.5: Schematic of data collection in a step-scan interferometer. (Top) The mirror moves a discrete distance, stops, the photochemical process is triggered and the temporal change in intensity is recorded over time. (Bottom) The interferogram at any time  $t$ . Fourier transformation gives the IR spectrum. (from 20)*

As none of the throughput is blocked by slits, the technique should be better suited to study processes that are not photo-reversible (e.g. photo-reactions), or where the compound is not highly photo-stable. (With dispersive IR, each frequency is averaged thousands of times) However, the technique is more sensitive to variation in measuring

conditions - e.g. a noise spike in the interferogram will affect the entire spectrum, whereas it will distort only a single point in the dispersive experiment. Also, dispersive IR allows the collection of data at one frequency of interest, giving accurate kinetic traces. An FT experiment requires the entire spectrum to be collected, followed by analysis of peaks of interest.

*2.1.3.3 Development of Technique*<sup>19</sup> Thus, initial work in TRIR spectroscopy used the conventional pump-probe approach, with a CW IR source and fast IR detector. CO and diode lasers were then used as IR source, giving higher throughput. However, S<sup>2</sup>-FTIR became technologically feasible<sup>21</sup> and the S<sup>2</sup>-FT-TRIR spectrum of the <sup>3</sup>MLCT states of Re(CO)<sub>3</sub>(polypyridyl)(X) were recorded in 1996.<sup>22</sup> Since then, M-CO and M-CN containing compounds have been studied successfully - these carbonyl and cyano groups are termed 'reporter ligands' as they have very strong chromophores which can change quite significantly on photo-excitation, depending on the extent of  $\pi$ -backbonding to the ligand.<sup>23</sup>

In 1993, the first microsecond TRIR spectrum of an excited state of an organic compound was reported, measured using a dispersive spectrometer.<sup>24</sup> The power of the technique for organic systems became apparent - 4-phenylbenzophenone has a well-characterised  $\pi, \pi^*$  state and the excited state spectrum of the compound reflected this (see below).

Since then several organic systems have been studied, mainly by Toscano and co-workers,<sup>25</sup> using the pump-probe approach. However, the technique is still relatively difficult and novel for organic compounds. Organic carbonyl chromophores have much lower extinction coefficients than their inorganic counterparts, and this coupled with the fact that IR detectors are less sensitive than UV/vis detectors means that the technique is still at the development stage. No S<sup>2</sup>-FT-TRIR spectra of organic compounds have



been reported, although George has studied benzophenone, 4-phenylbenzophenone and others successfully.<sup>26</sup>

**2.1.3.4 The TRIR Experiment** A schematic of the apparatus used in the University of Nottingham is shown below. (Fig. 2.6) Full experimental details are described in Chapter 5. Briefly, the sample is dissolved in *ca.* 20mL of solvent and degassed. A flow cell is used to minimise sample decomposition – during the experiment the sample is exposed to many thousands of laser flashes. As the moving mirror steps the range of frequencies, the sample is exposed to a laser flash at each step and the temporal change in IR absorbance monitored. The mirror moves to the next step and the process repeated. Therefore (after Fourier-transformation) a series of time-dependent spectra are collected and are available for processing. The change in intensity of any frequency in the spectrum (*i.e.* the decay profile) can also be analysed. exponentially over time).

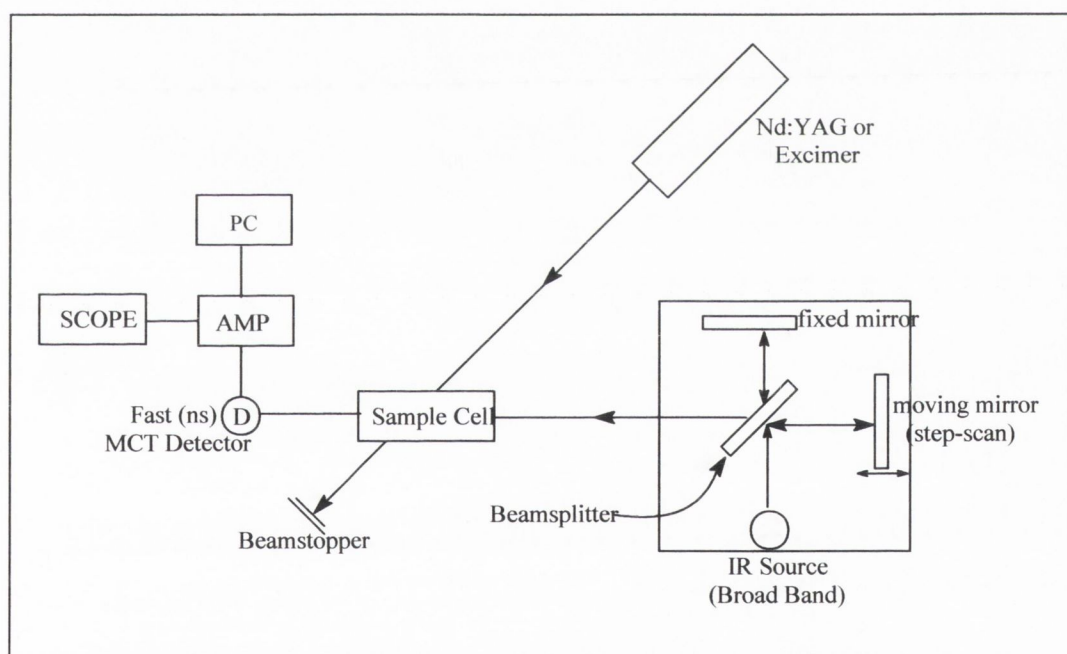


Fig. 2.6: Schematic of the TRIR apparatus at Nottingham

When assigning peaks, spectra over a time range were analysed to ensure that the peak was present across a range of time slices – indicating it is not an artefact. This was

important, especially when spectra had a poor signal to noise ratio. Examining the decay profile over time also allowed one to see if the peak was indeed due to a transient (*i.e.* decayed)

**2.1.3.5 Excited-State IR Spectra** Unlike UV spectra, which usually have broad featureless bands, IR spectra have characteristic 'fingerprints' and can reveal a lot of information about the system being studied. Spectra obtained are the *change* in infrared absorbance after laser flash. (Fig. 2.7) Therefore, any peaks corresponding to the ground-state of the molecule appear as negative absorbances in the spectrum, indicating the temporary disappearance of the ground state moiety. This is termed 'bleaching' and for ketones, the depletion of the ground-state carbonyl peak in the excited state IR spectrum is called the 'parent bleach'. The appearance of any positive peaks in the excited state spectrum is due to new species formed as a result of photolysis. In other words, positive peaks in the spectrum are due to either transient species or photoproducts.

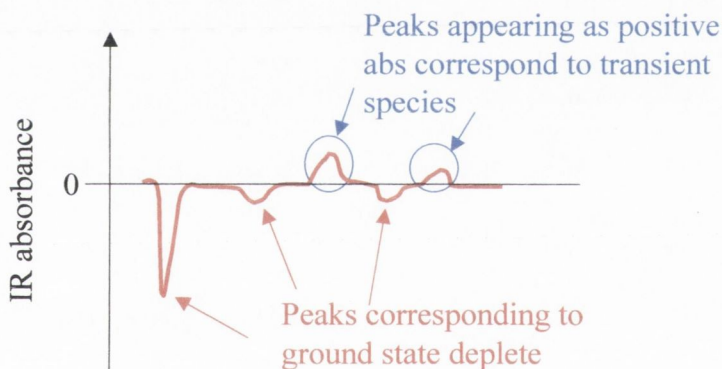


Fig. 2.7: Schematic of a transient infrared spectrum showing depletion of ground state peaks (bleaching) and formation of excited state peaks

**2.1.3.6 Interpreting the Excited-State IR of Organic Ketones** There are very few reports of excited state IR spectra of organic ketones, with the first - an excited state spectrum of 4-phenylbenzophenone - being reported only in 1993.<sup>24</sup> Other compounds studied

include benzophenone,<sup>26</sup> *p*-methoxy- and *p*-trifluoromethyl-acetophenone.<sup>27</sup> However, even these few reports give an indication of how useful the technique is for studying the excited states of these systems.

The difference in frequency between the parent bleach and the peak assigned as being due to excited state carbonyl band indicates the nature of the excited state. (Fig. 2.8) This has been elegantly demonstrated by comparing the excited state IR spectra of *p*-methoxyacetophenone and *p*-trifluoroacetophenone.<sup>27</sup> The former has been well characterised as having a  $^3(\pi,\pi^*)$  excited state, whereas the latter has a  $^3(n,\pi^*)$  excited state (using phosphorescence lifetimes, rate constants of quenching by H-donors, etc.)<sup>28</sup>

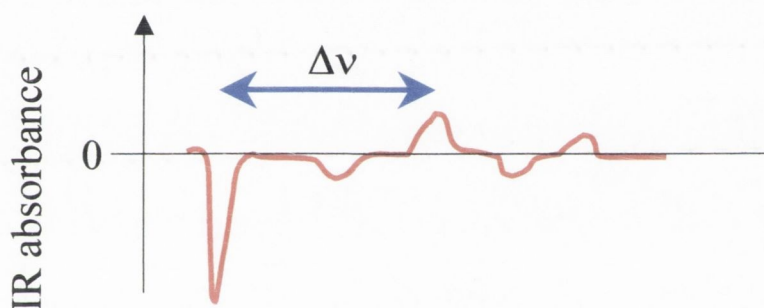


Fig. 2.8: Schematic transient infrared spectrum with the difference between ground state carbonyl and excited state carbonyl,  $\Delta\nu$ , marked

The methoxy-compound had a parent bleach at  $1664\text{cm}^{-1}$ , with a transient peak corresponding to the excited state carbonyl bond appearing at  $1462\text{cm}^{-1}$ , indicating a shift,  $\Delta\nu$ , of  $202\text{cm}^{-1}$ . This relatively small shift ties in with the fact that in a  $\pi,\pi^*$  system, the carbonyl bond retains much of its double bond character, and so the stretching frequency is not strongly affected.

Conversely, for the trifluoromethyl derivative, the parent bleach is at  $1696\text{cm}^{-1}$ , and the transient peak is at  $1326\text{cm}^{-1}$ , a shift of  $370\text{cm}^{-1}$ . This much larger shift correlates with the fact that in  $n,\pi^*$  systems, the excited state is localised on the carbonyl bond, and it is



C-O single bond in nature. Hence, the transient peak reflects this, and the frequency is significantly lower than that of a double bond.

These results are reflected in excited state IR spectra of benzophenone  $^3(n,\pi^*)^{26}$  and 4-phenylbenzophenone  $^3(\pi,\pi^*)^{24}$ . For benzophenone, the carbonyl C=O stretch shifts from  $1665\text{cm}^{-1}$  to  $1222\text{cm}^{-1}$ , a shift of  $443\text{cm}^{-1}$ ; whereas the shift for 4-phenylbenzophenone is much smaller at  $113\text{cm}^{-1}$ . (Fig. 2.9) These results correlate with those from time-resolved resonance Raman spectroscopy.

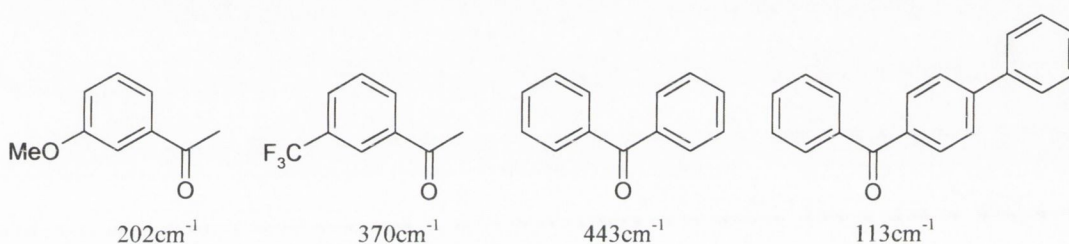


Fig. 2.9: Observed shifts in C=O frequency of model systems as measured by TRIR

#### 2.1.4 Current Study

The photophysics and photochemistry of two enones – 3-phenylcyclopentenone (PCP) and 3-phenylcyclohexenone (PCH) have been studied extensively in this laboratory.<sup>3</sup> The photocycloaddition reaction with (*E*)- and (*Z*)- 1-phenylpropene has also been studied with flash photolysis and  $^1\text{H}$  NMR. Some relevant data is summarised in Table 2.2.<sup>5</sup> PCP has a long transient lifetime at infinite dilution ( $14\mu\text{s}$  in acetonitrile), although it is very sensitive to concentration of the enone (self-quenching rate of the order of  $10^8\text{ dm}^3\text{ mol}^{-1}\text{ s}^{-1}$ ). On cycloaddition to (*E*)-1-phenylpropene, PCP gives two adducts, but with very low quantum yield. The dominant process is alkene isomerisation.

PCH on the other hand has a shorter transient lifetime at infinite dilution ( $3.9\text{ }\mu\text{s}$  in acetonitrile) but is much less sensitive to enone concentration. ( $k_{\text{sq}} < 10^6\text{ dm}^3\text{ mol}^{-1}\text{ s}^{-1}$ ) On

cycloaddition to (*E*)-1-phenylpropene, only one adduct is formed, with a reasonable quantum yield.

*Table 2.2: Quenching rate constants, limiting lifetimes and quantum yields of adduct formation with E-1-phenylpropene for PCP and PCH in acetonitrile<sup>5</sup> (Values  $\pm 10\%$ )*

	PCP	PCH
$k_{sq}$ ( $\text{dm}^3\text{mol}^{-1}\text{s}^{-1}$ )	$1.9 \times 10^8$	$< 2 \times 10^6$
$k_q$ (E-1PP) ( $\text{dm}^3\text{mol}^{-1}\text{s}^{-1}$ )	$1.5 \times 10^9$	$3.3 \times 10^7$
$\tau_0$ ( $\mu\text{s}$ )	14	3.9
$\Phi_{\text{adduct}}$	0.04	0.24

Given these data it was decided to study the excited state of PCH and its interaction with (*E*)-1-phenylpropene by TRIR. High concentrations ( $\sim 10^{-2}$  M) are required for TRIR experiments, and the low self-quenching rate of PCH means that this high concentration will not hinder the experiment. In addition, the fact that only one adduct is formed, and in reasonable yield, on cycloaddition to (*E*)-1-phenylpropene means that transient spectra will not be complicated by two separate adducts.

## 2.2 RESULTS

### 2.2.1 Design of Experiment

As TRIR is a relatively new technique for organic compounds, it was necessary to think carefully about the system to study, and the conditions to be used in the experiment.

#### 2.2.1.1 Solvent:

The solvent for the experiment was chosen to be deuterio-acetonitrile  $\text{CD}_3\text{CN}$ . This solvent has a 'window' (*i.e.* does not absorb) between  $1200\text{-}1800\text{cm}^{-1}$ , where the region of interest is. (Fig. 2.10) Other 'traditional' solution IR solvents - chloroform and carbon tetrachloride - were not used as it was feared that chlorine atoms would be liberated on laser excitation.

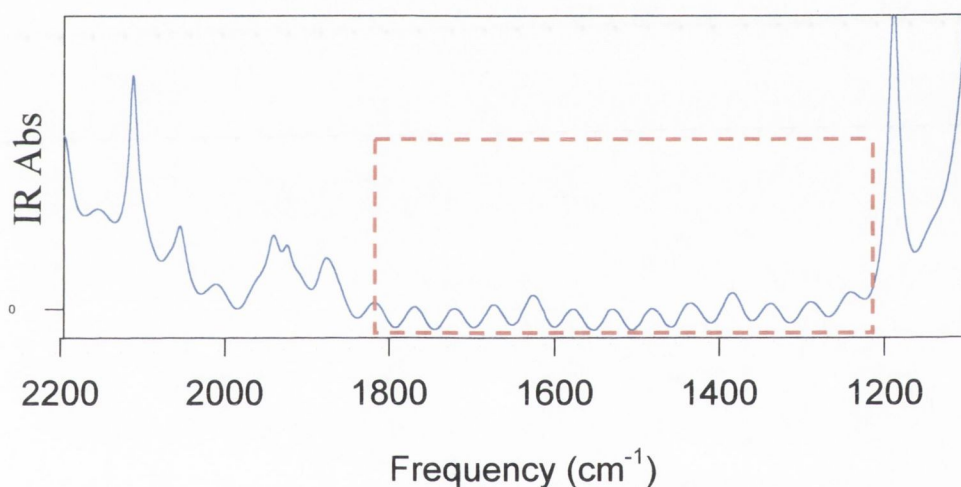


Fig. 2.10: IR absorbance spectrum of deuterioacetonitrile (Pathlength = 0.1mm)

2.2.1.2 Sample Concentration To minimise solvent absorption, a small pathlength is used in the IR cell. ( $P/L=0.1\text{mm}$ ) Also, IR detectors are less sensitive than UV detectors, and IR extinction coefficients are relatively low. Therefore, the Beer-Lambert law requires that a high sample concentration is required to record sufficient absorption. A sample concentration of 10mM is used.



*2.2.1.3 Excitation Wavelength* Flash photolysis studies on this compound were previously carried out using a XeCl laser, exciting at 308nm. PCH absorbs well in this region ( $\epsilon_{308} = 2710 \text{ dm}^3 \text{ mol}^{-1} \text{ cm}^{-1}$ ) but for UV experiments, low concentrations ( $10^{-4} \text{ M}$ ) are used. For TRIR, concentrations of 10 mM are used. Absorbances at 308nm at this concentration were  $>2$ . Preliminary experiments showed that excitation at 308nm gave an overriding 'shock' signal – caused by too high a UV absorbance relative to the IR absorbance. In this case the IR signal is overridden and spectra cannot be collected. Therefore, although the absorbance is low at 355nm, ( $\epsilon_{355} = 80 \text{ dm}^3 \text{ mol}^{-1} \text{ cm}^{-1}$ ) at the concentrations used it was sufficient, and hence a Nd:YAG laser was used to excite the sample at 355nm.

## **2.2.2 The Photophysical Properties of 3-Phenylcyclohexenone**

*2.2.2.1 UV/vis Absorption Spectrum* A highly allowed transition at 278nm in cyclohexane is assigned to a  $\pi, \pi^*$  band, as it shifts to the red on increasing solvent polarity. (Fig. 2.11) A shoulder is observed at 340nm which blue shifts on increasing polarity and is assigned as  $n, \pi^*$ . The extinction coefficients at wavelengths of interest are given in Table 2.3.

Table 2.3: Extinction coefficients at wavelengths of interest for PCH in acetonitrile

Wavelength (nm)	278	308	340	355
$\epsilon$ (dm <sup>3</sup> mol <sup>-1</sup> cm <sup>-1</sup> )	16110	2710	126	80

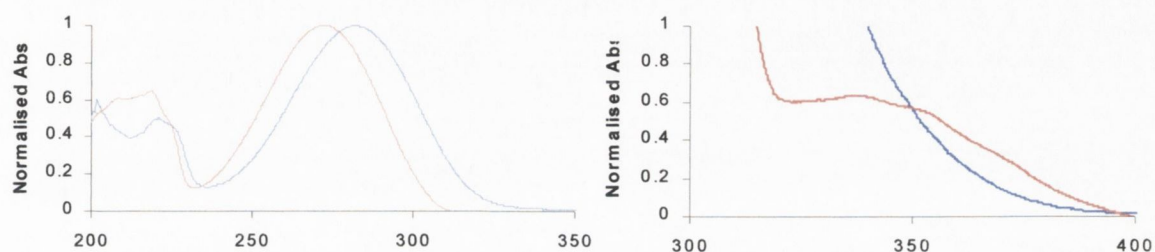


Fig. 2.11: (Left) UV/vis absorption Spectrum of PCH (0.1mM) in cyclohexane (red) and ethanol (blue); (Right) of PCH (1mM)

#### 2.2.2.2 Laser Flash Photolysis

Laser flash photolysis is usually carried out with sample concentrations of  $\sim 10^{-4}$  M in acetonitrile but in order to compare results with those from the TRIR experiments, sample concentrations of 10 mM were used. Laser excitation at 355 nm produced a transient species. Monitoring the change in absorbance of this species as a function of wavelength, gives the transient absorption spectrum, shown below.

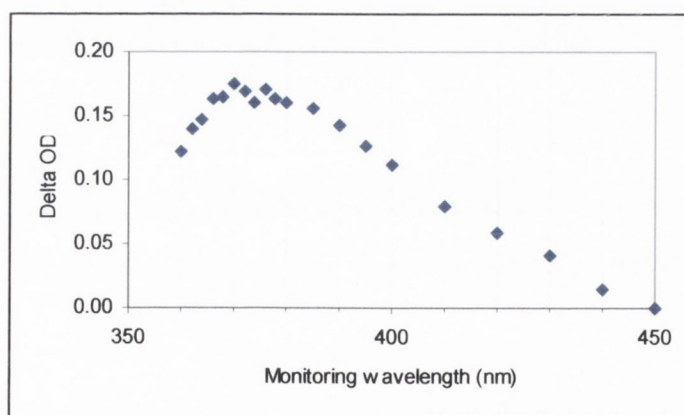


Fig. 2.12: Transient Absorption Spectrum of PCH(10mM) immediately after laser flash

This spectrum shows a broad maximum, centred around 375nm, with a  $\Delta OD$  value of 0.17. Some fine structure is apparent, and the points were repeated 3 times, giving the same result. However, within the margin of error, it is difficult to say if this fine structure is real. Monitoring the decay profile of any of these peaks and fitting the curve allows the rate of decay to be calculated. (Fig. 2.13)

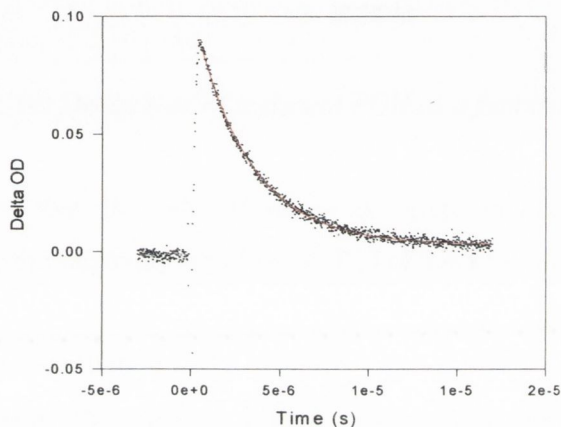


Fig. 2.13: Decay profile of transient observed at 370 nm after photolysis of PCH (10mM)

Decay rates of  $3.0 \pm 0.3 \times 10^5 \text{ s}^{-1}$  were calculated across the wavelength range 360 - 400nm. Decays were unimolecular. Rate constants were slightly slower at shorter wavelengths ( $k_{360\text{nm}} = 2.9 \times 10^5 \text{ s}^{-1}$ ) than at longer wavelengths ( $k_{400\text{nm}} = 3.2 \times 10^5 \text{ s}^{-1}$ ), but all were within 10% margin of error. The rate of decay as a function of concentration was examined. (Fig. 2.14) Fitting the plot to equation 2.1 gives a slope of  $k_{\text{sq}}$ , the self-quenching rate constant.

$$k_{\text{obs}} = k_0 + k_{\text{sq}} [\text{PCH}] \quad \text{Equation 2.1}$$



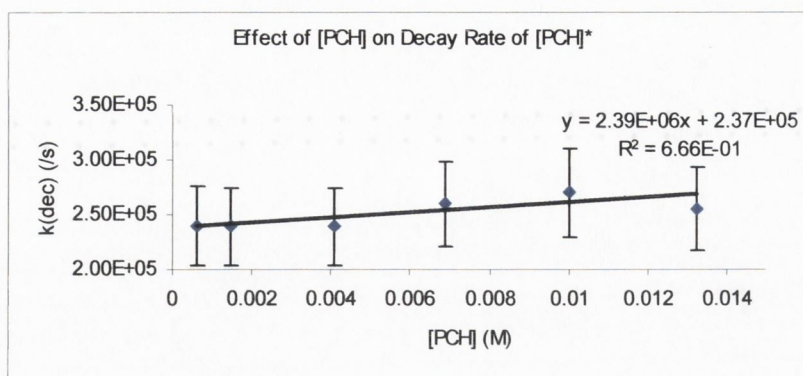


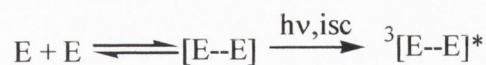
Fig. 2.14: Decay rate of transient PCH as a function of [PCH]

This graph shows that the rate of decay is relatively unaffected by increasing concentration, and the relatively small slope ( $k_{sq}$ ) of  $2.4 \times 10^6 \text{ dm}^3 \text{ mol}^{-1} \text{ s}^{-1}$  reflects this.

A study of lower concentration PCH - 0.6mM - also showed mono-exponential decays across all wavelengths 360 - 400nm. Fitting curves gave a rate constant of  $2.4 \pm 0.3 \times 10^5 \text{ s}^{-1}$ . The maximum transient in this case was much smaller, a delta OD value of 0.06.

Interestingly, for the lower concentration case, the maximum transient absorption was between 360 and 365nm, 10nm lower than the higher concentration case. This experiment was repeated twice, giving the same graph in each case. This shift indicates that for low and high concentration experiments a different transient is being observed.

Experiments on low (*i.e.*  $\sim 10^{-1}$  mM) and high (*i.e.*  $\sim 10^1$  mM) concentration samples were carried out to examine what was causing this effect. There were two possibilities - that at high concentration, PCH was forming a ground state complex, E-E, (E=enone) which when excited formed an excimer, - or that the triplet enone was dimerising with another ground state to form E-E\*.



or



Ground state aggregation was studied using two methods - varying concentration across the range of interest, and looking for deviation in Beer-Lambert law; and variation of concentration and looking for any change of shift in  ${}^1\text{H}$  NMR. Both these experiments showed no indication of ground-state aggregation - a plot of absorbance against concentration ( $0.05\text{mM} < [\text{PCH}] < 0.02\text{M}$ ) gave a straight-line fit. ( $R^2 = 0.9993$ ). (Fig. 2.15)  ${}^1\text{H}$  NMR of varying concentrations in  $d_3\text{-MeCN}$  ( $0.5\text{mM} < [\text{PCH}] < 0.02\text{M}$ ) showed no shift in any peaks in the spectrum. (Fig. 2.16)

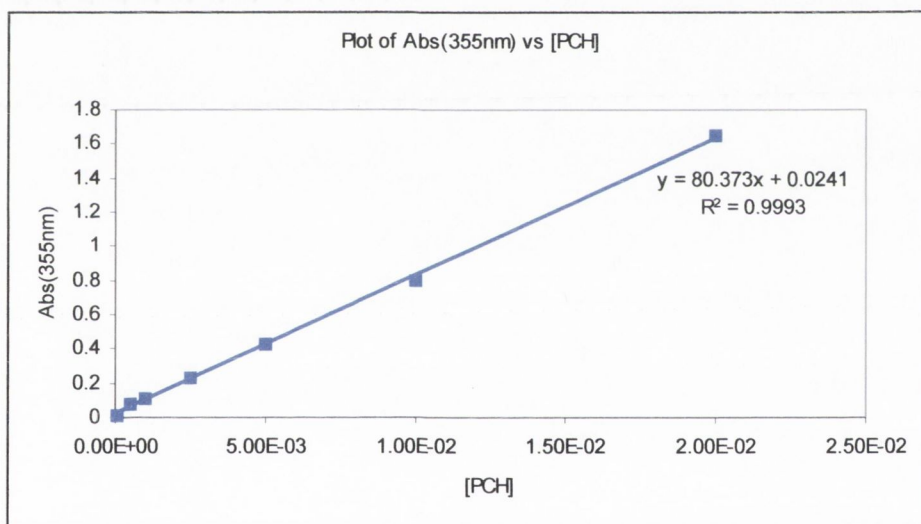


Fig. 2.15: Plot of Absorbance at 355nm as a function of [PCH]

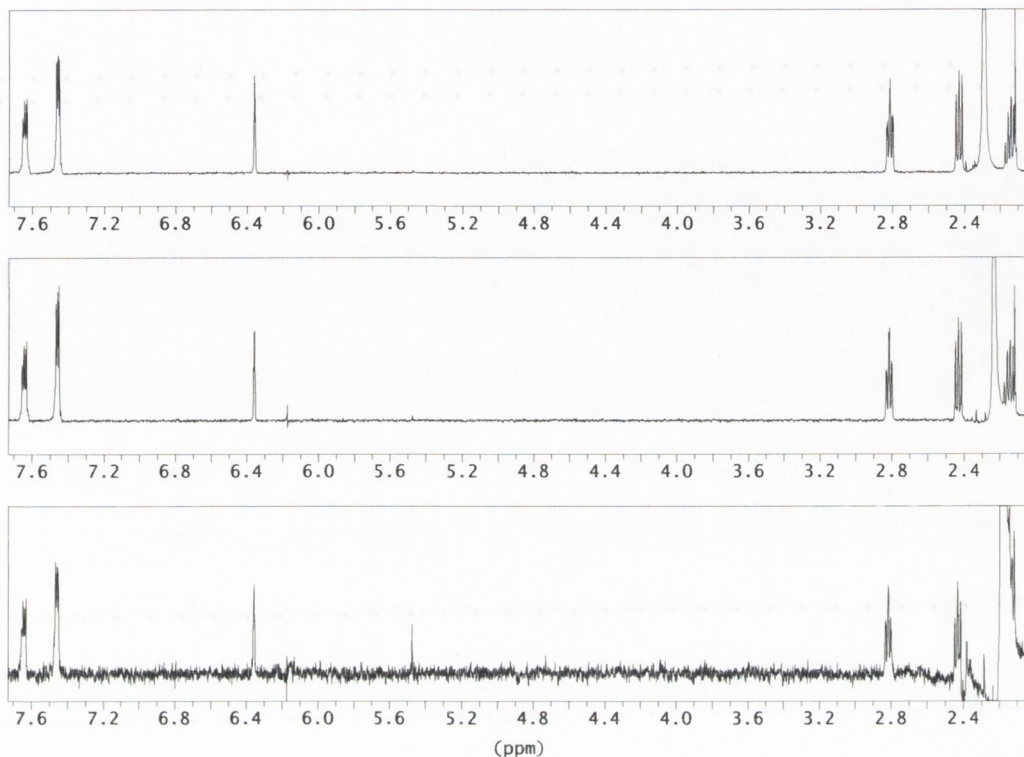


Fig. 2.16:  $^1\text{H}$  NMR of high (10mM), medium (2mM) and low (0.5mM) [PCH]

## 2.2.3 Infrared Spectroscopy

### 2.2.3.1 Ground-State Infrared Absorption Spectrum

The infrared spectrum of PCH in acetonitrile (Fig. 2.17) shows the carbonyl band at  $1666\text{cm}^{-1}$ . The extinction coefficient  $\epsilon_{\text{C=O}}$  is calculated as  $900\text{ dm}^3\text{mol}^{-1}\text{cm}^{-1}$ . The band at  $1607\text{cm}^{-1}$  is assigned to the C=C stretch, enhanced due to its conjugation with the carbonyl bond. Bands at  $1575$  and  $1498\text{cm}^{-1}$  are assigned to the phenyl ring stretches. All bands appearing in the spectrum are given in Table 2.4 with tentative assignments.



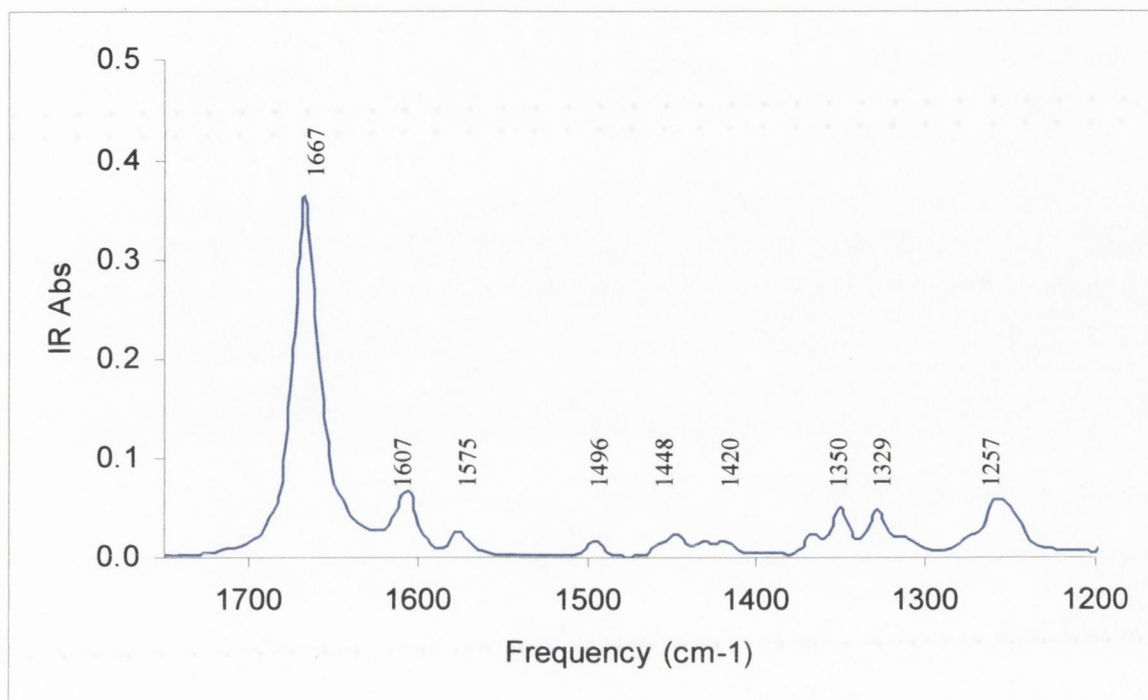


*Fig. 2.17: Infrared absorption spectrum of PCH (10mM)*

*Table 2.4: Assignments of bands appearing in IR absorption spectrum (Fig. 2.17)*

Frequency (cm <sup>-1</sup> )	Assignment
1667	Carbonyl bond
1607	Enone C=C bond
1575	Phenyl C-C
1496	Phenyl C-C
1448	Cycloalkane C-C
1420	Unassigned
1350	Cycloalkane C-C
1329	Cycloalkane C-C
1257	Unassigned

2.2.3.2 *Excited-State Infrared Absorption Spectrum* Photolysis of PCH (10mM) in deuterated acetonitrile at 355nm gave the excited spectrum shown. (Fig. 2.18) All bleaching peaks match with the ground state spectrum, indicating that there is a temporary disappearance of ground state species. In addition, several positive peaks were observed. In all spectra recorded for this compound, the peak at  $1488\text{cm}^{-1}$  was consistently the most intense band.

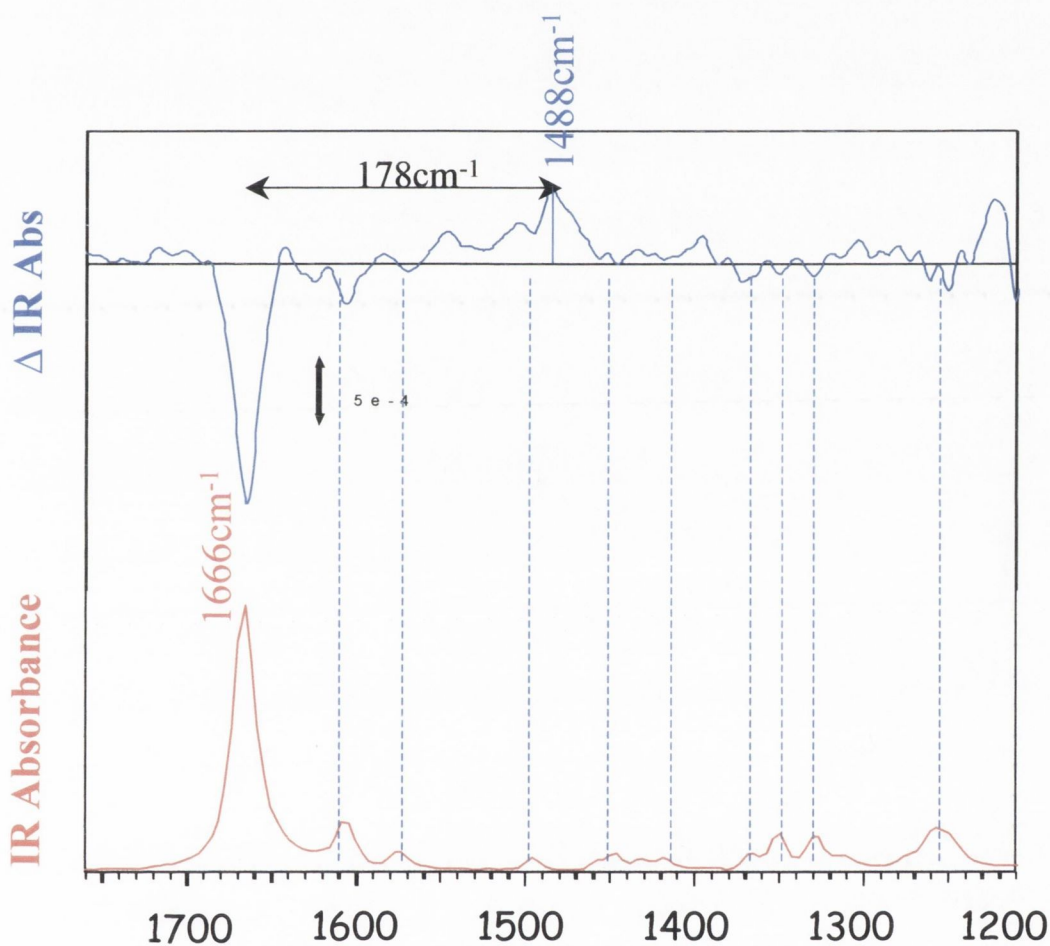


Fig 2.18: Ground state (bottom) and excited state (top) infrared absorption spectra of PCH (10mM) Bleaching peaks in the excited state spectrum are marked with the corresponding peaks in the ground state spectrum

In addition, the kinetics of decay (see below) equated with those of the excited state as measured by flash photolysis. For these reasons, (intensity and kinetics of decay) this peak was assigned as the excited state carbonyl frequency. The difference between the ground state bleach and this transient band is  $178\text{cm}^{-1}$ .

*2.2.3.3 Number of scans* The spectra below show the effect of varying number of scans. Spectra taken after 12, 32 and 44 scans are shown. (*Fig. 2.19*) Increasing the number of scans increases signal to noise ratio, although the effect is small - the signal to noise ratio increases with the square root of the number of scans.



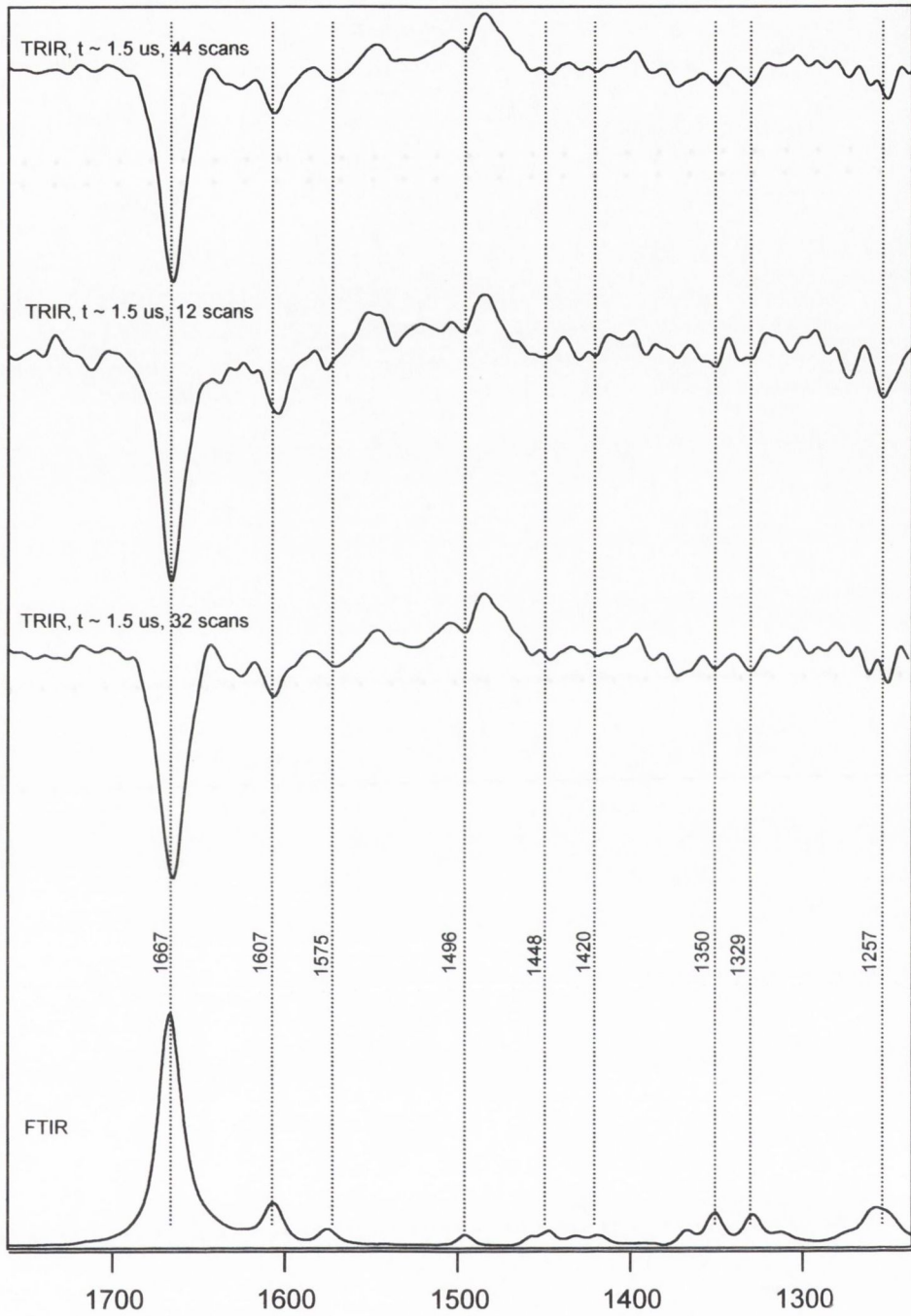


Fig. 2.19: Effect on spectral resolution of varying number of scans: Top 44 scans; centre 12 scans and bottom 32 scans

2.3.3.4 *Varying Resolution* The effect of varying resolution was also examined. Higher resolution requires that the moving mirror in the FTIR interferometer takes a greater number of steps, therefore increasing the signal to noise ratio. The lower and higher resolution spectra are shown in Fig. 2.20. Little extra information is obtained, but it is useful in terms of experimental design to compare the spectra.

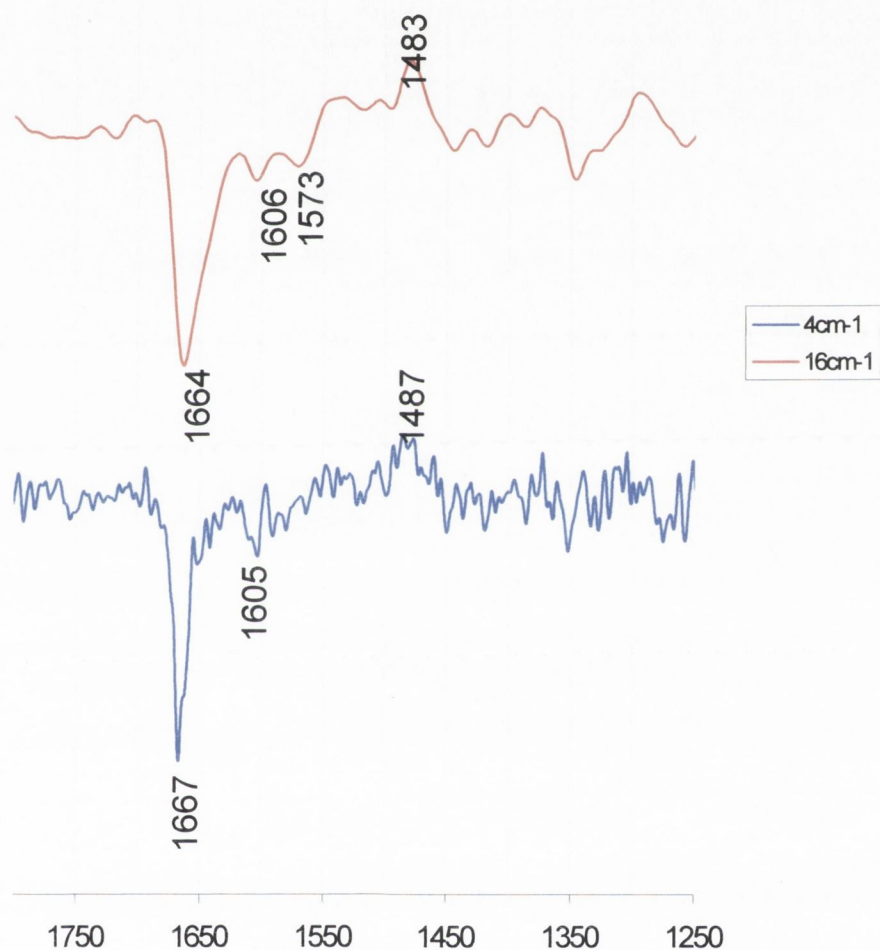


Fig 2.20: Effect of resolution on spectral quality - top 16cm<sup>-1</sup> and bottom 4cm<sup>-1</sup> resolution

The  $4\text{cm}^{-1}$  spectrum is the result of 36 scans, requiring 36 hours collection time. The spectrum is of poor quality, and it is only by comparing it to lower resolution work that peaks of interest can be identified. The  $8\text{cm}^{-1}$  spectrum (Fig. 2.16) is the result of 44 scans, requiring 22 hours collection time. The quality of the spectrum is adequate - bleaching peaks can be easily identified and the main transient peak can be assigned. The  $16\text{cm}^{-1}$  spectrum is the result of 16 scans, requiring just 4 hours data collection time. Bleaching peaks are clear as are the main and other transient peaks. This indicates that excited state IR spectra can be obtained with relative ease at this resolution.

*2.2.3.5 Decay Kinetic Profiles* TRIR spectra are three dimensional, and the decay of any peak as a function of time can be plotted. Therefore it is possible to fit curves and obtain kinetic data. (Table 2.5) The recovery of the ground state carbonyl and the decay of the excited state band at  $1488\text{cm}^{-1}$  are plotted below. (Fig. 2.21) By flash photolysis standards, they are noisy and therefore will have large errors associated with the rate constants derived from them. Nevertheless, it appears that recovery and decay profiles are approximately equal, apart from the  $16\text{cm}^{-1}$  spectrum. This is surprising, given that there is less noise associated with this spectrum, but it may be due to the fact that fewer averages were taken.

Table 2.5: First order decay constants for PCH (10mM) of parent bleach ( $1666\text{cm}^{-1}$ ) and excited state peak ( $1488\text{cm}^{-1}$ )

	$k_{\text{rec}} (1666\text{cm}^{-1})$	$k_{\text{dec}} (1488\text{cm}^{-1})$
$4\text{cm}^{-1}$	$9.7 \pm 1 \times 10^5 \text{s}^{-1}$	$1.0 \pm 0.5 \times 10^6 \text{s}^{-1}$
$8\text{cm}^{-1}$	$8.6 \pm 1 \times 10^5 \text{s}^{-1}$	$8.8 \pm 1 \times 10^5 \text{s}^{-1}$
$16\text{cm}^{-1}$	$5.2 \pm 0.5 \times 10^5 \text{s}^{-1}$	$1.9 \pm 2 \times 10^5 \text{s}^{-1}$

*2.2.3.6 Dimerisation* An FTIR spectrum of the reservoir containing the sample being analysed was taken after the experiment. No dimer peaks were observed. This indicates that dimerisation is unfavourable, a result previously observed by  $^1\text{H}$  NMR spectroscopy.<sup>4</sup>



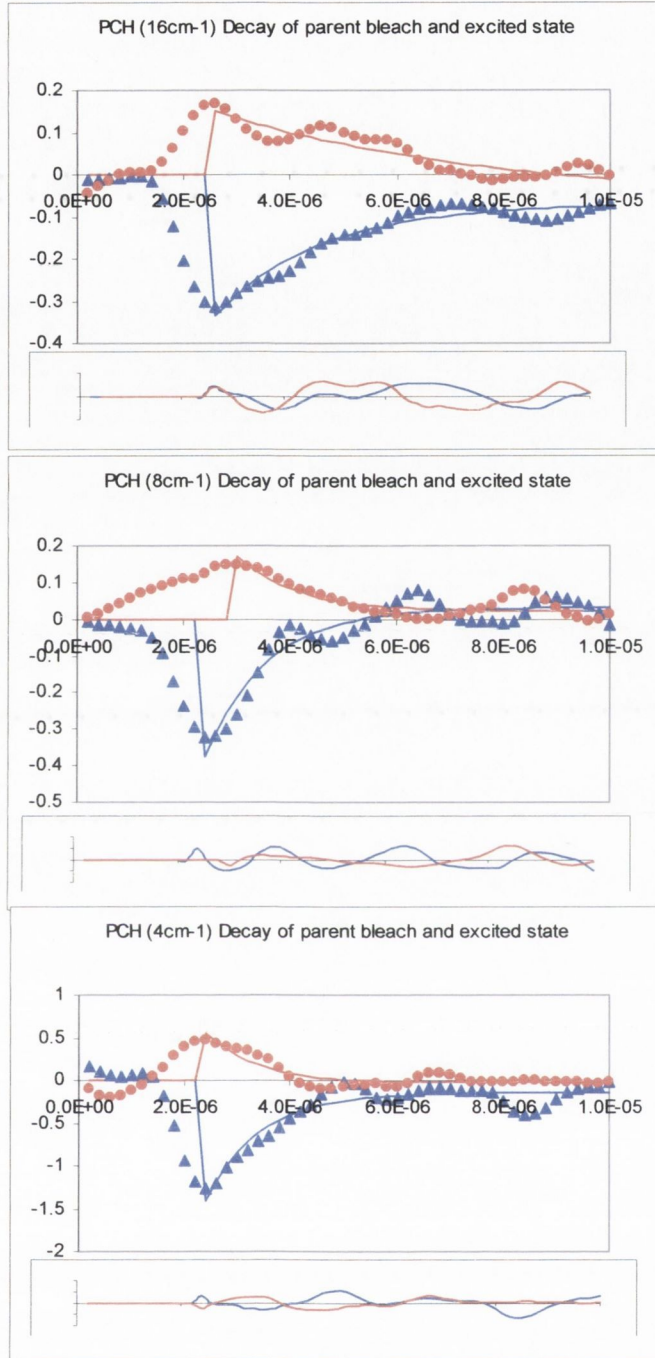
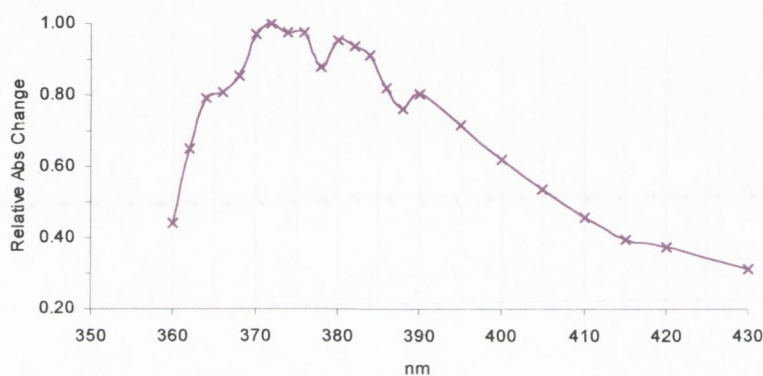


Fig. 2.21: Decay profiles, best fits and residuals for parent bleach(▲) and excited state(●) at different resolutions From top:  $16\text{cm}^{-1}$ ,  $8\text{cm}^{-1}$  and  $4\text{cm}^{-1}$ . Solid lines represent best fit lines according to the expression  $f(x) = a + b.\exp(-kt)$  and residuals from these traces are shown underneath

## 2.2.4 The Photolysis of PCH and trans-1-Phenylpropene (1PP)

**2.2.4.1 Laser Flash Photolysis** The transient absorption spectrum immediately after laser flash (*Fig. 2.22*) of PCH (10mM) and 1PP (10mM) was similar to that of 10mM PCH, indicating that the transient being monitored was probably the same in both cases. Again some fine structure is apparent, but within margin of error it is difficult to say if it is real. The decay trace was fitted to a mono-exponential fit, giving a decay rate of  $1.0 \pm 0.1 \times 10^6 \text{ s}^{-1}$ , across all wavelengths.



*Fig. 2.22: Transient absorption spectrum of PCH (10mM) in the presence of 1PP (10mM) immediately after laser flash.*

Finally, rates of decay of the transient enone (10mM) against varying concentrations of 1PP ( $1\text{mM} < [1\text{PP}] < 30\text{mM}$ ) were examined. The results were plotted, and the data fitted to a straight line. (*Fig. 2.23*) The slope of the line was found to be  $2.9 \times 10^7 \text{ dm}^3 \text{ mol}^{-1} \text{ s}^{-1}$ , corresponding to the rate of quenching by the alkene. A value of  $3.3 \times 10^7 \text{ dm}^3 \text{ mol}^{-1} \text{ s}^{-1}$  was reported previously for a dilute solution.<sup>5</sup>

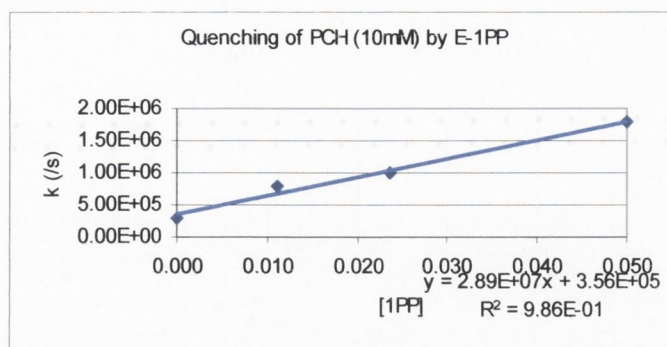


Fig. 2.23: Effect on decay rate of PCH (10mM) on increasing alkene concentration

2.2.4.2 *Time-Resolved Infrared Spectroscopy* Initial work carried out on his experiment was at  $8\text{cm}^{-1}$  resolution, with PCH (10mM) and 1PP (10mM). At that time, software and computer capability meant that kinetic traces could not be produced. The TRIR spectrum obtained is shown in Fig. 2.24. There are several features of note. The excited state band at  $1488\text{cm}^{-1}$  is still present at this relatively short timescale (600ns). The adduct band is forming ( $1695\text{cm}^{-1}$ ) (The adduct carbonyl stretch has been previously characterised in Nujol as  $1690\text{cm}^{-1}$ )<sup>4</sup> In addition, there are new bands, at  $1548\text{cm}^{-1}$  (not dominant in this spectrum but see below for  $16\text{cm}^{-1}$  work) and  $1710\text{cm}^{-1}$ .



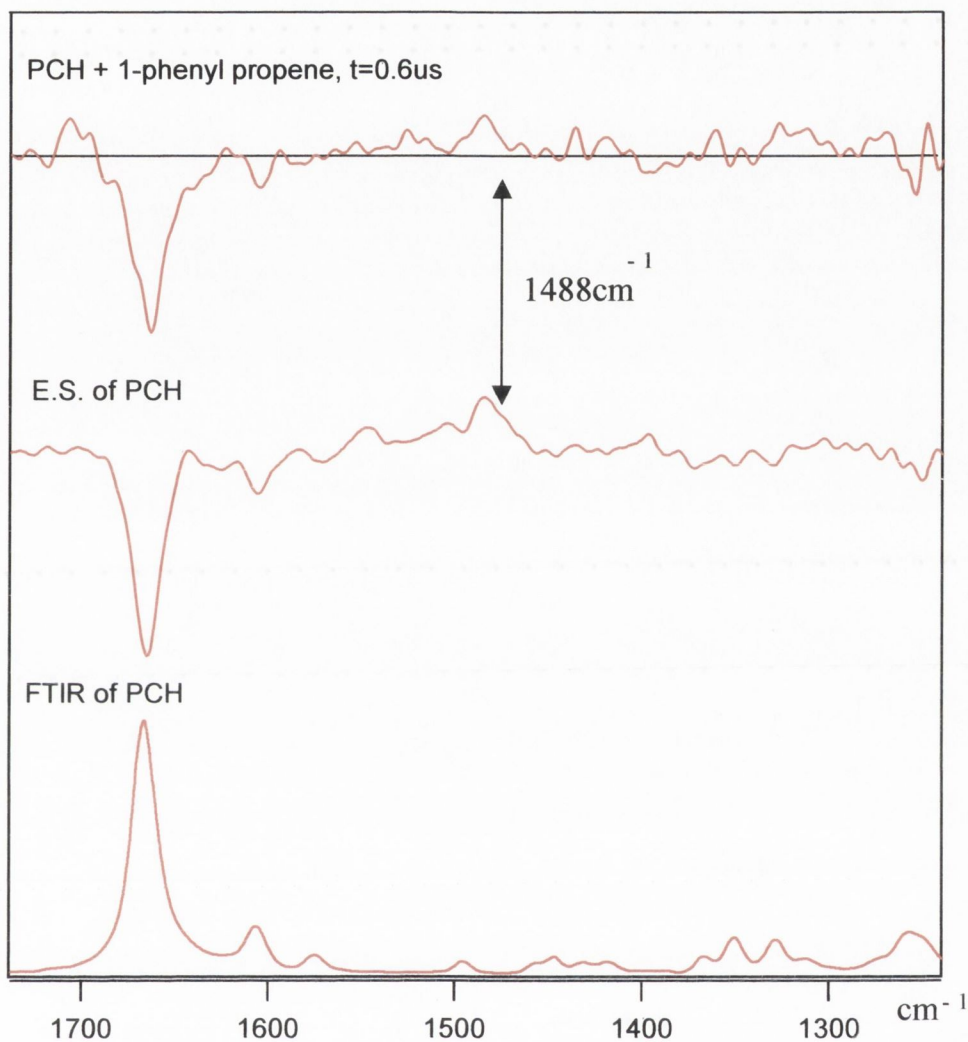
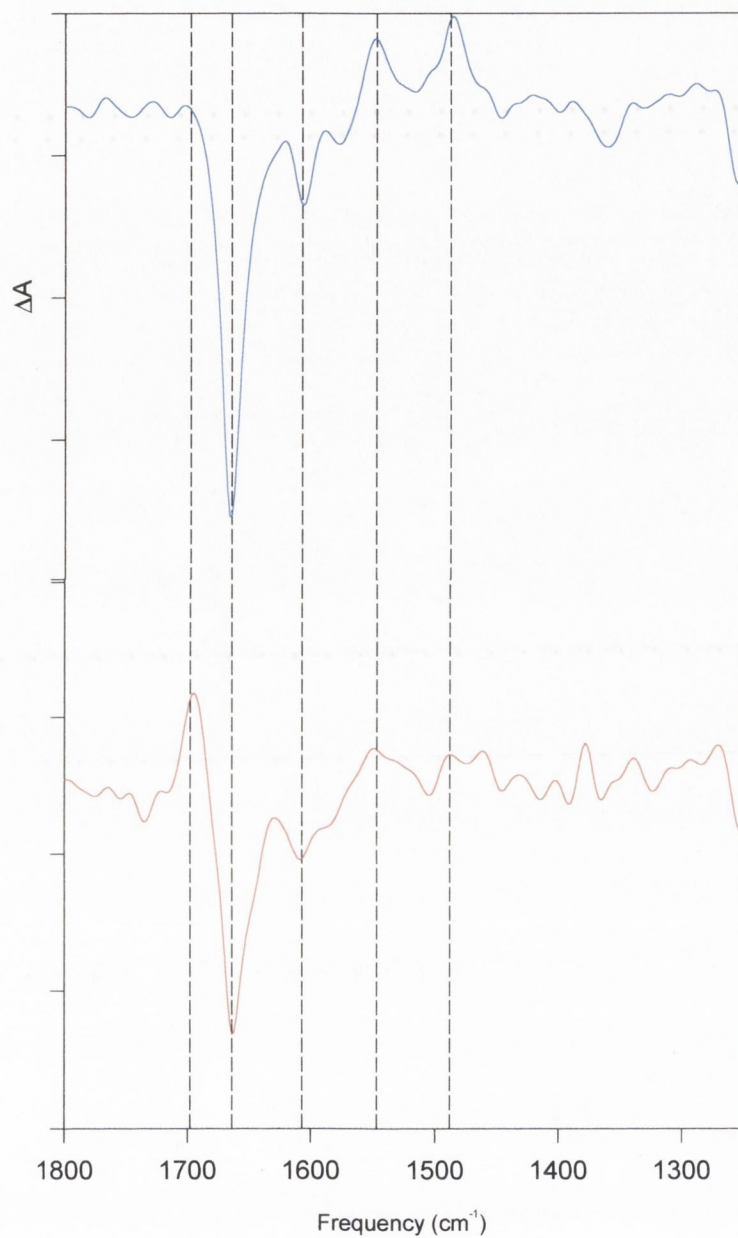


Fig. 2.24: Ground state absorption spectrum of PCH (10mM) and 1PP (10mM) (bottom), transient infrared spectrum of PCH (10mM) (centre) and transient infrared spectrum of PCH (10mM) in the presence of 1PP (10mM). All spectra at  $8\text{cm}^{-1}$  resolution

Given the success of the  $16\text{cm}^{-1}$  work for pure PCH, it was decided to continue the study of the reaction using this lower resolution. Two spectra obtained at different times are shown in Fig 2.25. At early time (250ns), the excited state peak is dominant, along

with the peak at  $1548\text{cm}^{-1}$  observed in the  $8\text{ cm}^{-1}$  spectrum. This latter peak is practically equal in intensity to the excited state peak, and is not visible in the pure PCH spectrum. This indicates the presence of a subsequent intermediate.

The spectrum at later time shows the adduct at  $1690\text{cm}^{-1}$  is now dominant, with the excited state band depleted. Unfortunately lower resolution means that the second peak in the region cannot now be distinguished.



*Fig. 2.25: Transient infrared spectrum of PCH (10mM) in the presence of IPP (10mM) 250ns (top) and 3 $\mu$ s (bottom) after laser flash. Spectral resolution is 16cm<sup>-1</sup>. Solid lines represent best fit lines according to the expression  $f(x) = a + b.exp(-kt)$  and residuals from these traces are shown underneath*



Increasing the concentration of [1PP] to 30mM results in the adduct forming on a faster timescale. (Fig. 2.26)

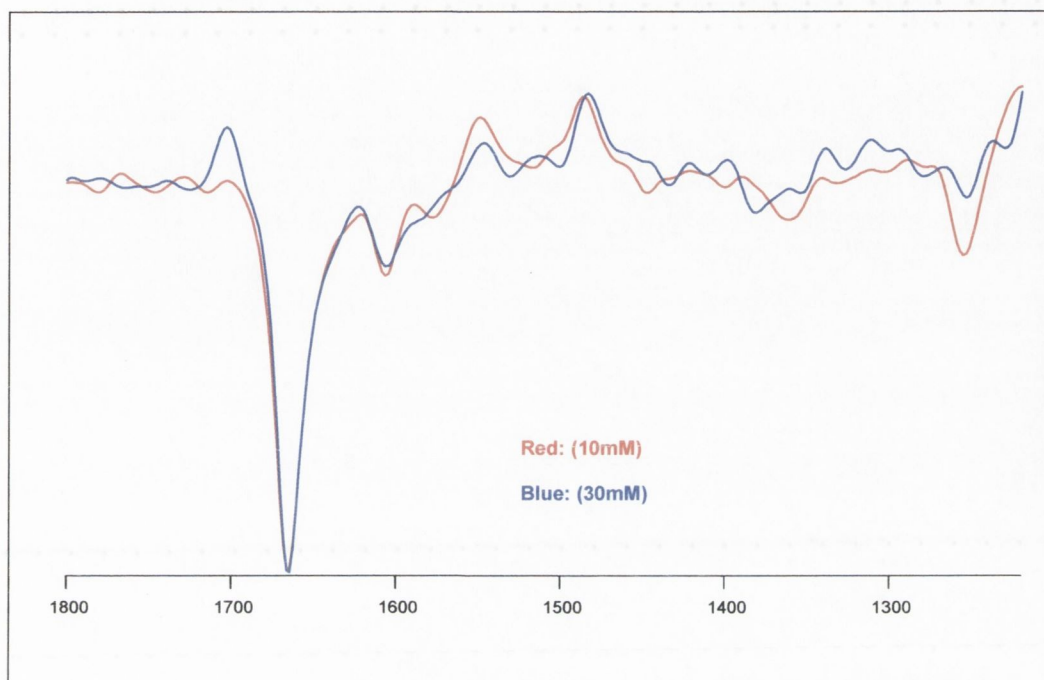


Fig. 2.26: Transient infrared spectra of PCH (10mM) and 1PP (10mM, red) (30mM, blue) 250ns after laser flash.

2.2.4.3 Decay Kinetic Profiles Again, change in intensity as a function of time of any peak of interest can be plotted. (Fig. 2.27) This is useful in this case for analysing which of the peaks are products and which are transients. Product peaks 'grow in', whereas transients decay over time. Decay rates of the transients and the recovery rate of the ground state can be fitted to exponential decays, and are given below (Table 2.6).

Table 2.6: First order decay constants for PCH (10mM) in the presence of 1PP (10mM) of parent bleach ( $1666\text{cm}^{-1}$ ), excited state peak ( $1488\text{cm}^{-1}$ ) and peak at  $1548\text{cm}^{-1}$

	$1488\text{cm}^{-1}$	$1548\text{cm}^{-1}$	$1666\text{cm}^{-1}$
$k_{\text{dec}} (\times 10^6 \text{ s}^{-1}) (\pm 10\%)$	2.2	1.4	1.4

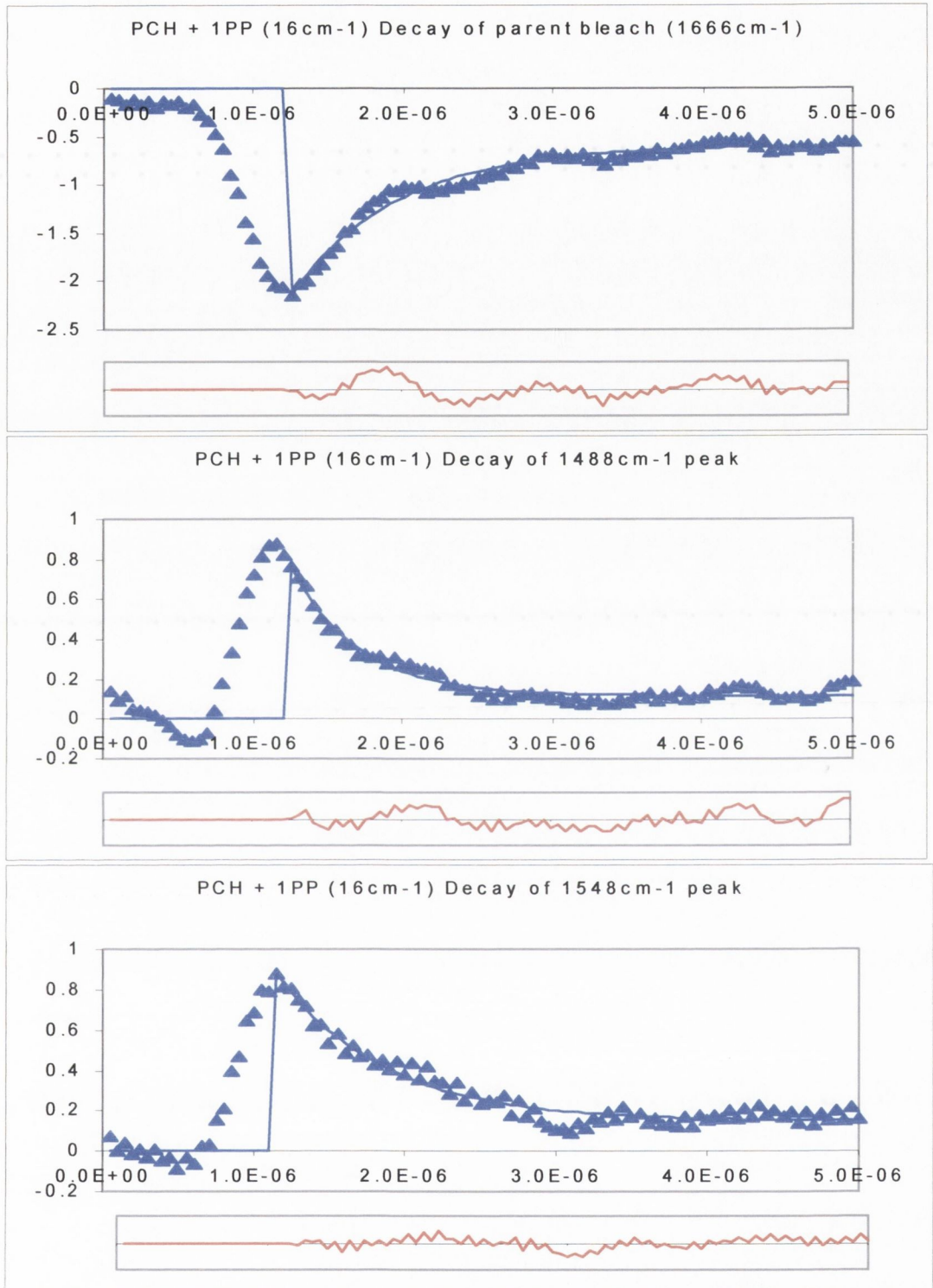


Fig. 2.27: Decay profiles, best fits and residuals for parent bleach ( $1666\text{cm}^{-1}$ , top), excited state ( $1488\text{cm}^{-1}$ , centre) and peak at  $1548\text{cm}^{-1}$  (bottom).

## 2.3 DISCUSSION

### 2.3.1 General Comments

The aims of this work were to characterise the excited state of 3-phenylcyclohexenone and its interaction with 1-phenylpropene using transient UV and IR spectroscopy. In addition, the use of S<sup>2</sup>-TRIR as a technique for studying organic excited states was examined.

Laser flash photolysis created a transient species with a broad absorption maximum. Decay traces of the transient were exponential. The transient, identified as triplet enone, is not susceptible to self-quenching. TRIR experiments require higher concentration than that for UV, and the low self-quenching rate of PCH meant that it was a suitable compound for analysis by this technique.

### 2.3.2 The Step-Scan - TRIR Experiment

*2.3.2.1 Experimental Design* Several points were noted about experimental design. The excitation wavelength was chosen where the compound absorbs weakly. If a wavelength where the compound absorbs well was used, the experiment was unsuccessful as the high UV absorbance 'shocked' the system with noise, and the relatively small IR signal could not be detected.

*Deutero-acetonitrile* was an excellent solvent for this system, and would be for other organic carbonyl compounds. It does not absorb strongly in the region of interest, and is insensitive to laser excitation. The prohibitive factor is cost - experiments were usually carried out with a 20-30mL reservoir, and for many scan-experiments this solution would need to be refreshed periodically.



In general the experiment was more successful at lower resolutions. TRIR spectra of organic compounds at higher resolution may still be some time away, from a technological point of view. Experiments at low resolution became routine after other experimental problems were overcome, and it has been shown that obtaining an excited state IR spectrum of an organic compound at low resolution can be obtained with relative ease.

### 2.3.3 TRIR Spectrum of the excited state of PCH

*2.3.3.1 Excited state spectrum* The excited state of PCH has previously been characterised as  $^3(\pi,\pi^*)$ , so it is no surprise that the shift,  $\Delta\nu$ , in carbonyl frequency on going from ground to excited state is relatively small, at  $178\text{cm}^{-1}$ . This small shift agrees well with other  $\pi,\pi^*$  systems such as 4-phenylbenzophenone ( $113\text{cm}^{-1}$ )<sup>24</sup> and 4-methoxyacetophenone ( $202\text{cm}^{-1}$ ).<sup>27</sup>

The main bleach-peaks in the  $16\text{cm}^{-1}$  spectrum are the parent (C=O) bleach at  $1664\text{cm}^{-1}$ , and C-C double bond peaks at  $1606\text{cm}^{-1}$ , and  $1573\text{cm}^{-1}$ . This spectrum shows possible peaks between  $1500$  and  $1550\text{cm}^{-1}$ . These are clearer in the  $8\text{cm}^{-1}$  spectrum and are most likely to be excited state C=C bond peaks. This is probable, given that in other experiments on aromatic ketones mentioned above (acetophenone derivatives), excited state C-C peaks appear in this region.<sup>27</sup> Of course, definitive assignment could only be achieved by experiments on  $^{13}\text{C}$  and/or  $^{18}\text{O}$  isotopomers.

The rate of self-quenching for PCH is low, at  $\sim 2 \times 10^6\text{dm}^{-3}\text{mol}^{-1}\text{s}^{-1}$ , and the TRIR spectrum reflects this. Self-quenching leading to dimerisation is not evident. No dimerisation was observed in FTIR spectra taken after experiments.

2.3.3.2 *Kinetics* The kinetics of decay of excited state and reformation of ground state are equal and are of the order of  $10^5 \text{ s}^{-1}$  for all resolutions. Decay traces of ground and excited state mirror each other, indicating that the transient is formed as a direct result of exciting the ground state. Decay curves of the ground state return to zero, verifying that little or no photo-dimer is formed.

Self-quenching of enones has been found to observe the linear equation below (Eqn. 2.1), where  $k_0$  is the rate constant at infinite dilution, and  $k_{sq}$  is the rate constant for self-quenching.

$$k_{dec} = k_0 + k_{sq} [\text{enone}] \quad \text{Eqn 2.1}$$

Comparison of IR, flash and predicted values are shown in Table 2.7.

Table 2.7: Comparison of expected and experimental results for decay rate of PCH (10mM) ( $\pm 10\%$ )

	Predicted <sup>†</sup> (CH <sub>3</sub> CN)	Flash Photolysis (CH <sub>3</sub> CN)	Decay 1664cm <sup>-1</sup> (CD <sub>3</sub> CN)
$k_{dec} \text{ (s}^{-1}\text{)}$	$2.6 \times 10^5$	$3.3 \times 10^5$	$5.2 \times 10^5$

The predicted<sup>†</sup> value and the flash photolysis value are in reasonable agreement. Flash photolysis of the enone in *d*<sub>3</sub>-MeCN gives a rate of decay similar to that found in the TRIR experiment. The lifetime of the transient is 3  $\mu\text{s}$ .

<sup>†</sup> Taking values of  $2.4 \times 10^5 \text{ s}^{-1}$  and  $2 \times 10^6 \text{ M}^{-1}\text{s}^{-1}$  for  $k_0$  and  $k_{sq}$  respectively

## 2.3.4 TRIR Study of PCH and IPP

2.3.4.1 *TRIR Spectrum and kinetics* The spectrum was initially taken at  $8\text{cm}^{-1}$  resolution. This showed product peaks forming, but little information was gleaned. It was decided to use  $16\text{cm}^{-1}$  resolution, for subsequent work, as more spectra could be acquired - giving a better signal-noise ratio. The disadvantage of using low resolution is that if transient peaks in the reaction are close together, they will not be resolved.

The ground state depletion and subsequent recovery is similar to that of the excited state – except that recovery is not complete. This is due to the fact that some of the ground state, on excitation forms adduct (quantum yield  $\sim 0.2$ )<sup>5</sup> and therefore the absorbance of the ground state is reduced slightly. The rate of recovery is measured as  $1.4 \times 10^6 \text{ s}^{-1}$ . Again, the predicted value can be calculated, as above<sup>‡</sup>. This, and the value from flash photolysis experiments on the conditions used in TRIR are given in *Table 2.8*.

*Table 2.8: Comparison of expected and experimental results for decay rate of 10mM PCH + 10mM IPP ( $\pm 10\%$ )*

	Predicted	Flash Photolysis	Decay $1664\text{cm}^{-1}$
$k_{\text{dec}} (\text{s}^{-1})$	$6.5 \times 10^5$	$1.1 \times 10^6$	$1.4 \times 10^6$

2.3.4.2 *Evidence for intermediates* As well as excited state ( $1488\text{cm}^{-1}$ ) and adduct ( $1695\text{cm}^{-1}$ ) peaks, other peaks in the spectrum appear that do not appear in the pure PCH spectrum. In the  $8\text{cm}^{-1}$  spectrum, a second peak very close to the adduct peak is visible. It is conceivable that this peak is the carbonyl stretch of the biradical intermediate species, given its intensity (indicating it is most likely due to a carbonyl stretch) and its frequency. The biradical is more "adduct-like" in structure and it would be expected that its frequency is in the adduct region. Unfortunately, on moving to

<sup>‡</sup>  $k_{\text{dec}} = k_0 + k_q[\text{Q}]$ ; where  $k_0$  and  $k_q$  are  $3.6 \times 10^5 \text{ s}^{-1}$  and  $2.9 \times 10^7 \text{ M}^{-1}\text{s}^{-1}$  for respectively



lower resolution, this peak and the adduct peak could not be distinguished, so this peak could not be further examined.

At lower resolution, a peak at  $1548\text{cm}^{-1}$  is the most dominant feature apart from the excited state. As above, it is the *intensity* of this peak that is striking. This peak, with similar frequency and decay profile to the excited state may be due to an exciplex type intermediate. Reasons for this postulation are that given the intensity of the peak, it is most likely due to a carbonyl stretching frequency that is not excited state or product - *i.e.* is some other intermediate, and the fact that it is "excited-state" like. An exciplex intermediate would have a carbonyl stretch similar to the excited state.

Nevertheless, there is no *direct* evidence for these assignments. It has been suggested<sup>29</sup> that examining the PCH-alkene reaction using 4-propenylanisole (anethole) and 4-propenylbenzotrile and the effect that the electron-donating and withdrawing substituents have on the position of these peaks relative to the excited state peaks would yield further information on the nature of these peaks.

### 2.3.5 Conclusions

- The excited state of 3-phenylcyclohexenone has been characterised by time-resolved absorption and infrared spectroscopy. The lifetime of the transient species has been measured by both techniques.
- The reaction of PCH with 1-phenylpropene has been examined by flash photolysis to obtain quenching rates and by TRIR to investigate any intermediates.
- New peaks in the reaction spectra were observed, and possible assignments are given, although further work will be required for definitive assignments.

## 2.6 References Cited

1. See for example A. C. Weedon, *Synthetic Organic Chemistry*, W. M. Horspool, Ed., Plenum Press, New York, 1984, pp 61-144; S. W. Baldwin, *Organic Photochemistry*, A. Padwa, Ed., Marcel Dekker, New York, 1981, Vol. 5, pp 123-225; H. A. J. Carless, *Photochemistry in Organic Synthesis*, J. D. Coyle, Ed., Royal Soc. Chem., London, 1986, pp 95-117.
2. R.V. Benasson, E.J. Land and T. G. Truscott, *Excited States and Free Radicals in Biology and Medicine*, Oxford University Press, New York, 1993.
3. J. F. D. Kelly, J. M. Kelly and T. B. H. McMurry, *J. Chem. Soc. Perkin Trans. 2*, 1996, 1933 and refs within.
4. T. B. H. McMurry, A. G. Murphy, D. N. Work and J. P. James, paper submitted.
5. J. F. D. Kelly, PhD. Thesis, University of Dublin, 1998.
6. E. J. Corey, J. D. Bass R. LeMahieu and R. B. Mitra, *J. Am. Chem. Soc.*, 1964, **86**, 5570.
7. R. O. Loutfy and P. de Mayo, *J. Am. Chem. Soc.*, 1977, **99**, 3559.
8. A. Rudolph and A. C. Weedon, *J. Am. Chem. Soc.*, 1989, **111**, 8756.
9. Indirect evidence has been reported. R. A. Caldwell, D. C. Hrcir, T. Munoz Jr. and D. J. Unett, *J. Am. Chem. Soc.*, 1996, **118**, 8741 report a second transient as well as enone triplet which they assign to an exciplex, Kelly *et al* (ref. 3) report a second transient independent of enone concentration.
10. B. Stuart, D.J. Ando and W. O. George, *Modern Infrared Spectroscopy*, Wiley, 1996.
11. P. Fellgett, 1st International Conference on Fourier Transform Spectroscopy, Aspen, USA, 1970, p. 139.
12. P. Jacquinot, 17<sup>e</sup> Congres du GAMS, Paris, 1954.
13. J. Connes and P. Connes, *J. Opt. Soc. Am.*, 1966, 56, 896.
14. J. P. Toscano, *The Spectrum*, (1999), 8-14
15. K. Iwata and H-o Hamaguchi, *Appl. Spect.*, 1990, **44**, 1431.

16. T. Yuzawa, C. Kato, M. W. George and H-o Hamaguchi, *Appl. Spect.*, 1994, **48**, 684.
17. M. W. George, M. Poliakoff and J. J. Turner, *Analyst*, 1994, **119**, 551.
18. M. W. George and J. J. Turner, *Coord. Chem. Rev.*, 1998, **177**, 201.
19. P. C. Ford, J. S. Bridgewater and B. Lee, *Photochem. Photobiol.*, 1997, **65**, 57.
20. X. Z. Sun, PhD. Thesis, University of Nottingham, 2000.
21. R. A. Palmer, J. L. Chao, R. M. Dittmar, V. G. Gregoriou and S. E. Plunkett, *Appl. Spect.*, 1993, **47**, 1297.
22. J. R. Schoonover, C. A. Bignozzi and T. J. Meyer, *Coord. Chem. Rev.*, 1997, **165**, 239.
23. K. M. Omberg, G. D. Smith, D. A. Kavaliunas, J. R. Schoonover, R. A. Palmer and T. J. Meyer, *Inorg. Chem.*, 1999, **38**, 951.
24. M. W. George, C. Kato and H-o Hamaguchi, *Chem. Lett.*, 1993, 873.
25. See for example Y. Wang and J. P. Toscano, *J. Am. Chem. Soc.*, 2000, **122**, 4512.
26. M. W. George, Personal Correspondence
27. S. Srivastava, E Yourd and J. P. Toscano, *J. Am. Chem. Soc.*, 1998, **120**, 6173.
28. N. C. Yang, D. S. McClure, S. L. Murov, J. J. Houser and R. Dusenbery, *J. Am. Chem. Soc.*, 1967, **89**, 5466; N. C. Yang and R. L. Dusenbery, *J. Am. Chem. Soc.*, 1968, **90**, 5899; P. J. Wagner, A. E. Kemppainen and H. N. Schott, *J. Am. Chem. Soc.*, 1973, **95**, 5604.
29. D. I. Schuster, personal correspondence with J. M. Kelly.

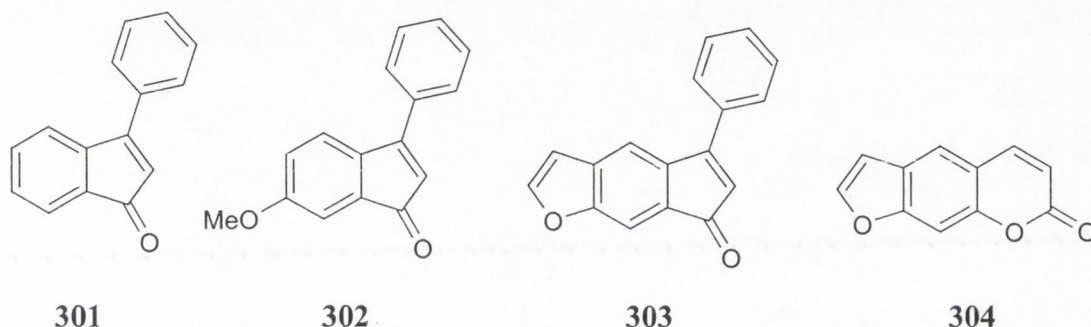


*Chapter Three*

*The Synthesis of 3-Phenylindenones*

### 3.1 INTRODUCTION

Previous workers in this laboratory have studied the photophysics and photochemistry of 3-arylcycloalkenones.<sup>1</sup> These enones are of interest from a synthetic point of view as they undergo [2+2] cycloaddition with alkenes to give cyclobutane adducts and from a photophysical point of view as they have relatively long ( $\mu\text{s}$ ) triplet lifetimes allowing their excited states to be characterised readily.



It was decided to synthesise 3-phenylindanone and derivatives, and examine the effect of the fused ring on the photochemistry and photophysics. 3-Phenylindanone (**301**) and 6-methoxy-3-phenylindanone (**302**) were the primary targets. The methoxy derivative is of interest as it is a synthetic precursor to a furanoindanone (**303**) - a compound with analogies to the phototherapeutic drug psoralen (**304**). Psoralen has two sites available for photoinduced [2+2] cycloaddition,<sup>2</sup> as does the furanoindanone. Thus the methoxy derivative, aside from the interest in examining the effects the methoxy substituent will have on the photochemistry of the indanone, is an important precursor to future work.

Literature methods for synthesis of indanones are generally in the following categories: (1) dehydrogenation of the corresponding indanone; (2) acid-catalysed ring closure of 1,3-diphenylsubstituted propanediones and (3) the annulation of 1,2-substituted alkynes by *o*-halobenzaldehyde. (*Fig. 3.1*)

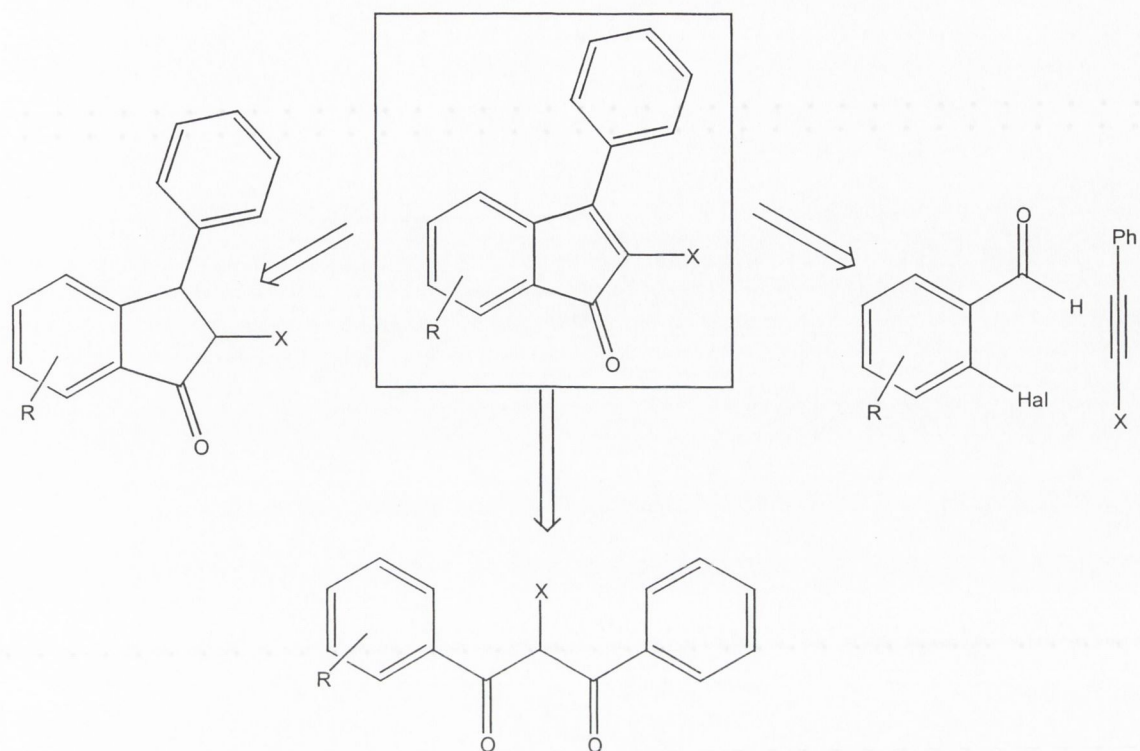


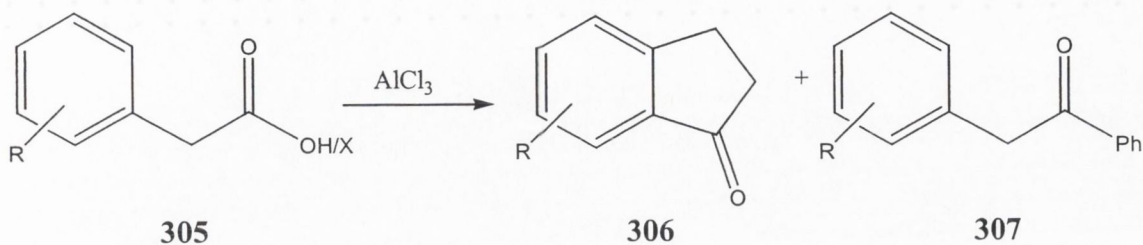
Fig.3.1: General literature procedures for synthesis of 3-phenylindanone derivatives

### 3.1.1 Synthesis of indanones

This method involves the synthesis of indanones and the subsequent dehydrogenation via oxidation or halo-dehalogenation. Methods for the synthesis of indanones are discussed below.

**3.1.1.1 Friedel-Crafts Acylation** Ring-closure of 3-arylpropionic acid or their acid chlorides give indanones. (Scheme 3.1) For example, ring-closure of 3-(*p*-methoxyphenyl)propionic acid chloride (**305**, R=6-MeO, X=Cl) gives 6-methoxyindanone (**306**, R=6-MeO).<sup>3</sup> This method was initially carried out by adding acid chloride to benzene containing excess aluminium chloride (1.7eq). This gave poor yields (21%) of 1-indanone and a side product (**307**, R=6-MeO; X=C<sub>6</sub>H<sub>5</sub>), which was formed by acid-chloride-aluminium chloride attack on solvent. Also, it appeared that aluminium chloride was complexing to the methoxy-substituent, reducing its electron-donating capacity, which would stabilise the Friedel-Crafts intermediate.

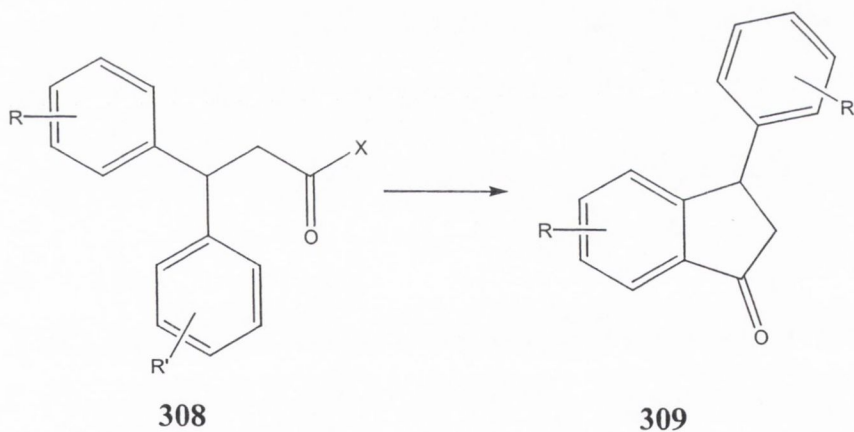




*Scheme 3.1: Synthesis of indanone from 3-phenylpropionic acid chloride*

The method was improved by adding, slowly, aluminium chloride to the acid chloride in large volumes of benzene.<sup>4</sup> In this case, 78% yields of 6-methoxyindanone were reported.

The other common reagent is polyphosphoric acid (PPA).<sup>5-8</sup> An example is the ring closure of 3-(*p*-methoxyphenyl)propionic acid to give 6-methoxyindanone. (*Scheme 3.2*)



*Scheme 3.2: Synthesis of 3-arylindanones*

3-Phenylpropionic acids containing a second 3-arylsupstituent (**308**, R=H) yield 3-arylsupstituted indanones (**309**, R=H) or 4- or 6- supstituted indanones (**309**, R = 4- or 6- supstituent, R'=H), depending on direction of ring closure.<sup>5,6</sup> (*Scheme 3.2*) **For 3,3-**

diarylpropionic acid (**308**, R, R'  $\neq$  H), the direction of ring closure depends on the substituents R and R'.<sup>5,6,9</sup>

In general, for R = electron donating group (EDG) and/or R' = electron withdrawing group (EWG), ring closure to the ring with R occurs. However, when R' = H, directed ring closure is not observed. Indeed, for R = OMe and R' = H, ring closure to the R containing ring was observed.<sup>10</sup> This is unexpected and unlikely, given that an electron donating methoxy- group would be expected to stabilise the cationic intermediate. (Fig. 3.2)

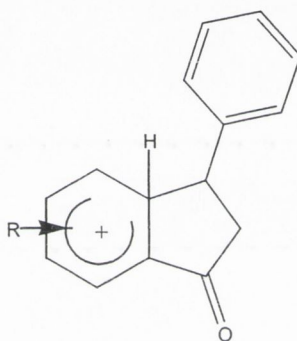
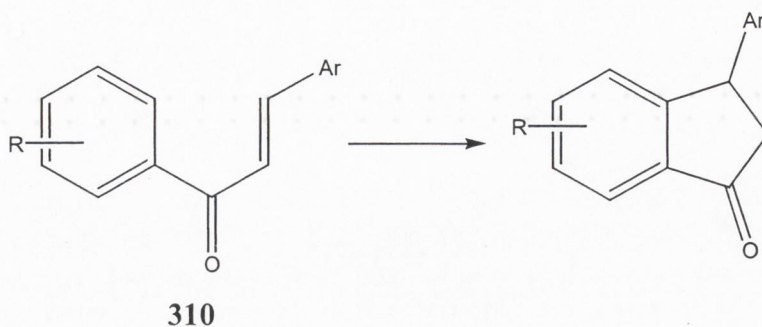


Fig. 3.2: Intermediate in propionic acid ring-closure

**3.1.1.2 Friedel-Crafts Alkylations** Ring closure of chalcone derivatives (**310**) yield indanones. (Scheme 3.3) In this case, ring-closure is dependent on the presence of an electron-donating group on the aromatic ring to which closure is occurring. This is necessary, in order to stabilise the intermediate. Chalcones inherently have an acyl (electron-withdrawing) group. Without the presence of an electron donor, ring closure does not occur. Ring-closure may occur where there is both an electron donating and electron-withdrawing group.<sup>9</sup>



*Scheme 3.3: Ring-closure of chalcone*

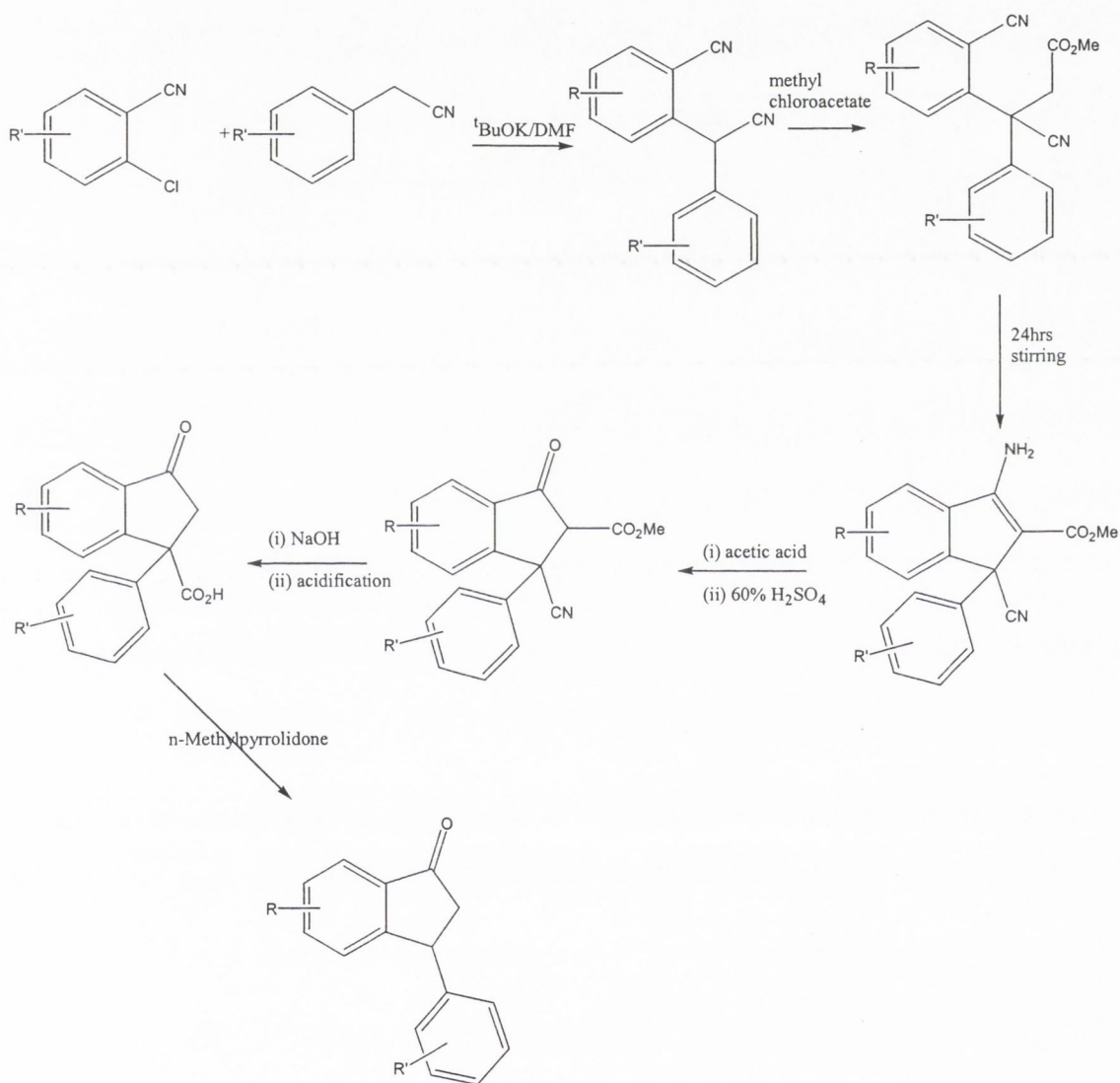
Catalysts commonly employed include protic acids - polyphosphoric, (PPA),<sup>11</sup> hydrofluoric, sulphuric and trifluoroacetic acid,<sup>12</sup> and Lewis acids - usually aluminium chloride<sup>13</sup> and boron trifluoride.<sup>14</sup> PPA is the most frequently used, and has been used to synthesise a range of 3-arylindanones.

**3.1.1.3 Acylation vs. Alkylation** The question arose of whether to use acylation or alkylation in the synthesis of the desired indanones. Acylation has the advantage that it is Friedel-Crafts 'allowed'. However, uncertainty in the direction of ring closure, and subsequent regioisomers formed on ring-closure (*i.e.* 4- or 6- isomer) meant that where possible, alkylation was favoured. Alkylations, with electron-donating groups on the ring have been reported. Ring closure can only occur to one ring - removing that degree of uncertainty. Also, electron-donating groups in the 3'-position appear to be *p*-directing, yielding the desired 6-isomer.

For these reasons, ring closure of chalcone was chosen as the preferred method for the synthesis of indanones. The chalcones themselves can be easily synthesised by aldol condensation of benzaldehyde and a substituted acetophenone,<sup>13,14</sup> a range of which are available commercially.



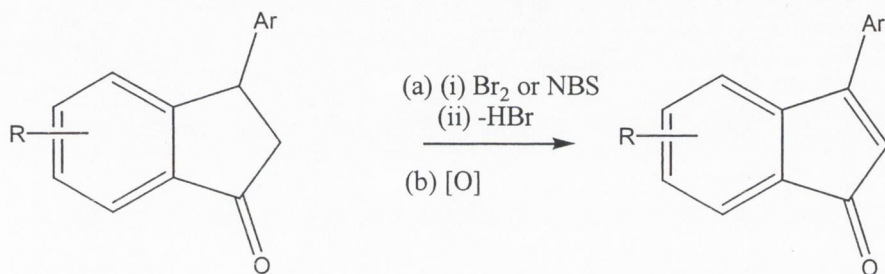
**3.1.1.4 Newer Method** A third method, described by Sommer *et al* is described in Scheme 3.4.<sup>15</sup> As other methods were available to synthesise the desired indanone, this method was not investigated further. However, this method has the distinct advantage of not being subject to restrictions of substituents as the Friedel-Crafts reactions are, and many 4- and 6- halo substituted indanones were reported. Another advantage is that it is regioselective. The only limitation is whether or not the precursors can be synthesised.



Scheme 3.4: Alternative route to 3-arylidanones as described by Sommer *et al*<sup>15</sup>

### 3.1.2 Indenones from indanones

There are relatively few references in the literature for 2-unsubstituted-3-substituted indenones. Of those formed from the corresponding indanone, the majority of reports use bromination-dehydrobromination as a means of creating  $\alpha,\beta$ -unsaturation. (Scheme 3.5)



Scheme 3.5: Two methods for creating  $\alpha,\beta$ -unsaturation

**3.1.2.1 Bromination-dehydrobromination** The bromo-dehydrobromination method has been used widely in creating  $\alpha,\beta$ -unsaturation in a range of cyclic ketones - including cortisone,<sup>16</sup> methylcyclohexenone<sup>17</sup> and many others.

Jones and Marmon<sup>18</sup> describe the synthesis of 3-methylindenone from the corresponding indanone. This was brominated by irradiating in the presence of N-bromosuccinimide (NBS) and benzoyl peroxide in  $\text{CCl}_4$ . Triethylamine was used to dehydrobrominate, giving an overall yield of 12%.

This method is based on that of Marvel and Hinman,<sup>19</sup> who used these conditions to synthesise 3-bromoindanone, which was dehydrobrominated using *sym*-collidine. (17%) It was used also by Friedrich and Tam, who synthesised 5-methyl (5%) and 5-methoxy (20%) indenone. They preferred this method over that of House and McDaniel,<sup>20</sup> who used bromine in ether - a method which creates the  $\alpha$ -bromopropyl. House does not perform dehydrobromination, and his yields of 2-bromo-6-methoxyindanone was 53%.

Other reported methods for dehydrobromination include lithium chloride in DMF,<sup>16,17</sup> lithium bromide/lithium carbonate in DMF,<sup>21</sup> and 1,8-diazabicyclo[5.4.0]undec-7-ene (DBU) in benzene, among others.<sup>22</sup>

**3.1.2.2 Oxidation** In general, oxidation of aliphatic compounds to give a double bond in a specific location is not usually a feasible process.<sup>23</sup> In the case of the conversion of indanones to indenones, however, there are two advantages: (1) only one location is available for oxidation (i.e. the  $\alpha,\beta$ -bond) and (2) the double bond formed is in conjugation with existing double bonds (C=O and phenyl group).

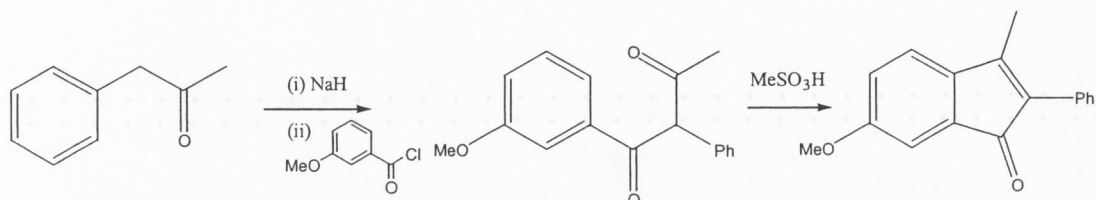
Examples of oxidising agents successfully used include selenium dioxide, used in <sup>t</sup>BuOH which was employed in the selective  $\alpha,\beta$ -oxidation of a steroid.<sup>24</sup> Selenium dioxide has also been used to dehydrogenate 1,4-diketones<sup>25</sup> and 1,2-diarylalkanes. In all cases, the double bond being formed is in conjugation with an existing double bond.

Cyclopentenone has been dehydrogenated to the corresponding enone by palladium chloride,<sup>26</sup> ferric chloride<sup>27</sup> and benzene selenic anhydride.<sup>28</sup> Thiessen has used palladium chloride to oxidise a range of cyclo and bicycloalkanones to the corresponding  $\alpha,\beta$ -alkenones.<sup>29</sup>

### 3.1.3 Indenones from propanedione derivatives

This method provides an elegant route for the making of 2,3-disubstituted indenones, although the synthesis of 3-substituted compounds has not been reported using this method. The synthetic method involves condensation of the 1-arylpropan-2-one derivative with, for example, *m*-anisic acid chloride to give the 1,2-diaryl-3-substituted propanedione. (*Scheme 3.6*)



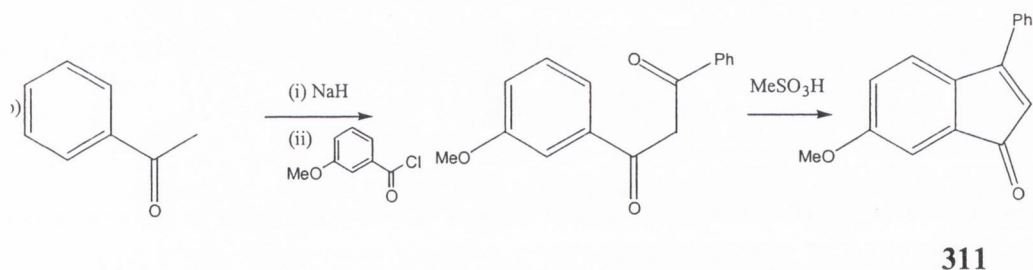


Scheme 3.6: Example of Anstead synthesis (a) and modified method to synthesis 3-substituted indenones(b)

One-pot ring closure and dehydration with methanesulfonic acid<sup>30</sup> gives 2-aryl-3-substituted indenones. Anstead synthesised a broad range of indenones using this method,<sup>31-32</sup> but in all cases they were (1) 2-aryl-3-substituted (e.g. 3-alkyl) and (2) all disubstituted - no 2-unsubstituted compounds were synthesised.

### 3.1.4 Routes devised for synthesis of 3-phenylindenones.

For the synthesis of indenones **301** and **302**, both the Friedel-Crafts alkylation method and a modified Anstead method were used (Fig. 3.3). The third method described, annulation of alkyne derivatives was not attempted.



Scheme 3.7: Modified Anstead method for synthesis of 3-phenylindenones

The modified Anstead method is shown in Scheme 3.7. It involves the condensation of acetophenone and *m*-anisic acid chloride to give the 1,3 diarylpropanedione and subsequent ring closure-dehydration to give the desired indenones.

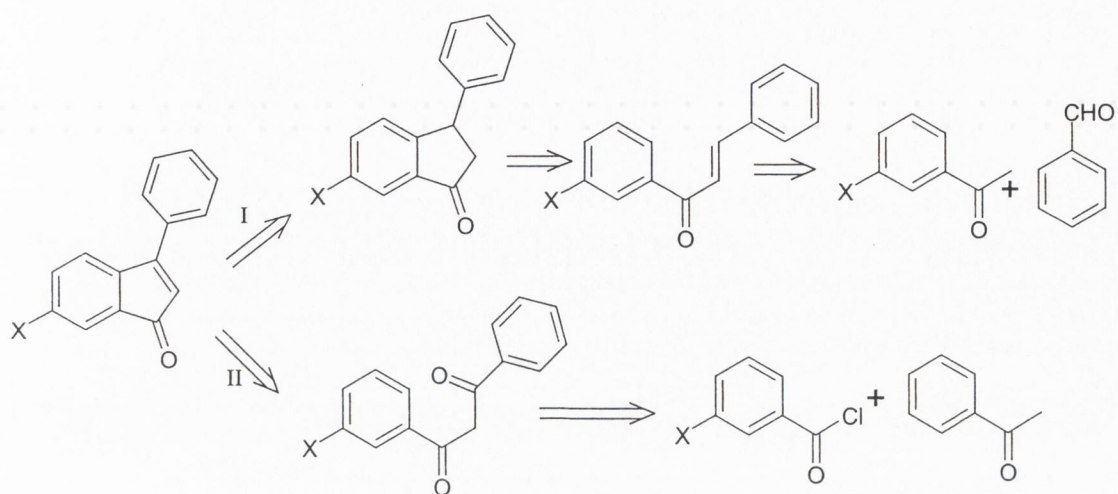


Fig. 3.3: Retrosynthetic analysis showing possible routes to indenones ( $X=H, OMe$ )

appearance of product spots. On working up, the product was a sticky tar, which was only partially soluble in dichloromethane. Both the insoluble 'tar' and the solution were analysed. The IR spectrum of the solution contained a carbonyl peak at  $1684\text{cm}^{-1}$ , whereas the indanone product was expected to have a value of  $1700 - 1720\text{cm}^{-1}$ . (cyclopentanone fused to benzene ring) Also, the  $^1\text{H}$  NMR – which was complicated – showed the absence of a methoxy peak – expected at  $\sim 4.0\text{ppm}$ . The IR and  $^1\text{H}$  NMR spectra of the tar did not show peaks which were expected of the indanone. This experiment was repeated, again unsuccessfully, and was abandoned.

#### *Sulfuric Acid*

Sulfuric acid was added to a solution of chalcone in cyclohexane. Again a 'tar' was obtained on work-up. The IR spectrum of the extracted compound (brown powder) gave a carbonyl bond stretch of  $1675\text{cm}^{-1}$ . The method was abandoned.

#### *Titanium Tetrachloride*

Titanium tetrachloride was added to the chalcone in dichloromethane. The mixture was refluxed for 24 hours, but only starting material was obtained on work-up. The reaction was repeated in toluene, to allow a higher reflux temperature, but again, starting material was recovered.

#### *Boron Trifluoride*

Murphy *et al*<sup>14</sup> describe this reaction using boron trifluoride diethyl etherate as a catalyst for ring closure. The experiment was repeated under their conditions (nitromethane, three days at room temperature). The IR spectrum of the crude product showed a carbonyl stretch at  $1705\text{cm}^{-1}$ . This is the expected frequency for the indanone carbonyl bond.  $^1\text{H}$  NMR showed three sets of double doublets, corresponding to the  $\alpha$ - and  $\beta$ -hydrogens of the indanone (ABX system). Although this reaction worked, yields were low, with a by-product being dominant. This by-product precipitated out on work-



up. Analysis by  $^1\text{H}$  NMR showed it contained no aliphatic protons. We have not identified it.

A suggestion by Murphy<sup>33</sup> that we incorporate acetic anhydride in the reaction mixture (based on work by Vyas *et al*<sup>34</sup>) gave rise to increased yields and a cleaner reaction.

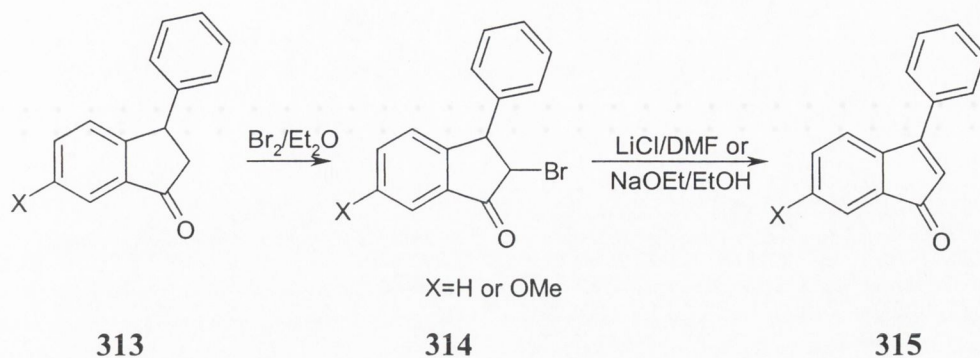
### *Trifluoroacetic Acid*

Johnson *et al*<sup>35</sup> has described ring closure of a methoxy chalcone using trifluoroacetic acid as catalyst. In repeating his method at room temperature, but at these conditions only minimal conversion was observed, and the route was initially abandoned. But after difficulties with boron trifluoride, (see above), the reaction was modified. Refluxing the chalcone in neat TFA for 18 hours gave the desired product in modest to good yields. Purification by column chromatography (dichloromethane) gave the indanone as a pale yellow powder.

Ring closure of *trans*-chalcone (formed by condensation of acetophenone and benzaldehyde) failed using the conditions used for the methoxy derivative. However 3-phenylindanone, the precursor to **301** is available commercially or can be synthesised by ring-closure of 1,3-diphenylpropionic acid using polyphosphoric acid.<sup>35</sup>

## **3.2.2 Bromination of indanones**

**3.2.2.1 Bromine** This method involved the synthesis of an  $\alpha$ -bromo-derivative followed by dehydrobromination to the indenone (*Scheme 3.9*).



*Scheme 3.9: Synthesis of indenone via bromo intermediate*

House *et al* used bromine in ether to make 2-bromoindanone<sup>20</sup> and his method was used to synthesise 2-bromo-6-methoxy-3-phenylindanone. This reaction goes easily (1 hour at 0°C).

The <sup>1</sup>H NMR of the crude product shows that α-bromination has occurred, as reported by House. This is confirmed by a hmqc spectrum, which shows that the two aliphatic protons in the molecule are on different carbons. The compound can be isolated by crystallising in ether, and purified by recrystallisation (ether).

In the overall reaction scheme (chalcone to indenone) this recrystallisation step was a useful point for purification of the 6-isomer from traces of the 4-isomer. The 4-isomer is formed by ring-closure to the carbon *ortho* to the methoxy, whereas the desired product is formed (preferentially) by ring-closure to the carbon *para* to the methoxy substituent. Thus, the 6-isomer is the dominant product, the 4-isomer being formed in negligible amounts. In the <sup>1</sup>H NMR of the crude bromo-mix, as well as the pair of doublets corresponding to the 6-isomer, (α- and β-H), there was a second pair of doublets, downfield, which were assigned to the 4-isomer. These protons were also on different carbons (hmqc), so they can be only assigned to the 4-isomer. The by-product could not be the 3-bromo-compound. We found that crystallisation at this point gave access to the pure 6-isomer. It is necessary to eliminate the by-product at this stage, as attempts to remove the 4-methoxyindenone from its 6-isomer proved extremely difficult. Obviously

for any photophysical work, the presence of a small amount of compound with similar characteristics to the one undergoing study would produce erroneous results.

Bromination of the parent indanone (3-phenylindanone) proved to be much slower than of the methoxy-derivative, requiring longer reaction times. The compound did not crystallise out in ether, and required chromatography for purification.

**3.2.2.2 *N*-bromosuccinimide** There are several references in the literature to the bromination of cycloalkanones using NBS.<sup>36</sup> We studied several conditions with the indanone system: NBS + UV; NBS + peroxide + UV and NBS + peroxide + reflux - all with varying reaction times. In general, reactions did not proceed or proceeded to give unidentified products. This method was discarded in favour of bromination using bromine itself.

### 3.2.3 Dehydrobromination

**3.2.3.1 *Lithium Chloride/DMF*** Lithium chloride has been used to dehydrobrominate  $\alpha$ -brominated cycloalkanones, such as  $\alpha$ -bromocortisone.<sup>16</sup> The bromoindanone synthesised above was dissolved in refluxing DMF, and lithium chloride added. The mixture turned red with time. Work up gave the desired indenone, together with unreacted bromo-compound. The mixture could be separated by column chromatography. Longer reaction times and/or addition of more lithium chloride did not increase yields.

Dehydrobromination of 2-bromo-3-phenylindanone could not be effected under the conditions described above.



**3.2.3.2 Sodium ethoxide/ethanol** Sodium ethoxide in ethanol was also used to dehydrobrominate the methoxyindanone, although by-products were feared. However, these did not materialise, and the reaction proceeded quickly (starting material spot not visible on TLC after one hour at 80°C) and gave moderate yields of the indenone. Purification by column chromatography (dichloromethane) gave the indenone as a red powder. Samples contaminated with the 4-isomer could be incompletely separated by chromatography (3:2 dichloromethane:hexane).

This method was not attempted for the parent indanone, as oxidation (below) was used instead.

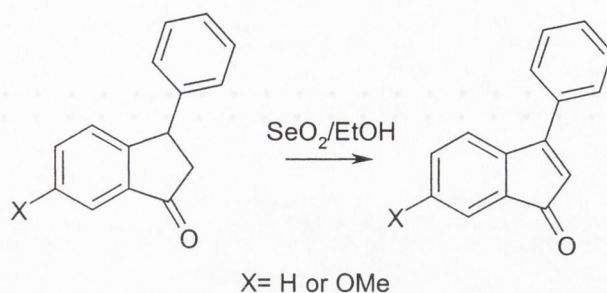
### **3.2.4 Oxidation of indanones to indenones**

Dehydrogenation can also be effected with an oxidising agent, and some palladium based<sup>26</sup> and selenium based<sup>25, 28</sup> catalysts have been described. Reactions usually involve the double bond to be formed in conjugation with an existing double bond.

With both parent and methoxy substituted indenone, the sample was dissolved in <sup>t</sup>BuOH and selenium dioxide added. After refluxing for three to seven days only starting material and product could be observed, and the latter obtained in modest yields. (*Scheme 3.10*).

For the methoxy-compound, yields of 20-30% were obtained, after 3 days. No other side products were observed. The two compounds (reactant and product) could be separated by chromatography, and the reactant recycled.

For the parent compound, yields of ~20% were obtained after seven days. The reaction was repeated in ethanol, giving similar results, and ethanol was chosen as the solvent of choice, as it was more easily purified and the reaction more easily worked up.

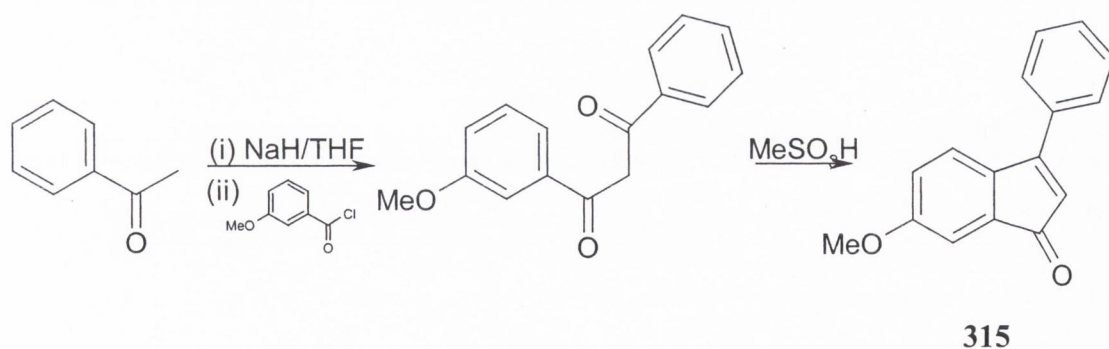


*Scheme 3.10: Synthesis of indenone by direct oxidation*

Yields of the indenone were ca. 20%, but chromatography (100% dichloromethane) isolated both product and starting material, and the latter could be recycled.

### 3.2.5 Modified Anstead Method

**3.2.5.1 Attempts to synthesise 6-methoxy-3-phenylindenone** Difficulties in the synthetic route described above prompted a rethink of synthetic strategy. Anstead synthesised 2,3-diphenyl indenone derivatives from 1,2,3-triphenylpropanediones, involving ring closure and dehydration using methane sulfonic acid in a one-pot synthesis.<sup>31, 32</sup> This two-step synthesis from simple starting materials appeared attractive, and a scheme to synthesise 6-methoxy-3-phenylindenone was devised. (*Scheme 3.11*)



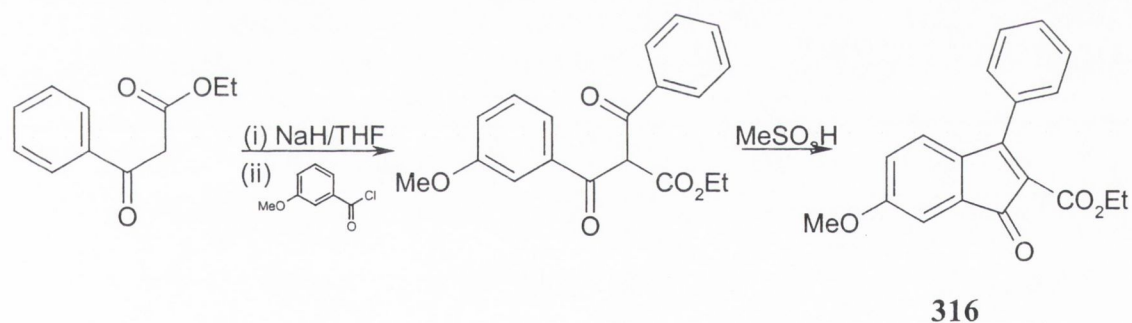
*Scheme 3.11: Proposed two-step synthesis following method of Anstead et al<sup>8</sup>*

The method involved condensation of anisoyl chloride and acetophenone to afford the dione, ring closure of which with acid would lead to the desired product. The formation

of the dione did not work using Anstead's conditions, but slower addition of the acid chloride to the acetophenone/sodium hydride mixture and longer reaction time gave 1-methoxyphenyl-3-phenylpropanedione. Ring closure was attempted using a wide range of conditions (various temperatures and reaction times) but in all cases, only starting material was obtained.

Ring closure with boron trifluoride gave a yellow powder on work-up. This powder was not the desired indenone, though it showed all the peaks in  $^1\text{H}$  NMR corresponding to indenone but with the singlet at 7 ppm instead of the expected 6.0ppm observed (and as reported) for the  $\alpha$ -H in indenones. This compound has not been identified.

**3.2.5.2 Synthesis of 2-carbethoxyindenone ester** The above method worked well in the synthesis of 2,3-substituted indenones, and 2-carbethoxy-6-methoxy-3-phenylindenone was synthesised by this method (*Scheme 3.12*)



*Scheme 3.12: Synthesis of ester derivative*

This involved the condensation of anisoyl chloride and ethyl benzoyl acetate to give 2-carbethoxy-1-(*m*-methoxyphenyl)-3-phenylpropane-1,3-dione which ring closed easily with methanesulfonic acid. The product, as red crystals was recrystallised using hexane/ethyl acetate (10:1). Hydrolysis of this ester gave the acid 6-methoxy-3-phenylindenone-2-carboxylic acid, but attempts to decarboxylate this compound to 6-methoxy-3-phenylindenone were unsuccessful.



## Spectroscopic Analysis of Products

3.2.6.1 *NMR*  $^1\text{H}$  NMR spectroscopy was very useful in studying the reaction between chalcone and indenone, as the environment of the  $\alpha$ - and  $\beta$ - hydrogens change quite dramatically in each step. *Table 3.1* summarises the data obtained.

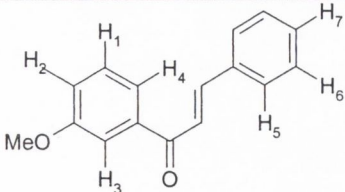
*Table 3.1:  $^1\text{H}$  NMR Data for the  $\alpha$ - and  $\beta$ - hydrogens in the reaction scheme from chalcone to indenone*

Compound	Observed Shifts for $\text{H}_\alpha$ and $\text{H}_\beta$
3'-methoxychalcone <b>312</b>	$\delta 7.5\text{ppm}$ (d), $\delta 7.8\text{ppm}$ (d)
6-methoxy-3-phenylindanone <b>313</b>	$\delta 2.7\text{ppm}$ (dd), $\delta 3.2\text{ppm}$ (dd); $\delta 4.5\text{ppm}$ (dd)
2-bromo-6-methoxy-3-phenylindanone <b>314</b>	$\delta 4.4$ (d); $\delta 4.6$ (d)
6-methoxy-3-phenylindenone <b>315</b>	$\delta 5.9\text{ppm}$ (s)

The data for compounds 3-phenylindanone (Aldrich) and 3-phenylindenone are similar, with the singlet in the latter appearing at  $\delta 6.0\text{ppm}$ . In all compounds, the methoxy shift was at *ca.*  $\delta 3.9\text{ppm}$ .

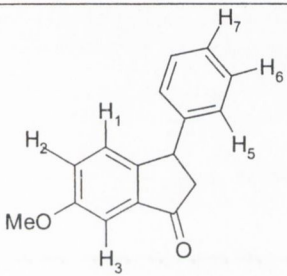
The protons of aromatic protons were difficult to assign, due to overlap of fused ring and phenyl ring peaks. The data for 3'-methoxychalcone is given in *Table 3.2*

*Table 3.2: Observed aromatic proton shifts 3'-methoxychalcone*

Compound <b>312</b>	Observed Shifts
	$\delta 7.1\text{ppm}$ (dd, 1H, $\text{H}_2$ ); $\delta 7.4\text{ppm}$ (m, 3H, Ph); $\delta 7.56\text{ppm}$ (t, 1H, $\text{H}_3$ ); $\delta 7.62\text{ppm}$ (dt, 1H, $\text{H}_4$ ); $\delta 7.69\text{ppm}$ (dd, 2H, Ph)

H<sub>2</sub> and H<sub>4</sub> were distinguished by an nOe experiment on *m*-methoxyacetophenone which showed proton H<sub>2</sub> to be a double doublet around 7.0ppm and H<sub>4</sub> to be a double triplet around 7.5ppm. Table 3.3 gives the <sup>1</sup>H NMR data for the fused ring compound.

Table 3.3: Observed aromatic proton shifts 3-phenylindanone

Compound 313	Observed Shifts
	δ7.14ppm, 2H, dd(7, 1.5Hz), H <sub>5</sub> ; δ7.18ppm, 2H, d(1.5Hz), H <sub>1</sub> & H <sub>3</sub> overlapping; δ7.26ppm, 2H, m, H <sub>2</sub> & H <sub>7</sub> ; 7.3ppm, 2H, m, H <sub>6</sub> .

In the second method, *via* propanedione derivatives, <sup>1</sup>H NMR was again useful in studying the products formed. The compound 1-(*m*-methoxyphenyl)-3-phenyl-2,3-propanedione exists in both keto and enol form. (Fig 3.5)

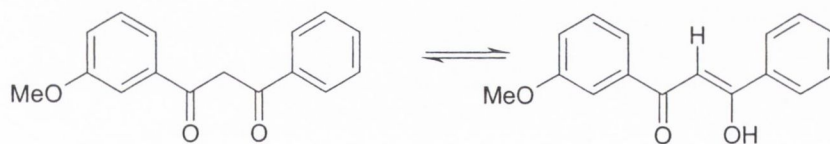
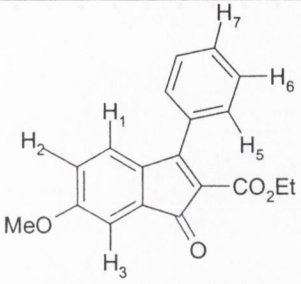


Fig. 3.5: Keto-enol tautomers of propanedione derivatives

The ratio of keto:enol is 1:4, obtained from integrating the respective signals. (This compound also had a positive ferric chloride test, indicating the presence of an enol) The compound 2-carbethoxy-6-methoxy-3-phenylindenone had a very simple <sup>1</sup>H NMR spectrum (Table 3.4)

Table 3.4: Observed aromatic proton shifts 2-carbethoxy-6-methoxy-3-phenylindanone

Compound <b>316</b>	Observed Shifts
	$\delta$ 1.2ppm, 3H, t (7Hz), Me; $\delta$ 4.2ppm, 2H, q (7Hz), OCH <sub>2</sub> , $\delta$ 6.8ppm, 1H, dd (8.5, 2.5Hz), H <sub>2</sub> ; $\delta$ 7.1ppm, 1H, d (8Hz), H <sub>1</sub> ; $\delta$ 7.2ppm, 1H, d (2.5Hz), H <sub>3</sub> , $\delta$ 7.5ppm, s, 5H, Ph)

3.2.6.2 **Infrared Spectroscopy** Because of the change in environment of the carbonyl substituent during the chalcone to indenone reaction scheme, IR is another useful tool for studying the structures of the products obtained. Table 3.5 summarises the data.

Table 3.5: Change in carbonyl frequency through reaction sequence

Compound	$\nu(\text{C=O})$ (cm <sup>-1</sup> )
3'-methoxychalcone <b>312</b>	1660
6-methoxy-3-phenylindanone <b>313</b>	1709
2-bromo-6-methoxy-3-phenylindanone <b>314</b>	1713
6-methoxy-3-phenylindenone <b>315</b>	1700

### 3.2.6.3 X-ray Crystallography

Crystal structures were collected for 2-bromo-6-methoxy-3-phenylindanone (Fig 3.6) and the corresponding enone (Fig. 3.7). (It was found that indenones substituted at the 2- and 3-position recrystallised more easily than those with substituents only in the three position). For the bromoindanone, the  $\alpha$ - $\beta$  carbon bond length was 1.531 Å, and the



phenyl torsion angle was  $60^\circ$  to the plane of the indenone. For the indenone, the  $\alpha$ - $\beta$  carbon bond length was 1.356 Å, and the torsion angle of the phenyl substituent was  $59^\circ$ . These, and other parameters are summarised in *Table 3.6*.

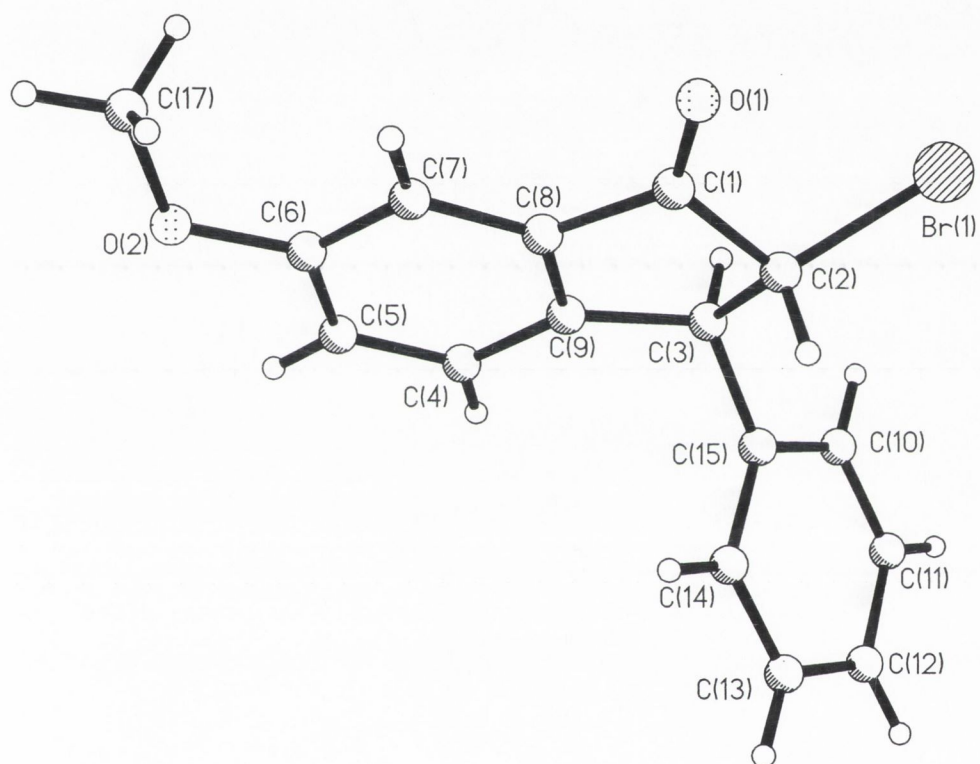


*Fig. 3.6: X-Ray crystal structure of 2-bromo-6-methoxy-3-phenylindenone 314*

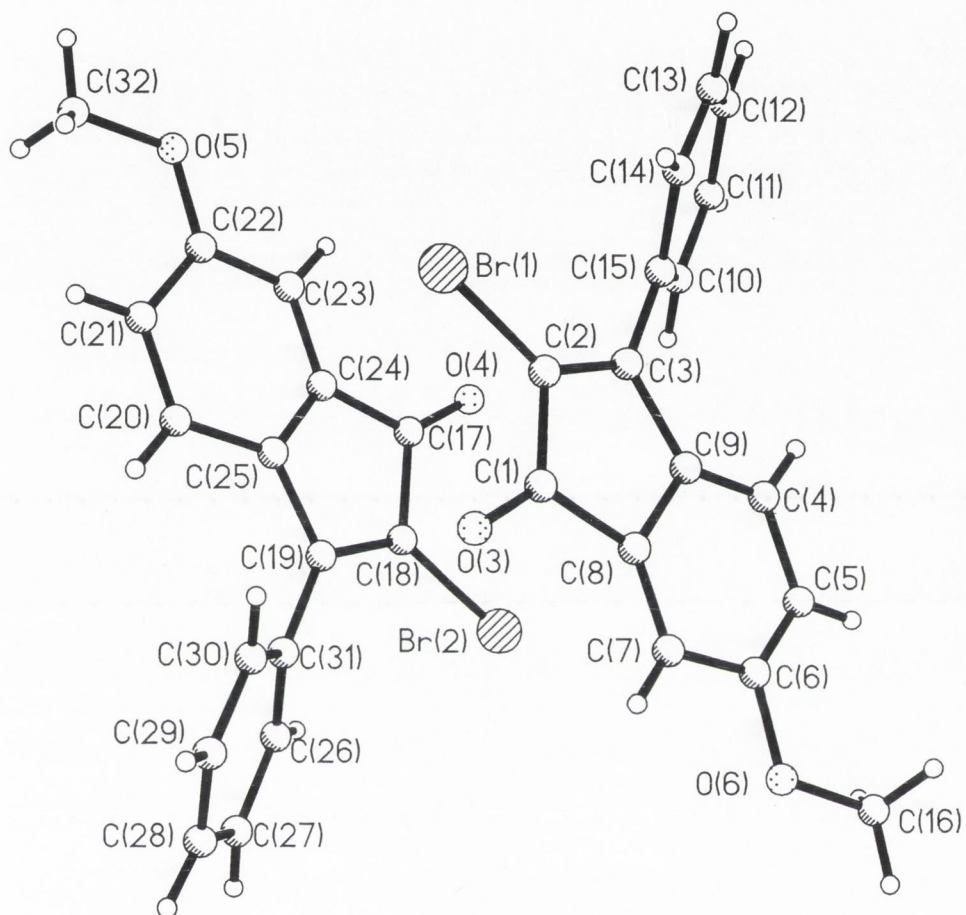


*Fig. 3.7: X-ray crystal structure of 2-bromo-6-methoxy-3-phenylindenone*

*Table 3.6: Important parameters derived from X-ray crystal structure data\**

	2-bromo-6-methoxy-3-phenylindanone <b>314</b>	2-bromo-6-methoxy-3-phenylindenone
Formula	C <sub>16</sub> H <sub>13</sub> Br O <sub>2</sub>	C <sub>16</sub> H <sub>11</sub> Br O <sub>2</sub>
Crystal System	Monoclinic	Triclinic
C <sub>α</sub> -C <sub>β</sub>   (Å)	1.531	1.356
Phenyl Torsion angle (°)	60	59
C-O  (Å)	1.210	1.205

\*Full data table in Appendix



### 3.3 DISCUSSION

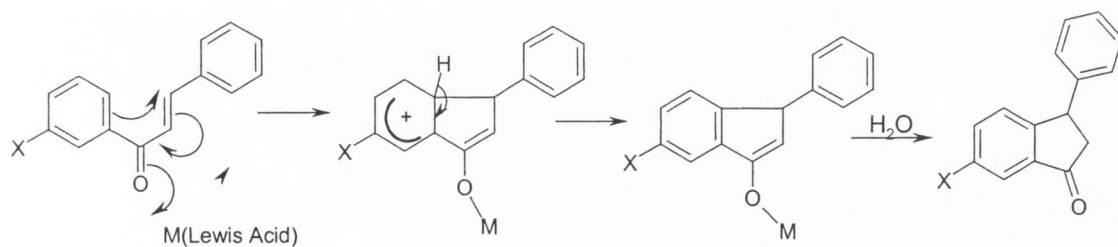
#### 3.3.1 6-methoxy-3-phenylindanone

It was decided to synthesise the indanone using Friedel-Crafts alkylation over acylation, as it was feared that acylation would give a mixture of 3-phenyl and 3-arylidene. In retrospect, acylation could have been attempted, as it would appear that ring-closure to the aryl ring with the electron-donating methoxy substituent would be favoured over ring-closure to the unsubstituted phenyl ring.

Fears that ring-closure of 3'-methoxychalcone would yield both 4- and 6- isomers were allayed by the work of both Murphy<sup>14</sup> and Gaviña,<sup>13</sup> who reported that the 6-isomer was the major product.

The 4-isomer, formed by ring closure to the carbon *ortho* to the methoxy substituent was removed by crystallisation and recrystallisation of 2-bromo-6-methoxy-3-phenylindanone (major product) to give a purity of >99%.

Although the aldol condensation to give the chalcone was facile, ring closure proved to be frustratingly difficult. This is probably due to the fact that Friedel-Crafts alkylation is disfavoured when there is an electron withdrawing group on the ring, as this destabilises the cationic intermediate (*Scheme 3.13*)



*Scheme 3.13: Mechanism for ring-closure of chalcone*

In the case of 3'-methoxychalcone ( $X=OMe$ ), the methoxy substituent acts as an electron-donating group, which provides some stabilisation, and so ring closure can occur, with some difficulty. However, if an activating and deactivating group are both present on ring, Friedel-Crafts alkylation can be accomplished.<sup>9</sup> This is supported by the fact that chalcone ( $X=H$ ) does not undergo ring-closure under the conditions used for the methoxy derivative.

Of the catalysts used, boron trifluoride and trifluoroacetic acid were the ones that gave desired product. The use of trifluoroacetic acid gave fewer side products, required less reaction time and so was the catalyst of choice.

Aluminium chloride is known to complex to electron-donating substituents such as  $-OR$ ;  $-OH$  and  $-NR_2$ , thus deactivating their electron donating capacity.<sup>9, 23</sup> This may have happened in this case, as in the work up of this reaction, the  $^1H$  NMR of the crude product showed no sign of a MeO substituent, indicating that the  $MeO \rightarrow OH$  transformation had occurred (via  $[AlCl_3-OMe]$  complex).

### 3.3.2 Dehydrogenation of Indanones

**3.3.2.1 Methoxy-derivative** Two methods were used in the dehydrogenation step (indanone to indenone). Both have distinct advantages and disadvantages. The first – bromination-dehydrobromination – involves two steps, and on a small scale (mmol) is difficult, with an oily bromo-intermediate. Dehydrobromination was attempted with LiCl in dimethylformamide, and proved to be slow, with small conversion to product. Purification of the indenone was difficult. However, on scale-up, this reaction showed its virtues. In this experiment, the bromo-intermediate crystallised out. Dehydrobromination using sodium ethoxide in ethanol was much more successful than LiCl.

Thus, the overall reaction from aldol condensation to indenone was as follows. The chalcone was synthesised and the crude product dissolved in trifluoroacetic acid. The crude indenone was brominated in ether. It was at this point that the first purification took place. As stated above, ring-closure of the chalcone gives predominantly the 6-isomer, but some 4-isomer is present. The 4-isomer was difficult to remove after indenone formation, but could be removed by several recrystallisations of the bromo-ketone stage. The methoxy peak in  $^1\text{H}$  NMR spectrum (singlet at 3.9 ppm) was used as a diagnostic tool to test for purity, and samples were recrystallised until purity was greater than 99%. Dehydrobromination could then be effected, and final purification of the indenone yielded pure product suitable for photophysical/chemical analysis.

The fact that  $\alpha$ -bromination had occurred (*Scheme 3.13*) was verified with a C-H COSY spectrum. This confirmed that the two aliphatic protons were on different carbon atoms.

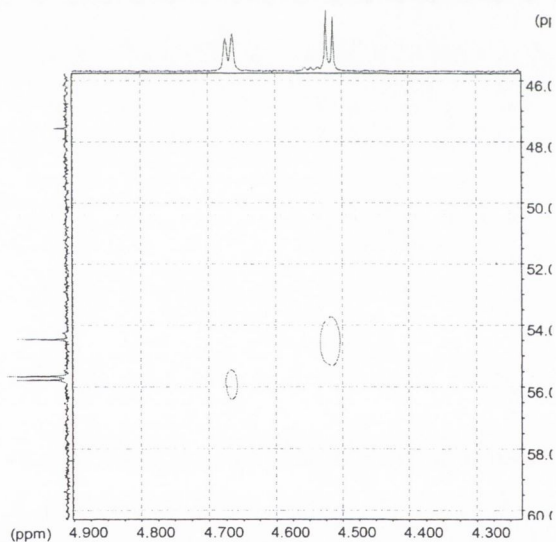


*Fig 3.8: C-H COSY showing the  $^1\text{H}$  peaks of the  $\alpha$ - and  $\beta$ - hydrogens are on different carbon atoms*

This was to be expected. Previous reports of brominations show that bromine brominates the position  $\alpha$ - to the carbonyl, whereas NBS brominates the  $\beta$ -carbon.  $\alpha,\alpha$ -dibrominated product was also obtained, which on dehydrobromination gave the  $\alpha$ -



bromoindenone. This was separated from the desired product by column chromatography. A crystal structure of this compound confirms  $^1\text{H}$  NMR assignments: namely – no aliphatic protons, indicating the  $\alpha$ -position is substituted and the  $\alpha,\beta$ -bond is unsaturated. Also it confirms that the methoxy substituent is indeed at the 6-position.

The second method – oxidation of the alkanone to the alkenone using selenium dioxide – had the advantages that it was one-step reaction and that the reaction is clean (when freshly distilled and dried solvent is used). However, low conversion rates (7 days gives a ratio of 2:3 product : starting material) make these advantages less attractive. Starting indanone can be recovered by chromatography and recycled.

Overall, the first method was favoured for the synthesis of the methoxy derivative, as large quantities of the corresponding crude indanone can be brominated in the knowledge that the bromo-product can be easily isolated and purified.

#### 3.3.2.2 *Parent compound:*

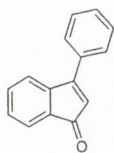
Attempts to brominate 3-phenylindanone using the conditions for the methoxy-compound resulted in low conversion rates. Longer reaction times were required. The bromo-compound could not be isolated as easily as its methoxy derivative. Dehydrobromination could not be effected successfully - either using the same conditions as for the methoxy derivative, or with longer reflux times.

Oxidation, using selenium dioxide, was therefore preferred in the synthesis of 3-phenylindenone. The results were similar to the methoxy derivative - modest yields, but the indanone could be isolated and recycled.

**3.3.3 *Anstead Method*** This method seemed attractive – a two-step synthesis to the desired indenone. The first step – the synthesis of the propanedione – was slower than Anstead reported for his compounds. This was expected. In Anstead's systems, the

carbanion formed by deprotonation with sodium hydride is further stabilised by aryl substituent. In this modified reaction, deprotonation of the methyl group of acetophenone affords no such additional stabilisation. The propanedione was synthesised, and existed predominantly in an enolic form. Ring closure with methanesulfonic acid failed under all conditions attempted.

### 3.4 EXPERIMENTAL



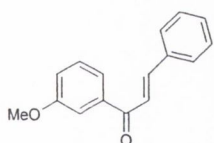
**3-Phenylindanone<sup>37</sup> (313, X=H)** 3-Phenylindanone (0.5g) (Aldrich) was dissolved in dry ethanol (20ml). The solution was set to reflux under an atmosphere of nitrogen and selenium dioxide (0.3g) added. The mixture was let reflux for 48 hours after which it was let cool, and added to water. The product was extracted with dichloromethane and washed with aqueous sodium hydrogen carbonate and water. The organic extract was dried over magnesium sulphate and the solvent removed. <sup>1</sup>H NMR of the crude red oil showed a singlet at 5.9ppm, corresponding to the  $\alpha$ -hydrogen. Purification by column chromatography (100% dichloromethane,  $R_f = 0.8$ ) gave 100mg (20%) of product as a red oil.

<sup>1</sup>H NMR (CDCl<sub>3</sub>):  $\delta$ 6.0, 1H, s,  $\alpha$ -H;  $\delta$ 7.3, 7.4, 2H, dt (6.5, 1), 5- & 6-H;  $\delta$ 7.4, 7.5, 2H, d (6.5), 3- & 7-H

<sup>13</sup>C NMR (CDCl<sub>3</sub>):  $\delta$ 121.6, 7-C,  $\delta$ 122, 5-C,  $\delta$ 123, 2-C,  $\delta$ 127, *m*-Ph,  $\delta$ 129, *o*-Ph,  $\delta$ 129, 6-C,  $\delta$ 130, 4-C,  $\delta$ 132, 8-C,  $\delta$ 133, *p*-Ph,  $\delta$ 163, 3-C,  $\delta$ 197, 1-C

IR (neat) 1704cm<sup>-1</sup> (C=O)

ESMS M<sup>+</sup> = 207.0743 (calculated for C<sub>15</sub>H<sub>11</sub>O 207.0810)



**3'-Methoxychalcone<sup>13, 14</sup> 312** KOH (2.18g) was dissolved in water (20ml) and cooled in ice. *m*-Methoxyacetophenone (5.7ml) was dissolved in 95 % ethanol and the alkali added to this solution. Benzaldehyde (4.6ml) was added and the resulting clear yellow solution let stir for 8 hours. The solution was cooled in an ice-bath to prompt precipitation of product, which came out as a pale yellow powder. However, it sometimes formed an oil which was isolated and purified by column chromatography (hexane:ethyl acetate 10:3,  $R_f = 0.5$ ) yielded 6.5g (69%) of product as a yellow powder.

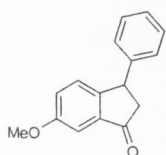
<sup>1</sup>H NMR (CDCl<sub>3</sub>):  $\delta$ 3.9, 3H, s, OMe;  $\delta$ 7.15, 1H, ddd (8, 2.5, 1), 4'-H;  $\delta$ 7.4, 3H, m *m*- & *p*-Ph;  $\delta$ 7.54, 1H, d (15.5), 2-H;  $\delta$ 7.57, 1H, t(1.5), 2'-H;  $\delta$ 7.62, 1H, d (8), 5'-H;  $\delta$ 7.65, 2H, dd (6, 2), *o*-Ph;  $\delta$ 7.81, 1H, d (15.5), 3-H.



**IR**  $\nu(\text{C}=\text{O})$  1660 $\text{cm}^{-1}$  (Nujol)

**ESMS**  $\text{M}^+$  239.1058 (Calculated for  $\text{C}_{16}\text{H}_{15}\text{O}_2$  239.1072)

**UV/vis** (ethanol) 310 nm



**6-Methoxy-3-phenylindanone**<sup>13,14</sup> **313** 3'-Methoxychalcone (9.2g) from above was dissolved in trifluoroacetic acid (20ml) and refluxed for 2 days under an atmosphere of nitrogen. Work up (addition of water, extraction with dichloromethane dry over magnesium sulfate) and evaporation of solvent gave a red-brown oil. A sample was purified by column chromatography (100% dichloromethane,  $R_f = 0.4$ ) to give a yellow powder. Partially purified product could also be used in the oxidation step. (8.1g, 88%)

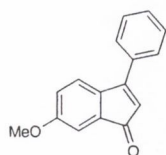
**$^1\text{H}$  NMR** ( $\text{CDCl}_3$ ):  $\delta$ 2.7, 1H, dd(19, 3.5), 2-H;  $\delta$ 3.3, 1H, dd(19, 7), 2-H;  $\delta$ 3.9, 3H, s, OMe; 4.5, 1H, dd(7, 3.5), 3-H;  $\delta$ 7.14, 2H, dd(7, 1.5), *o*-H;  $\delta$ 7.18, 2H, d(1.5), 4-H & 7-H overlapping;  $\delta$ 7.26, 2H, m, 5-H & *p*-H; 7.3, 2H, m, *m*-H.

**$^{13}\text{C}$  NMR** ( $\text{CDCl}_3$ ):  $\delta$ 43, 3-C,  $\delta$ 48, 2-C,  $\delta$ 55, OMe,  $\delta$ 104, 7-C,  $\delta$ 124, 5-C,  $\delta$ 127, 4-,  $\delta$ 127, *o*-Ph,  $\delta$ 127, *p*-Ph,  $\delta$ 128, *m*-Ph,  $\delta$ 138, 8-C,  $\delta$ 146, 3-C,  $\delta$ 160, 6-C,  $\delta$ 208, 1-C.

**IR:**  $\nu(\text{C}=\text{O})$  1705 $\text{cm}^{-1}$  (Nujol)

**Melting Point** 69-71°C

**ESMS**  $\text{M}^+$  239.1058 (Calculated for  $\text{C}_{16}\text{H}_{15}\text{O}_2$  239.1072)



**6-Methoxy-3-phenylindenone** **315** *Method A:* The oxidation was carried out analogous to above (0.5g indenone, 0.5g selenium dioxide) and after chromatography (100% dichloromethane) gave 140mg (28%) of product.

*Method B:* 6-Methoxy-3-phenylindanone (8.1g) was dissolved in ether and the solution cooled in ice. Bromine (0.1ml) was added dropwise, and the mixture was let stir for twenty minutes. At this time a precipitate started to fall out of solution. The solution was stirred for a further 10 minutes and water added. The solution was allowed to stand overnight and the precipitate that formed was collected by suction filtration. Recrystallisation (ether) gave an  $^1\text{H}$  NMR spectrum that corresponded to 2-bromo-6-methoxy-3-phenylindanone (6.1g, 55%) This was refluxed in sodium ethoxide for three hours under inert atmosphere. Work-up and purification (100% DCM, 3:2 DCM:hexane) gave product 6-methoxy-3-phenylindenone. (1.1g, 13.5% overall)

$^1\text{H}$  NMR ( $\text{CDCl}_3$ ):  $\delta$ 3.9, 3H, s, OMe;  $\delta$ 5.9, 1H, s,  $\alpha$ -H;  $\delta$ 6.8, 1H, dd(8, 2.5), 5-H;  $\delta$ 7.2, 1H, d(2.5Hz), 7-H;  $\delta$ 7.3, 1H, d(8), 4-H.

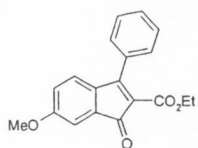
$^{13}\text{C}$  NMR ( $\text{CDCl}_3$ ):  $\delta$ 44, 3-C,  $\delta$ 60, OMe,  $\delta$ 107, 7-C,  $\delta$ 122, 5-C,  $\delta$ 125, 4-,  $\delta$ 126, *o*-Ph,  $\delta$ 126, *p*-Ph,  $\delta$ 127, *m*-Ph,  $\delta$ 137, 8-C,  $\delta$ 162, 6-C,  $\delta$ 200, 1-C.

IR:  $\nu(\text{C}=\text{O})$  1700  $\text{cm}^{-1}$  (Nujol)

Melting Point 81 - 83°C

Analysis: Reqd.: C 81.34, H 5.12%, Found: C 81.27, H 5.21%

ESMS  $\text{M}^+$  237.0922 (Calculated for  $\text{C}_{16}\text{H}_{13}\text{O}_2$  237.0916)



**2-Carbethoxy-6-methoxy-3-phenylindenone 316** Sodium hydride

(1.1g) was added to dry THF and the mixture set stirring. Ethyl benzoyl acetate (3.5 ml) was added and the mixture was left stirring for 1 hour. Anisoyl chloride (2.8ml) was added drop-wise over 45 minutes and the solution turned an intense red colour. The solution was carefully poured into cold 5% HCl solution and extracted with dichloromethane. After drying over  $\text{MgSO}_4$ , the resulting solution was evaporated to give a red oil.

This was dissolved in dichloromethane (30ml) and the solution cooled in a ice-bath and methane sulfonic acid (1ml in 10ml dichloromethane) was added dropwise over 45 minutes. The ice-bath was removed and the solution let stir for three days. The

red solution was worked up (NaHCO<sub>3</sub>, brine, MgSO<sub>4</sub>) and the solvent evaporated off. On addition of a hexane-ethyl acetate mixture, red crystals fell out of solution and these were filtered off giving the product indenone. (2.3g, 46.6% overall)

<sup>1</sup>H NMR (CDCl<sub>3</sub>): δ1.2, 3H, t (7), Me; δ4.2, 2H, q (7), OCH<sub>2</sub>, δ6.8, 1H, dd (8.5, 2.5), H<sub>2</sub>; δ7.1, 1H, d (8), H<sub>1</sub>; δ 7.2, 1H, d (2.5), H<sub>3</sub>, δ7.5, s, 5H, Ph)

<sup>13</sup>C NMR (CDCl<sub>3</sub>): δ15, CH<sub>3</sub>, δ56, OMe, δ61, CH<sub>2</sub>, δ110, 7-C, δ117, 5-C, δ125, 4-C, δ127, *o*-Ph, δ128, *p*-Ph, δ131, *m*-Ph.

**Analysis:** Reqd.: C 74.01, H 5.23%, Found: C 73.79, H 5.31%

**ESMS** M<sup>+</sup> 309.1218 (Calculated for C<sub>16</sub>H<sub>15</sub>O<sub>2</sub> 309.1127)



### 3.5 References Cited

1. J. F. D. Kelly, J. M. Kelly and T. B. H. McMurry, *J. Chem. Soc. Perkin Trans. 2*, 1996, 1933 and refs within.
2. R.V. Benasson, E.J. Land and T. G. Truscott, *Excited States and Free Radicals in Biology and Medicine*, Oxford University Press, New York, 1993.
3. H. O. House and J. K. Larson, *J. Org. Chem.*, 1968, **33**, 448.
4. H. O. House and C. B. Hudson, *J. Org. Chem.*, 1970, **35(3)**, 647.
5. K. P. Bøgesø, *J. Med. Chem.*, 1983, **26**, 935.
6. K. P. Bøgesø, A. V. Christensen, J Hyttel and T Liljefors, *J. Med. Chem.*, 1985, **28**, 1817.
7. J. Zhang, R. L. Hertzler, E. M. Holt, T. Vickstrom and E. J. Eisenbraun, *J. Org. Chem.*, 1993, **58 (3)**, 556.
8. R. G. Shotter, K. M. Johnston and J. F. Jones, *Tetrahedron*, 1978, **34**, 741.
9. Olah, "*Friedel Crafts and Related Reactions*" Wiley, New York, 1963-1965.
10. *J. Chem. Soc.*, 1956, 2928.
11. J. M. Allen, K. M. Johnston, J. F. Jones and R. G. Shotter, *Tetrahedron*, 1977, **33**, 2083.
12. J. P. Bradley, T. C. Jarvis, C. D. Johnson, P. D. McDonnell and T. A. P. Weatherstone, *Tet. Lett.*, 1983, **24(28)**, 2851.
13. F. Gaviña, A. M. Costero and A. M. González, *J. Org. Chem.*, 1990, **55(7)**, 2060.
14. W. S. Murphy and S. Wattansin, *J. Chem. Soc. Perkin Trans 1*, 1980, 1555.
15. M. B. Sommer, M Begtrup and K. P. Bøgesø, *J. Org. Chem.*, 1990, **55(16)**, 4817.
16. R. P. Holysz, *J. Am. Chem. Soc.*, 1953, **75**, 4432.
17. E. W. Warnhoff, D. G. Martin and W. S. Johnson, *Org. Syn. Coll.*, 1963, **4**, 162.
18. D. W. Jones and R. J. Marmon, *J. Chem. Soc. Perkin Trans 1*, 1993, 681.
19. C. S. Marvel and C. W. Hinman, *J. Am. Chem. Soc.*, 1954, **76**, 5435.
20. H. O. House and W. C. McDaniel, *J. Org. Chem.*, 1977, **42(12)**, 2155.

21. R. P. Holysz, *J. Am. Chem. Soc.*, 1953, **75**, 4432
22. S. F. Martin, S. K. Davidsen and T. A. Puckette, *J. Org. Chem.*, 1987, **52(10)**, 1962.
23. J. March, "*Advanced Organic Chemistry*", 4<sup>th</sup> Ed., Wiley, New York, 1992, p. 1164.
24. Bernstein and Littell, *J. Am. Chem. Soc.*, 1960, **82**, 1235.
25. Barnes and Barton, *J. Chem. Soc.*, 1953, 1419.
26. R. F. Heck, "*Palladium Reagents in Organic Synthesis*", Academic Press, New York, 1985, pp103-110.
27. Cardinale, Lean, Russell and Ward, *Recl. Trav. Chim Pay-Bas*, 1982, **101**, 199.
28. Barton, Huitey and Williams, *J. Chem. Soc. Perkin Trans 1*, 1982, 1919.
29. R. J. Thiessen, *J. Org. Chem.*, 1971, **36(6)**, 752.
30. A. A. Leon, G. Daub and I. R. Silverman, *J. Org. Chem.*, 1984, **49**, 4544.
31. G. M. Anstead, J. L. Ensign, C. S. Peterson and J. A. Katzenellenbogen, *J. Org. Chem.*, 1989, **54(7)**, 1485.
32. G. M. Anstead, R. Srinivasan, C. S. Peterson, S. R. Wilson and J. A. Katzenellenbogen, *J. Am. Chem. Soc.*, 1991, **113**, 1378.
33. W. S. Murphy, personal correspondence
34. D. M. Vyas, P. M. Skonezny, T. A. Jenks, and T. W. Doyle, *Tet. Letters*, 1986, **27(27)**, 3099.
35. J. M. Allen, K. M. Johnston, J. F. Jones, R. G. Shotton, *Tetrahedron*, 1977, **33**, 2083.
36. H. J. Dauben and L. L. McCoy, *J. Am. Chem. Soc.*, 1959, **81**, 4863.
37. R. C Larock, M. J. Doty and S. Cacchi, *J. Org. Chem.*, 1993, **58**, 4579.

*Chapter Four*

*The Photo-interaction of 6-methoxy-3-phenylindenone  
with 1-phenylpropene*



## 4.1 INTRODUCTION

As described in Chapter 1, the photocycloaddition between enones and alkenes yielding cyclobutane adducts is an important category of organic photochemical reactions. Many examples in the literature show the usefulness of this reaction in the synthesis of complex molecules.<sup>1</sup> Examples include work carried out in this laboratory on 3-phenylcyclopentenone (PCP) and 3-phenylcyclohexenone (PCH) with 1-phenylpropene.<sup>2</sup> Another recent example describes work on 2-aryl and 2-alkylcyclopentenones. 2-methylcyclopentenone (**401**) irradiated in the presence of the substituted cyclobutene **400** gives adduct **402** only in a 55% yield (*Fig. 4.1*).<sup>3</sup> This product undergoes ring opening on thermolysis and is a useful intermediate in longer synthetic sequences.

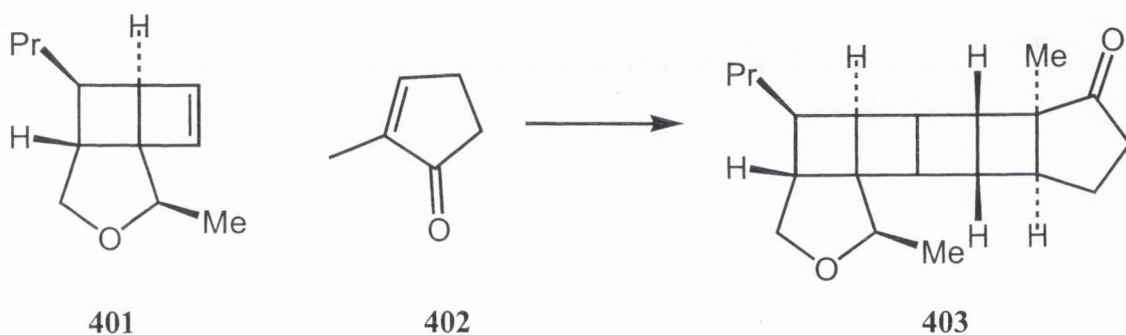


*Fig. 4.1: Irradiation of cyclobutene **400** in the presence of the substituted cyclopentenone **401** gives adduct **402** only*

In addition to intermolecular cycloaddition, intramolecular addition also provides access to useful intermediates. For example, irradiation of **403** gives quantitative conversion to the 2+2 adduct **404**, which was used as an intermediate in the total synthesis of ginkgolide (B) (*Fig. 4.2*).<sup>4</sup>

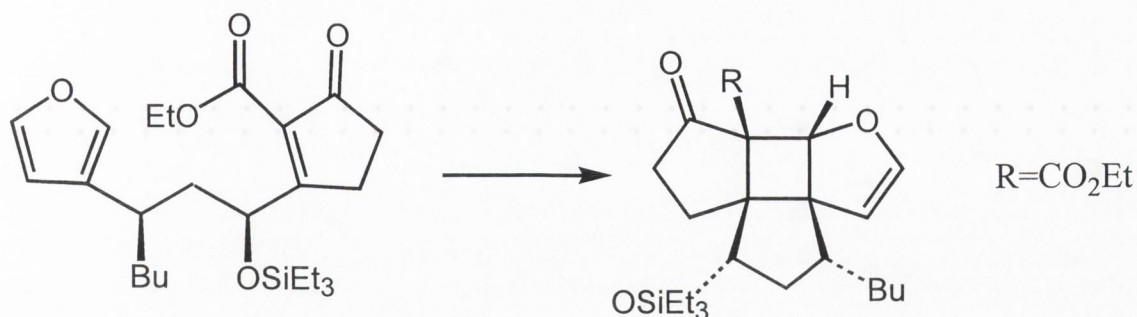


Fig. 4.2: Irradiation of enone **403** gives quantitative cycloaddition yielding adduct **404**

Workers in our laboratory have studied the cycloaddition of 3-phenylcyclic enones to various alkenes. Examples include the cycloaddition of 3-phenylcyclopentenone to 1-phenylpropene<sup>2</sup> (as described in Chapter 2) and various intramolecular cycloadditions, where the enone and alkene are within the same molecule (Fig 4.3).<sup>5</sup>

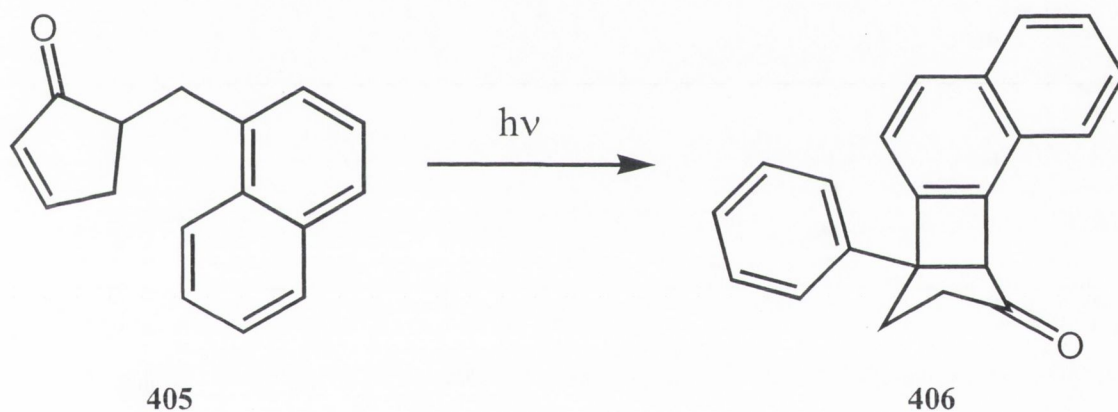
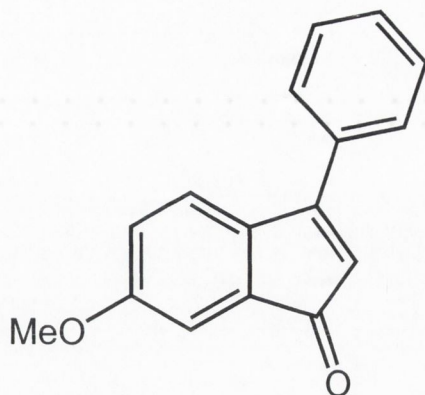


Fig. 4.3: Irradiation of naphthyl-substituted cyclopentenone **405** gives adduct **406**

As described in Chapter 2, the photo-reaction between both 3-phenylcyclopentenone and 3-phenylcyclohexenone to 1-phenylpropene has been studied by laser flash photolysis and NMR spectroscopy and in the case of 3-phenylcyclohexenone this interaction has been examined using time-resolved infrared spectroscopy. Having synthesised 6-methoxy-3-phenylindenone, **407**, it was decided to examine the photoreaction between this molecule and alkenes.



*Fig. 4.4: 6-methoxy-3-phenylindenone 407*

The following describes the experiments carried out on the indenones-alkene system. NMR spectroscopy is used as the diagnostic tool. The methoxy indenone is chosen as the methoxy-substituent is a good 'reporter' in NMR spectroscopy, giving a clean singlet in NMR spectra. Hence the disappearance of starting material indenone can be identified easily by the reduction in the intensity of the methoxy singlet.



## 4.2 RESULTS

### 4.2.1 6-methoxy-3-phenylindenone

**4.2.1.1 UV/Vis absorption spectrum** The UV spectrum of 6-methoxy-3-phenylindenone (**407**) is shown in Fig. 4.5. In ethanol, a long wavelength band is observed at 442 nm ( $\epsilon = 638$ ), and a shorter wavelength band observed at 298 nm ( $\epsilon = 18,500$ ). Both bands shift to the blue on decreasing solvent polarity. In cyclohexane, the long wavelength band appears at 424 nm, the shorter wavelength band at 298 nm. This represents shifts of 18 and 9 nm respectively to the blue. The same effect was observed for the carbethoxy derivative.

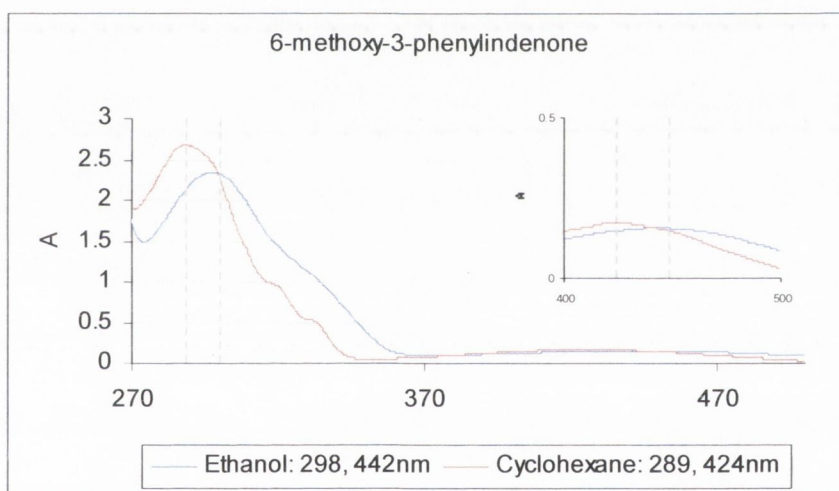


Fig. 4.5: UV spectrum of **407**

The short wavelength band is assigned as a  $\pi, \pi^*$  absorption band, which would shift to longer wavelengths on increasing solvent polarity. The long wavelength band is most likely a charge-transfer band, which again would be stabilised by increasing solvent polarity. The proposed charge transfer mechanism is shown below (Fig. 4.6)

**4.2.1.2 Flash Photolysis** Attempts to observe a transient species on excitation of **407** were unsuccessful. No transient was observed in the wavelength range 350 - 500nm

following laser excitation at 355 nm of a degassed solution of **407**. The extinction coefficient at this wavelength is *ca.* 300.

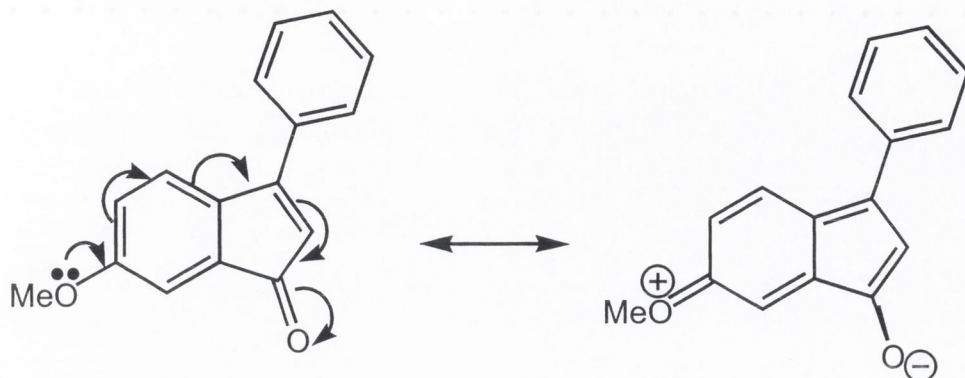


Fig. 4.6: Proposed Charge-Transfer mechanism for **407**

**4.2.1.3 NMR Spectrum** The NMR spectrum of **407** in  $d_3$ -acetonitrile is shown in Fig. 4.7. The methoxy-singlet appears at 3.8 ppm. The  $\alpha$ -hydrogen appears at 6.0 ppm. The hydrogens on the fused ring - the 4, 5, and 7-hydrogens appear at 7.4 ppm (doublet), 6.9 ppm (double doublet) and 7.1 ppm (doublet) respectively. The phenyl *o*- and *p*-hydrogens appear at 7.5 ppm and the *m*-hydrogens appear at 7.7 ppm.

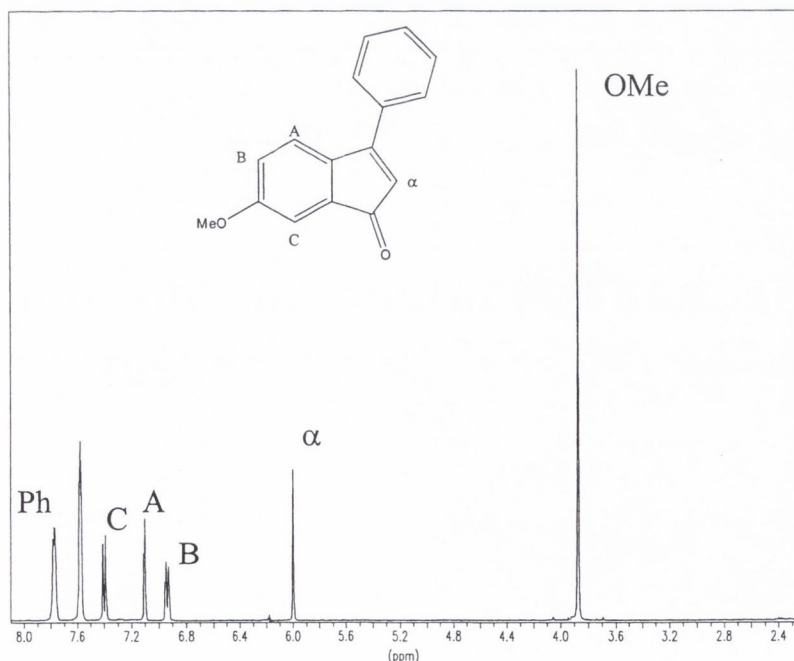
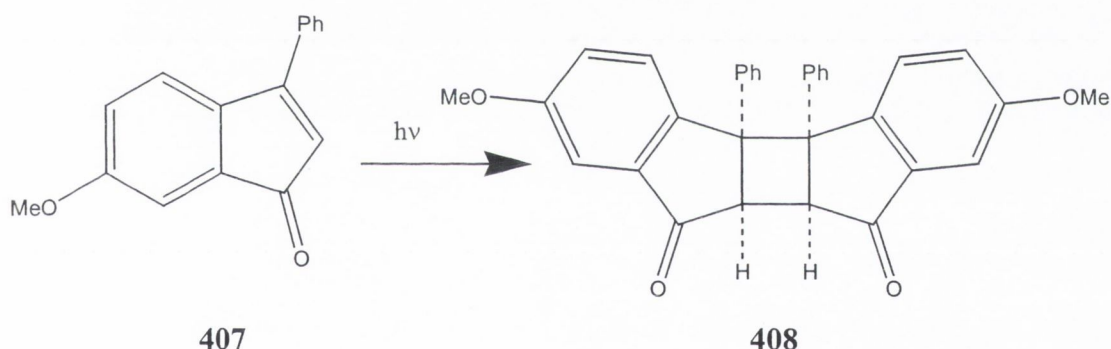


Fig. 4.7:  $^1\text{H}$  NMR spectrum of **407**

## 4.2.2 Irradiation of 6-methoxy-3-phenylindenone in the absence and presence of 1-phenylpropene

**4.2.2.1 6-methoxy-3-phenylindenone (acetonitrile) 407** (10 mM) in  $d_3$ -acetonitrile (1 mL) was degassed and exposed to UV irradiation. NMR spectra were recorded at various time intervals and the change in intensity of the peaks due to **407** (termed the 'monomer' hereon) monitored. On irradiation, the intensity of the peaks due to the monomer depleted, and some new peaks formed in the spectrum. Most significantly, singlets at 3.8 ppm and 3.7 ppm were observed. The ratio of these peaks in all spectra recorded was 3:1 respectively. It is thought that these peaks represent the dimerisation product, whose regiochemistry is most likely that shown in *Fig 4.8*, by analogy with reactions between pcp and pch with 1-phenylpropene.



*Fig. 4.8: Irradiation of 407 leading to dimer 408*

In this product the molecule is symmetrical, and therefore one methoxy singlet and one  $\alpha$ -hydrogen would be the only aliphatic hydrogens in this molecule. The ratio of these peaks would be 3:1. The spectra recorded at various times from 0 - 60 minutes is shown in *Fig 4.9(a)*, with the area 3.5 - 4.0 ppm shown in *Fig 4.9(b)*.



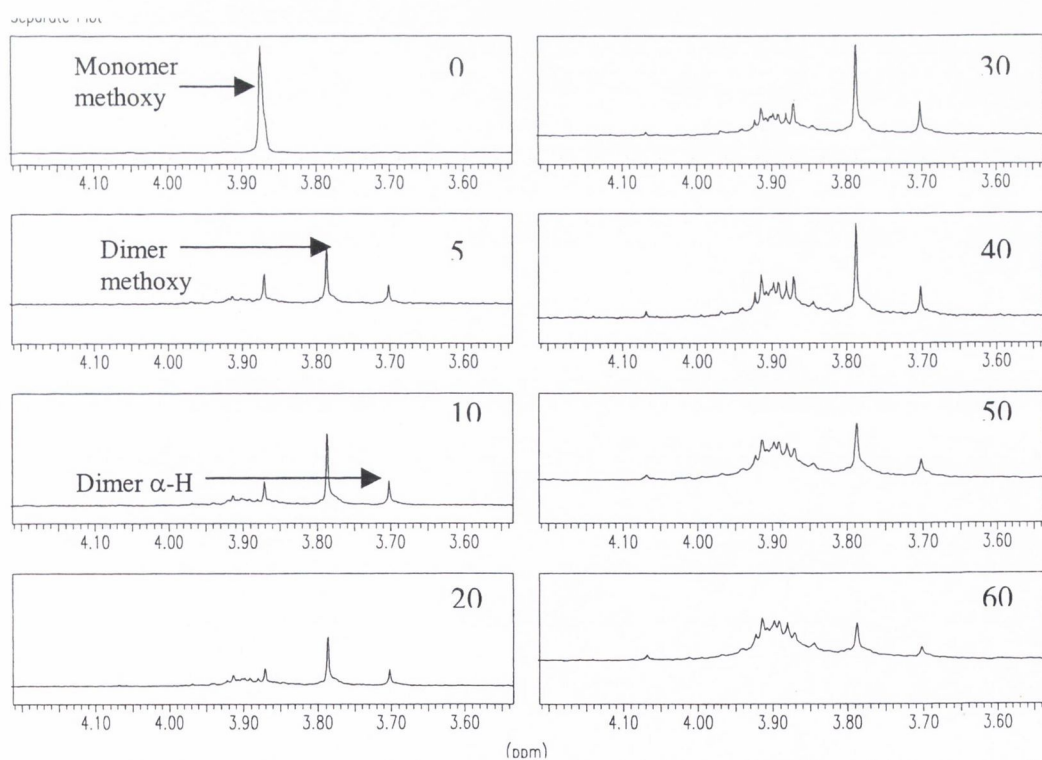
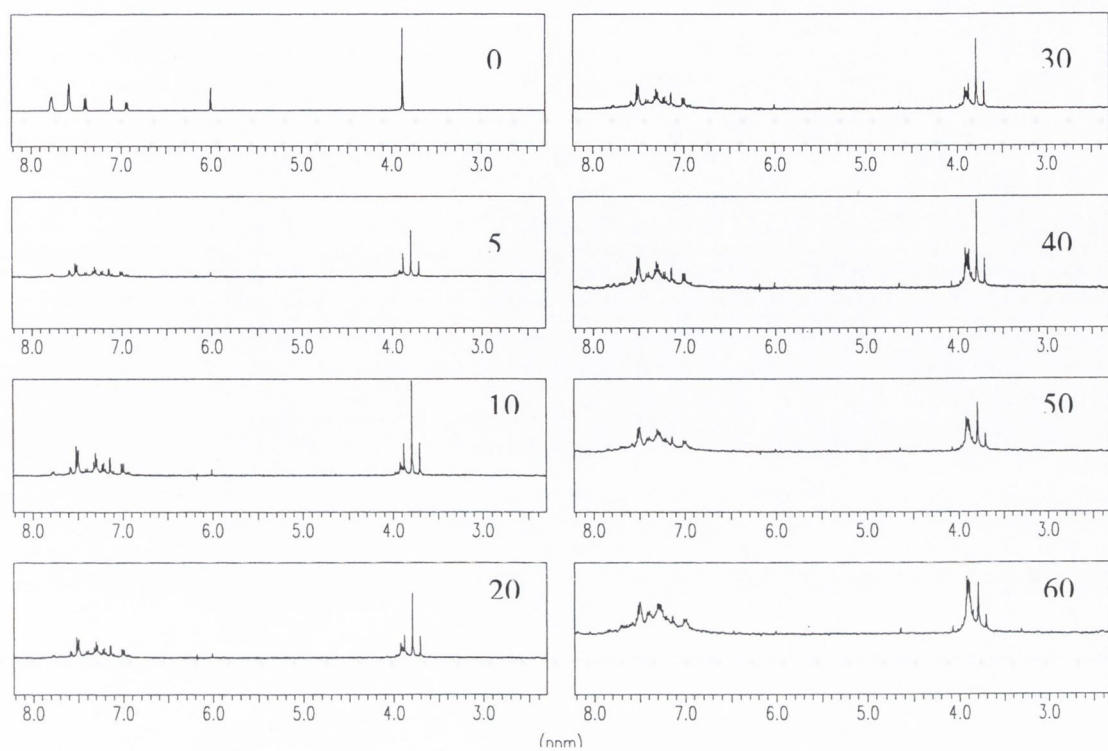


Fig. 4.9 (a) NMR spectra recorded on irradiation of 407 in  $CD_3CN$ ; (b) Region of interest expanded (time = 0 - 60 mins)

The ratio of the integrations of the monomer methoxy singlet : dimer methoxy singlet : dimer  $\alpha$ -hydrogen is shown in Fig. 10. The monomer methoxy singlet (at 3.87 ppm) decays rapidly from 100% at time  $t=0$  to *ca.* 30% after five minutes, and then the decay is slower, levelling off at about 20%. The errors in later time values are larger, due to difficulty in getting a good baseline for integration of the peak. The peak assigned as the dimer methoxy singlet rises quickly, to 55% after 5 minutes, levelling off to *ca.* 60%. The dimer-singlet mirrors this behaviour, except the ratio is one-third that of the methoxy substituent. Some other peaks are observed downfield of the monomer peak. It is difficult to say what these peaks are due to, as there is little resolution between them.

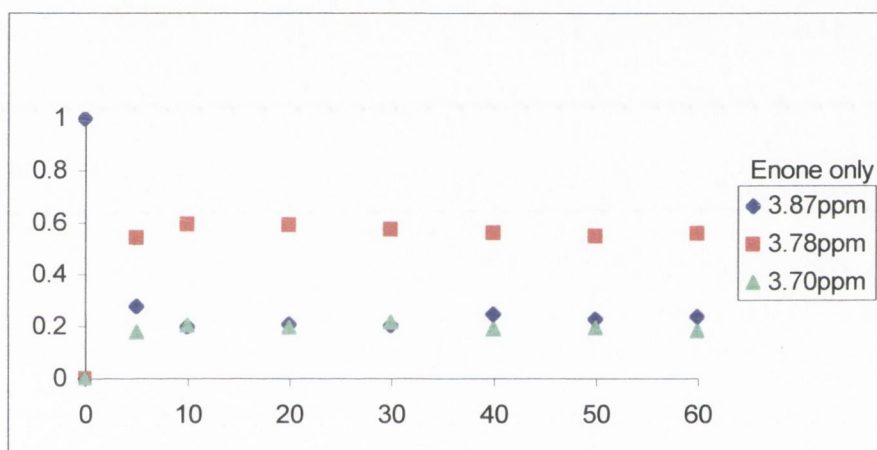


Fig. 4.10: Relative amounts of methoxy singlet of **407** (at 3.87 ppm), methoxy singlet of **408** (at 3.78 ppm) and  $\alpha$ -H (at 3.70 ppm) after irradiation in  $CD_3CN$

**4.2.2.2 6-methoxy-3-phenylindenone in the presence of 1-phenylpropene (acetonitrile) 407** (10 mM) was dissolved in acetonitrile and *E*-1-phenylpropene (50 mM) added. The solvent was deaerated, and the sample exposed to UV irradiation. Depletion of the monomer peaks was again observed, as was the appearance of the peaks assigned previously as the dimer at 3.8 and 3.7 ppm. Disappointingly however, there was little sign of appearance of the enone-alkene adduct methoxy group, which would be expected to be in an area similar to that of the monomer and dimer. A second peak close to the dimer  $\alpha$ -H peak is appearing, but it can't be assigned. The methoxy

peak would have the greatest intensity, so the fact that this cannot be viewed makes it very unlikely that aliphatic hydrogen peaks of the adduct would be visible.

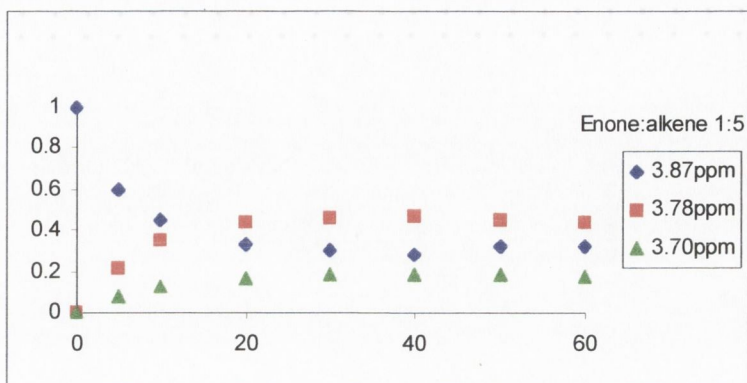


Fig. 4.11: Relative amounts of methoxy singlet of **407** (at 3.87 ppm), methoxy singlet of **408** (at 3.78 ppm) and  $\alpha$ -H (at 3.70 ppm) after irradiation in the presence of 1-phenyl propene in  $CD_3CN$  (E:A = 1:5)

The decay of the monomer, is plotted along with the appearance of the dimer methoxy and  $\alpha$ -H peaks. (Fig. 4.11) The decay in this case is slower, falling to *ca.* 40% over 20 minutes. The grow-in of the dimer methoxy peak grows to *ca.* 50% over 20 minutes. It should be stressed that these are ratios of the peaks relative to each other - they do not take into account other unassigned peaks in the spectrum.

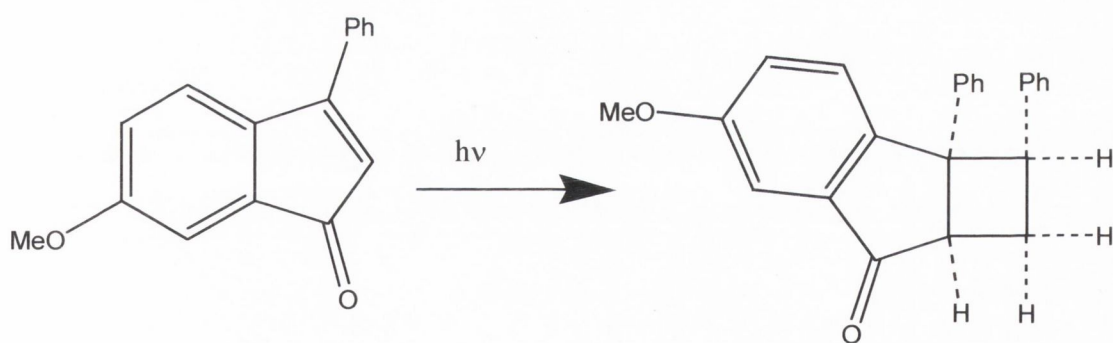


Fig. 4.12: Expected adduct to be formed on irradiation of **407** in the presence of 1-phenylpropene



Increasing the enone-alkene ratio to 1:10 has little effect on the above results. Again, the only definable product is that of the enone dimer. The rates of decay and grow in are shown (Fig. 4.12)

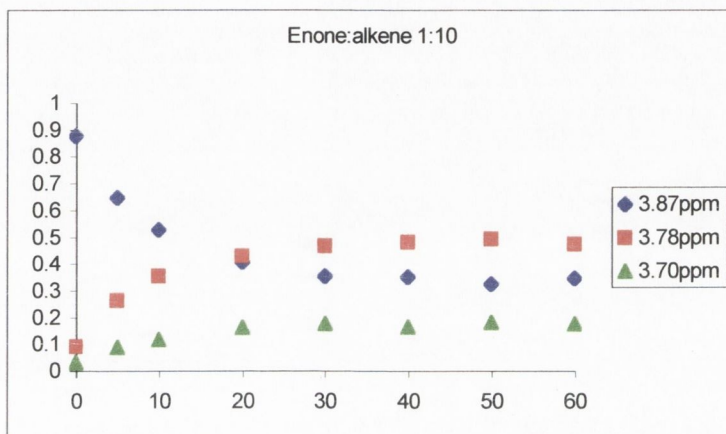


Fig. 4.12: Relative amounts of methoxy singlet of **407** (at 3.87 ppm), methoxy singlet of **408** (at 3.78 ppm) and  $\alpha$ -H (at 3.70 ppm) after irradiation the presence of 1-phenylpropene in  $CD_3CN$  ( $E:A = 1:10$ )

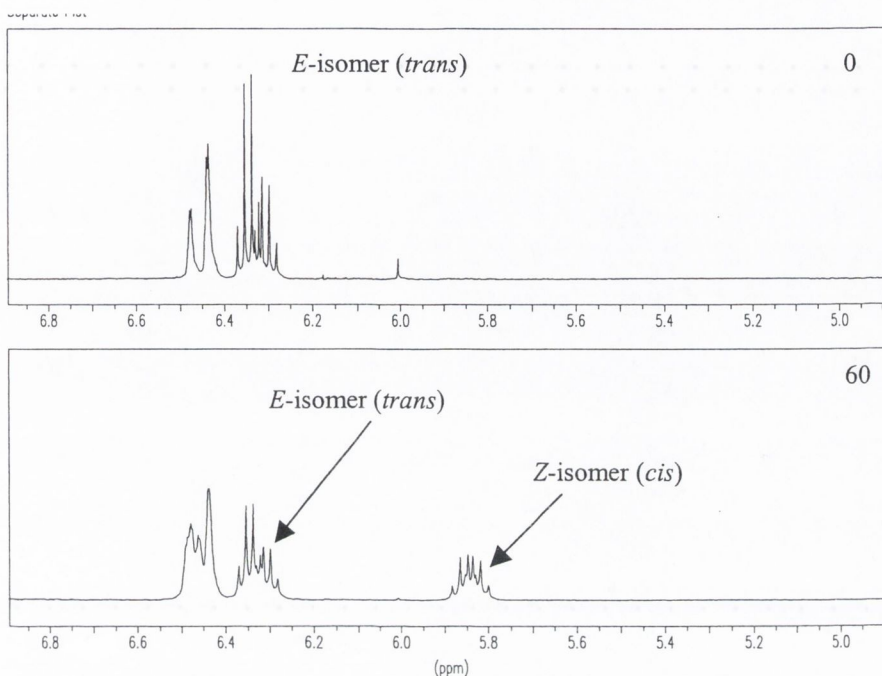


Fig. 4.13: Formation of *cis*-isomer on irradiation of solution containing *trans* isomer –  
 Top spectrum: no irradiation, bottom spectrum after 60 minutes irradiation

*Cis-trans* isomerisation of *E*-1-phenylpropene is also observed in the latter two experiments. (Fig. 4.13) As a glass filter is used in the experiment, this isomerism is most likely caused by the enone excited state. In both the enone-alkene experiments, there is a linear decrease of *trans* isomer with a corresponding increase in *cis* isomer.

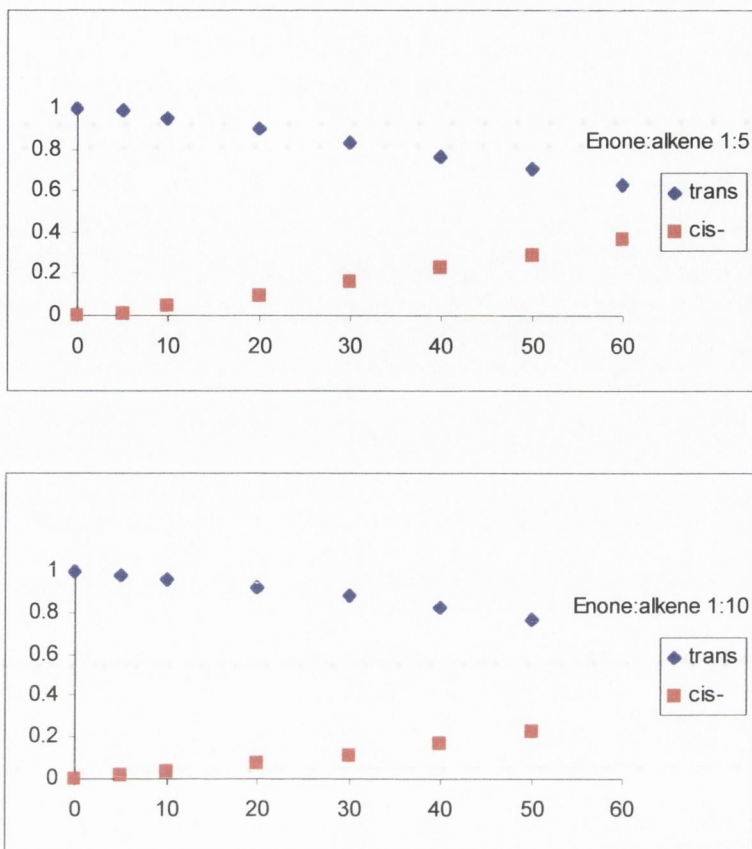


Fig. 4.13: Ratio of *trans*: *cis* isomers of 1-phenylpropene after irradiation time  $t$

**4.2.2.3 Irradiation of 6-methoxy-3-phenylindenone (benzene) 407** (10 mM) in degassed  $d_6$ -benzene was irradiated in an NMR tube in a manner analogous to above. Samples were monitored over a 70 minute time period. Over time, several new peaks appeared, and the peak due to initial starting material depleted. In the initial unexposed sample, the methoxy singlet of the enone is observed at 3.25 ppm. On irradiation, peaks at 3.15 and 3.9 ppm grow in. These integrate to a ratio of 3 : 1 respectively. These are therefore assigned as the methoxy singlet and  $\alpha$ -hydrogen of the dimer. There are no other peaks of interest in this region.



#### 4.2.2.4 6-methoxy-3-phenylindenone in the presence of 1-phenylpropene (benzene)

**407** (10 mM) was dissolved in  $d_6$ -benzene and *E*-1-phenylpropene (50 mM) added. The sample was exposed to UV irradiation as before, and the change in NMR spectra recorded. The dimerisation reaction observed above was again seen here - and it is the dominant reaction in this scheme.

Another sharp singlet is growing in at 3.0 ppm. The spectrum taken at 30 minutes shows this peak, and two others along with the peaks observed for the dimer in the 2 - 4 ppm range. The other two peaks, at 2.8 ppm and 3.4 ppm are a double doublet and a doublet respectively. These signals may be due to an adduct formed on cycloaddition between the enone and alkene. The evidence for this is as follows. The ratio of integrations of the signal assigned as adduct methoxy (3.0 ppm) to the peaks at 2.8 and 3.4 ppm is 3 : 1 : 1. The signal at 2.8 ppm is a double doublet, with splittings of 5 and 2 Hz. (Fig.4.15) The signal at 3.4 ppm is a doublet with a coupling constant of 2 Hz. The double doublet, if it is an adduct proton is therefore the hydrogen  $H_b$  (Fig.4.14), and the doublet either that marked  $H_a$  or  $H_c$ . A third signal, due to a third aliphatic hydrogen in the adduct is not observed.

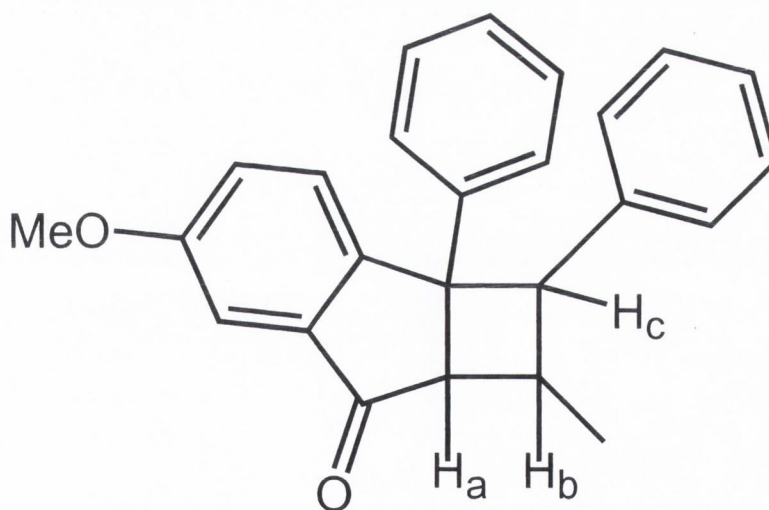


Fig. 4.14: Adduct that may be formed on irradiation of **407** in the presence of 1-phenylpropene

The formation of dimer is again preferential compared to the formation of adduct, although changing solvent from acetonitrile to benzene has had a positive effect on adduct formation. *Cis-trans* isomerisation is much less effective in benzene than was observed for acetonitrile. At thirty minutes, the ratio of *trans*- : *cis*- was 98 : 2. After 90 minutes the ratio was 91 : 9.

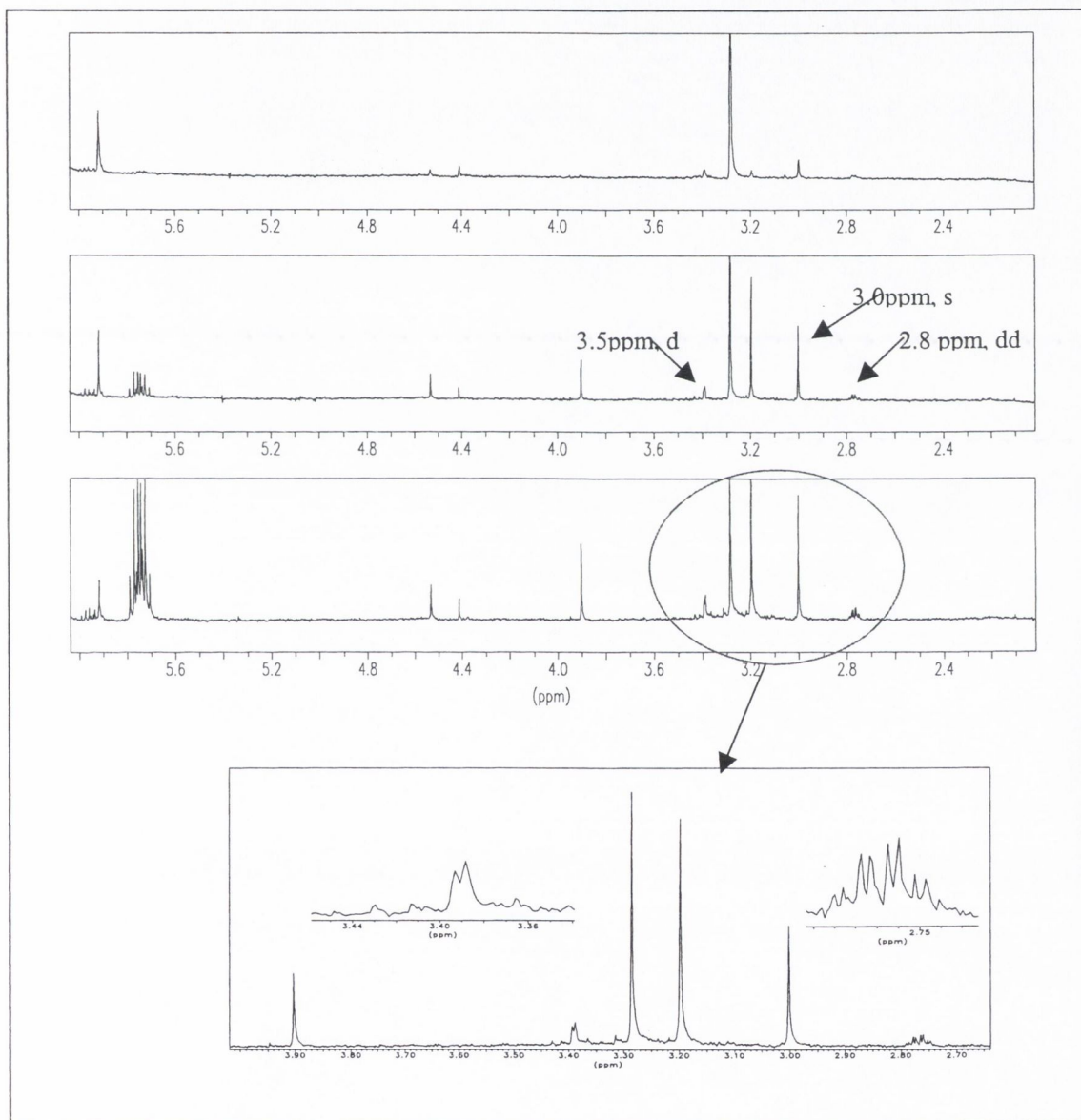


Fig. 4.15: NMR spectra of 407 after irradiation in the presence of 1-phenylpropene after 0, 30 and 90 minutes.

## 4.3 DISCUSSION

### 4.3.1 Experimental Procedure

The method of irradiation of samples in an NMR tube provided a convenient way of monitoring NMR spectra over time. Samples were degassed by bubbling with continuous stream argon for 30 minutes. Samples were then irradiated directly by a mercury lamp, after passage through a glass filter. A separate experiment, where the sample was degassed using the freeze pump thaw method, and the sample irradiated in the UV cell of the freeze-pump thaw apparatus was carried out. Samples were taken at various times and examined by NMR. There was little difference between the NMR spectra obtained for the samples degassed by bubbling and those degassed by freeze-pump thaw. The much more convenient method of degassing by bubbling was used. This had the added advantage that the whole sample could be directly monitored, so there was no change in concentration or environment.

### 4.3.2 6-Methoxy-3-phenylindenone

The UV spectrum of **407** shows two bands which have been assigned to  $\pi,\pi^*$  and charge-transfer (CT) bands. The assignment of this CT band is likely, given that 2-carbethoxy-6-methoxy-3-phenylindenone also has this long wavelength absorption, whereas 3-phenylindenone does not. The shift of 18 nm to the red on going from non-polar to polar solvent is relatively small compared to, for example, 3-(4'-N, N-dimethylaminophenyl)cyclopentenone, whose shift on going from cyclohexane to ethanol is 31 nm to the red.<sup>6</sup>

Flash photolysis of the enone in deaerated solution failed to produce any observable transient species. Various concentrations were tried. This is either due to the fact that the transient is too short lived (*e.g.* due to rapid self quenching) or the intensity of the transient is too low to be detected by the photomultiplier.



The NMR spectrum of **407** is relatively simple, showing an ABC type coupling of the fused ring hydrogens (double doublet and two doublets) in the aromatic region and both the methoxy and  $\alpha$ -hydrogen giving singlets in otherwise vacant aliphatic regions. It is very suitable therefore for analysis by NMR, as the decay of the enone can be monitored by the depletion of these singlets.

On irradiation of the enone, in both acetonitrile and benzene, the adduct is formed. The formation of dimer is more efficient in acetonitrile than in benzene. For example, after 40 minutes of irradiation of the enone in acetonitrile, the monomer peak is minimal compared to the dimer, whereas in benzene, the monomer : dimer ratio is 1:3 after 40 minutes. In addition the reaction in benzene is much cleaner than in acetonitrile. In particular, a lot of unassignable peaks occur just downfield of the monomer methoxy singlet in the acetonitrile reaction, whereas the benzene reaction is very clean.

The reason for different reactivities may be due to solvent type. In acetonitrile, the highly aromatic enone may associate, forming  $\pi$ -stack type arrays in the polar acetonitrile solvent (*Fig. 4.16*). On irradiation therefore, the enone excited state is very close to another enone ground state, and reaction will take place between the two quite quickly. Dimerisation therefore is quite efficient. However, no evidence of aggregation was observed by uv/vis spectroscopy - plots of absorption versus concentration were linear.

In benzene, there is no driving force behind the association of the enone molecules, as the benzene molecules may become part of this  $\pi$ -stacking, and so the enone disperses evenly through the solvent. Therefore on irradiation, [enone]\*-[enone] interaction is diffusion controlled, and so is lower than that observed in acetonitrile.

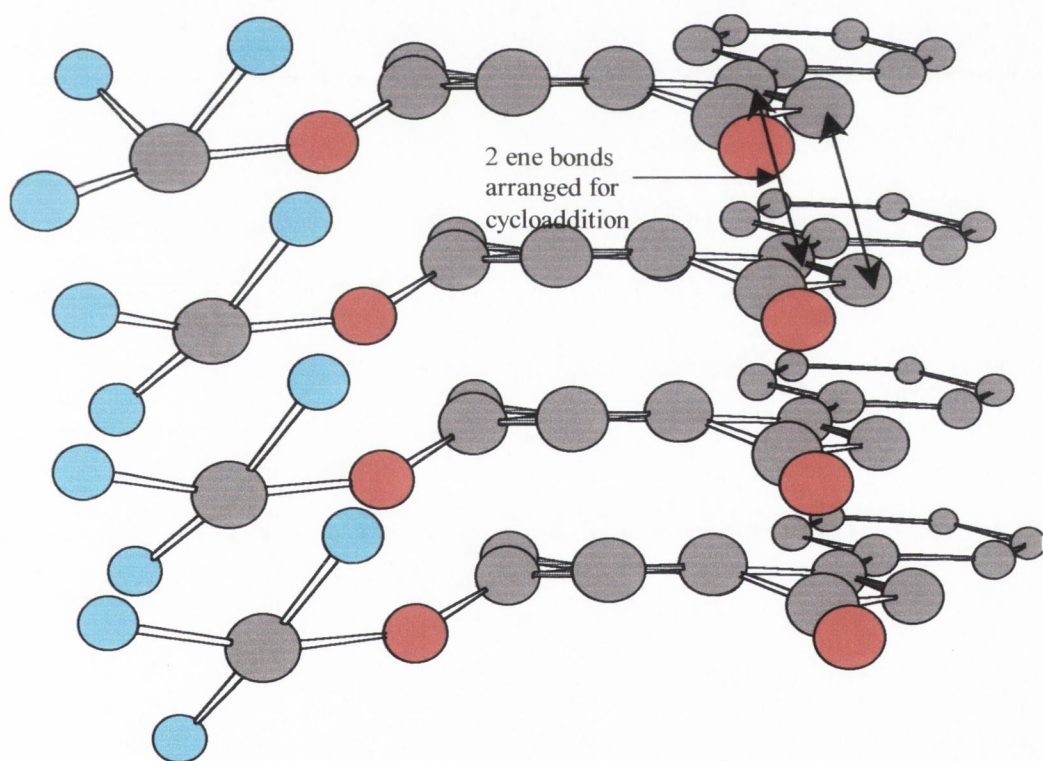
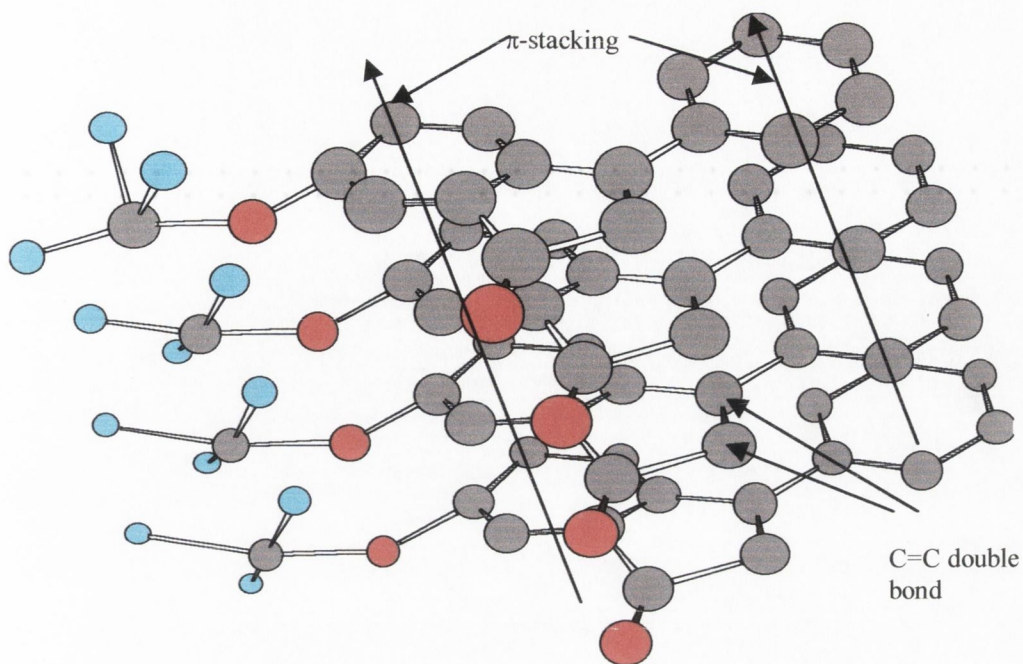


*Fig. 4.16 – Models of  $\pi$ -stacking of indenones – a process that may enhance dimerisation*



### 4.3.3 Irradiation of 6-Methoxy-3-phenylindenone in the presence of 1-phenylpropene

Irradiation of the enone in the presence of alkene produces mainly dimer, in both solvents. This was a disappointing outcome of the experiment, as the initial aim was to produce enone-alkene cycloadducts. In acetonitrile, no adducts were observed, and dimer formation was as rapid as it has been in the enone only case. In benzene, what is thought to be a small amount of adduct was observed. The dimer formation was slower in this case, after 90 minutes, the ratio of monomer to dimer was 1:1.

The difference in reactivity in the two solvents can be explained by a similar hypothesis to above. The enone-enone interaction described above remains strong in acetonitrile, and is overwhelmingly favourable to enone-alkene interaction. In addition, enone-alkene reactions do not appear to lead to ring closure in the majority of cases. Considering benzene, the enone-enone interactions are still dominant, but less so than in the enone only samples. There are two possibilities – that there are less enone-enone interactions leading to product or that the enone-alkene reactions do not lead to adducts. The former is unlikely – there is no reason to suggest that enone-enone interactions leading to product should be less efficient than in the enone only case. The latter reason therefore suggests that enone-alkene reactions do occur, but ring closure is very inefficient. This is supported by the fact that increasing the enone-alkene ratio from 1:1 to 1:10 had little effect on the reaction outcome.

### 4.3.4 *Cis-Trans* Isomerisation

Enone-alkene interactions have two possible outcomes: that the enone excited state is quenched by the alkene, resulting in energy transfer to the alkene/solvent, or that the interaction leads to an intermediate biradical, whose rate of reaction back to starting materials is faster than the forward reaction to products. The amount of *trans-cis* isomerisation is much greater in acetonitrile (4:1 after 40 minutes) than in benzene (9:1 after 90 minutes). Isomerisation is caused by the enone triplet being quenched by the



alkene. Therefore, using the idea of the different dispersion methods of the enone in different solvents, this would suggest that in acetonitrile, the alkene molecules themselves aggregate around the enone stacks (remembering that the 1-phenylpropene is itself  $\pi$ -electron rich), and are sensitised to the *cis*-isomer. In benzene, the two compounds are much more disperse, and so the interaction is lower.

The supposition above is that **407** forms a planar molecule which stacks in acetonitrile solution. To test this, some ab-initio geometry calculations were carried out. The model used was 3-phenylindenone, as the methoxy group will have little effect, and adds to computational requirements as it is difficult to find an optimal structure.

Calculations were carried out using the 6-31G\* basis set. The molecule was optimised and the torsion angle of the phenyl group rotated from its minimum through a range of angles. From the depth of the potential well created, it is possible to calculate the energy required for the phenyl group to rotate from its minimum to maximum.

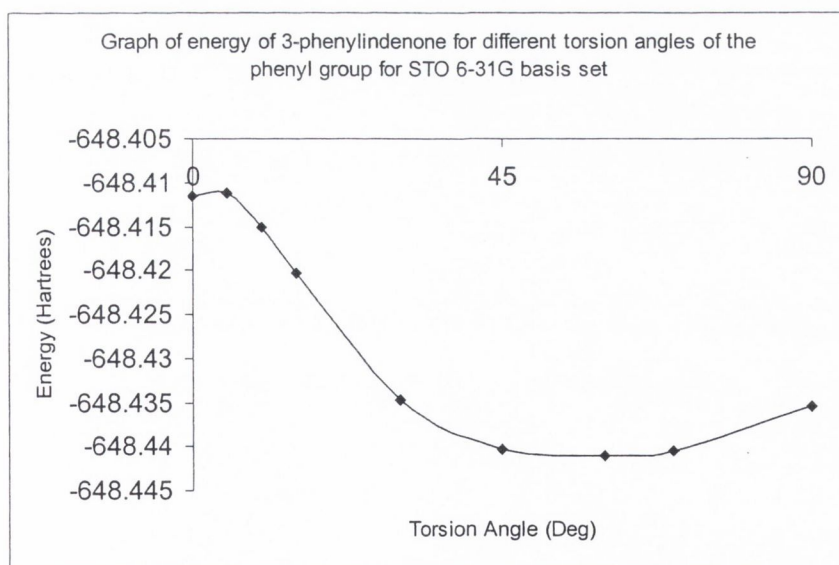


Fig. 4.17: Variation in energy of molecule on rotation of phenyl substituent

The results obtained are shown in Fig. #. It shows a broad minimum between 45 and 60°, which would be expected, comparing it to the crystal structures obtained for the

bromoindenone in Chapter 3. However, the energy well is quite low, about 0.03 Hartrees, which corresponds to about  $75 \text{ kJ mol}^{-1}$  (0.8 eV). Therefore the energy barrier for the molecule to rotate from its minimum at  $45 - 60^\circ$  to being planar is not prohibitive.

## 4.4 CONCLUSIONS

The reaction of 6-methoxy-3-phenylindenone to 1-phenylpropene has been studied. NMR was used as a diagnostic tool and proved to be very useful in following the reactions over time. It is found that this enone preferentially undergoes dimerisation. This has been attributed to the arrangement of the enone in the solvents, facilitating dimerisation over adduct formation.

## 4.5 References Cited

---

- 1 W. H. Horspool, *Photochemistry*, 2001, **32**, 74.
- 2 J. F. D. Kelly, J. M. Kelly and T. B. H. McMurry, *J. Chem. Soc. Perkin Trans. 2*, 1996, 1933 and refs within.
- 3 M. L. Randall, P. C. K. Lo, P. J. Bonitatebus and M. L. Snapper, *J. Am. Chem. Soc.*, 1999, **121**, 4534.
- 4 M. T. Crimmins, J. M. Pace, P. G. Nantermet, A. S. Kim-Meade, J. B. Thomas, S. H. Watterson and A. S. Wagner, *J. Am. Chem. Soc.*, 1999, **121**, 10249.
- 5 J. F. D. Kelly, M. E. Doyle, M. Guha, P. V. Kavanagh, J. M. Kelly and T. B. H. McMurry, *J. Chem. Soc. Perkin Trans. 2*, 1998, 1635.
- 6 J. F. D. Kelly, Ph.D Thesis, University of Dublin, 1998.



*Chapter Five*

*Materials and Methods*

## 5.1 MATERIALS

### 5.1.1 Reagents

All reagents used in synthesis of compounds as described were purchased from Aldrich Chemical Company, and used without further purification. 3-phenylcyclohexenone was prepared according to the procedure of Walker.<sup>1</sup> It was purified by vacuum sublimation according to Kelly *et al.*<sup>2</sup> Other reagents for photophysical and photochemical study were purchased from Aldrich Chemical Company and used as received.

### 5.2.2 Solvents

Solvents for synthesis and chromatography were obtained from the Hazardous Materials Facility, Trinity College. Ethyl acetate, hexane, dichloromethane were distilled prior to use. Diethyl ether was dried over calcium chloride and distilled sodium/benzophenone. Ethanol was distilled over magnesium turnings and iodine. Other solvents were used as received.

Solvents for spectroscopy were obtained as spectroscopic grade and used as received. Deutero solvents were used as received (99+% atom).

## 5.2 METHODS

### 5.2.1 NMR Spectroscopy

NMR spectra were recorded on a Bruker DPX 400 (<sup>1</sup>H at 400.13 MHz, <sup>13</sup>C at 100 MHz) instrument. NMR data are recorded in  $\delta$  values relative to tetramethylsilane at 0.0ppm. Splittings between peaks are given in Hz.

### **5.2.2 UV/vis Absorption Spectroscopy**

Absorption spectra were recorded on a Shimadzu UV-2401 PC spectrometer or a Cary 300 Scan spectrometer with the light sources in both cases being tungsten and deuterium. Samples were contained in a 1cm<sup>2</sup> cuvette with quartz windows.

### **5.2.3 Infrared Absorption Spectroscopy**

Infrared spectra were recorded on a Mattson Genesis II FTIR spectrometer. Samples were prepared either as Nujol mulls, applied neat to NaCl windows or dissolved in *d*<sub>3</sub>-acetonitrile and recorded between CaF<sub>2</sub> windows.

### **5.2.4 Electrospray Mass Spectrometry**

ESMS spectra were recorded on a Micromass LCG TOF mass spectrometer. Sample concentrations were made up to be less than 10<sup>-6</sup> M.#

### **5.2.5 Chromatography**

TLC analyses were run on Merck silica gel 60 f<sub>254</sub> precoated plates. Flash chromatography was performed in the manner of Still<sup>3</sup> using Merck grade flash silica.

### **5.2.6 Laser Flash Photolysis and Transient Absorption Spectroscopy**

Nanosecond laser flash photolysis was carried out using a Spectron Nd:YAG Q-switched laser which provided single shot pulses of 15 ns duration. Energies were measured periodically and averaged at *ca.* 38mJ per pulse at 355nm. The analysing light was provided by a 250 W xenon arc lamp at right angles to the laser pulse. The analysing light passed through the sample cell and into an Applied Photophysics f3/4 monochromator, onto a Hamamatsu R928 photomultiplier. The photomultiplier response was fed to a Tektronix TDS 380 digital oscilloscope. (*Fig. 5.1*)



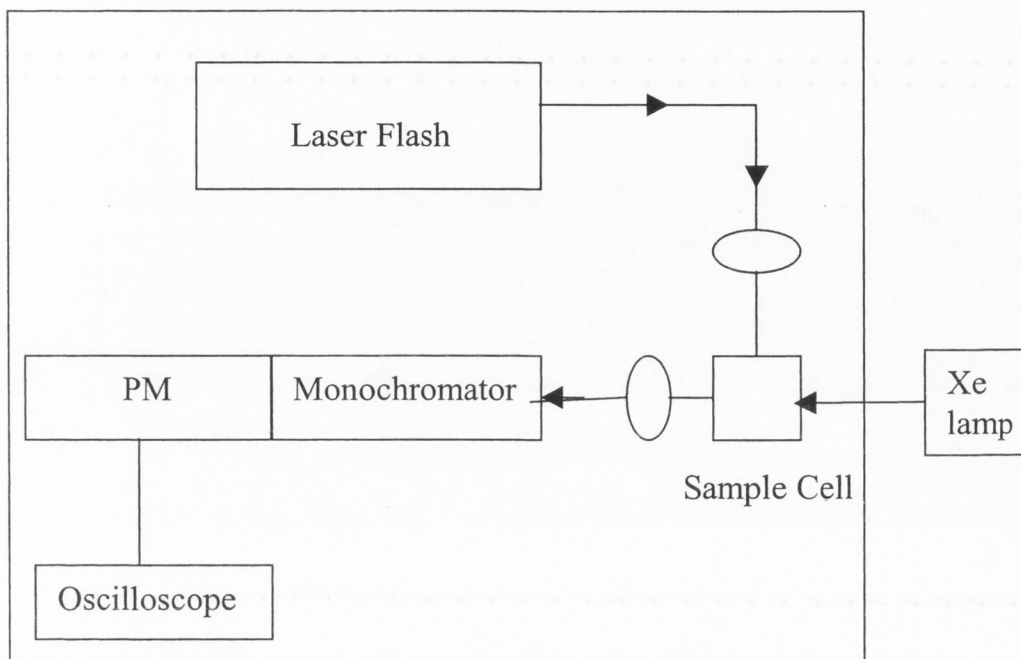


*Fig. 5.1: Schematic of laser flash photolysis apparatus (PM = photomultiplier)*

Operation of the apparatus is described briefly: The pump of the laser is turned on (“PUMP ON”) and left for ~30 minutes. A small flow of water is allowed in to the laser. The Xe lamp, if required is struck, and cooling water and fan turned on. All interlocks to the laser room (blinds, door) are closed and the interlock circuit switched on. “Reset” is pressed to activate the interlock. After the laser head is warmed up (30 minutes after turning on pump) the laser may be switched on. (“LASER ON”) All interlock LEDs should be off on the laser power supply box. The “External” LED indicates that the door interlock is not on, and needs to be activated. The interlock “Thermostat” may come on after some time of operation. This indicates that there is not enough external water flowing through the laser cooling system. In this case, the water pressure should be increased, (water will now flow out of the outlet pipe) and the pump turned off, turned on (at which point the “Thermostat” LED should be off) and the laser turned on again in immediate sequence. The outlet water flow should be monitored regularly. A similar procedure should be followed if the “Simmer” interlock LED is illuminated. In

this case, the interlock will switch off when the laser is powered on again. Other interlocks are described in the laser manual.

When powering down, the laser should be turned off (“LASER OFF”) and the pump left on for ~15 minutes, after which time the key can be turned off and removed. The door interlocks may be turned off as soon as the laser is turned off (*i.e.* the laser pump works without the door interlock activated). The external water flow should be turned off when the pump is turned off. For the Xe lamp, the water should be allowed to flow through for ~15 minutes after powering off.

Samples are prepared in a degassing cell (1cm<sup>2</sup> quartz cell) and the freeze pump thaw method used. At least three cycles are used. An absorbance of less than 0.8 at the excitation wavelength is optimum.

Transient absorption spectra are recorded by analysing the peak height of the transient  $\Delta I$  at sequential wavelengths. The change in optical density  $\Delta OD$  is given by the expression:

$$\Delta OD = \log_{10} \left( \frac{I_0 - \Delta I}{\Delta I} \right)$$

where  $I_0$  is the intensity of the incident light. Kinetic fits to decay traces were done by fitting the data points from the oscilloscope in the Sigma Plot v.4.0 analysis program.

### **5.2.7 Step-Scan Fourier Transform Time-Resolved Infrared Spectroscopy (s<sup>2</sup>-FT-TRIR)**

Time-resolved infrared spectroscopy (TRIR) was carried out in the University of Nottingham in the laboratories of Dr. Michael George, working with Dr. Chris Colley and Jixin Yang. The experimental set-up in Nottingham has been described<sup>4, 5</sup> and is outlined briefly here.

Carbon tetrachloride was analytical grade from Fisher Scientific, and acetonitrile was HPLC grade from Arcos Organics. *d*<sub>3</sub>-acetonitrile was purchased from Aldrich.

The technique is a combination of flash photolysis and fast infrared detection. The interferometer was a Nicolet Magna 860 and laser excitation was provided by a Nd:YAG laser (Spectron SL850G) at 355nm excitation wavelength or a Lumonics Excimer laser at 308nm. Power output for the Nd:YAG was measured to be ~150mJ per pulse at 355nm, and for the excimer ~100mJ per pulse at 308 nm. The detector was a mercury-cadmium-telluride (MCT) photovoltaic detector.

The infrared detector beam was passed through an external optical bench (Nicolet-TOM<sup>®</sup>), on which the MCT detector and sample cell is located. This is contained in a clear-walled box, flushed with dry air to minimise water vapour interaction.

UV spectra were recorded in a 1mm path length cell. FTIR spectra were recorded as a solution between CaCl<sub>2</sub> plates, separated with Teflon spacers. The path-length was checked with Vernier callipers.

Samples for TRIR spectroscopy were prepared as follows: solutions were made up to 10 – 20 mL volume of solvent and entered into a flow cell. The samples were degassed by evacuating the flow cell reservoir and shaking it vigorously several times. The flow system was evacuated and argon (2atm) entered. The reservoir was connected and the solution bubbled with argon. The whole system was evacuated and filled with argon three times, the final pressure of argon being 1.5 atm.

Output to the PC was in the form of a series of spectra across the time range being studied. One could view the entire range of spectra on a three-dimensional graph (although in general the signal: noise ratio was too poor for this to be of use) or look at individual spectra at any time. In identifying a peak, spectra across the time range were



examined to ensure that the peak was not an artifact at a particular time range – in other words – that the peaks decay profile was as would be expected (initial rise and decay for transient peaks, initial drop and re-growth for starting materials, rise and leveling for photoproducts) A useful tool was that which allowed the decay profile of any wavelength to be plotted against time. In this way artifacts could be avoided, and one could be reasonably assured that peaks identified were real transients. Decay profiles were fitted to single exponential curves using Igor Wavemetrics software.

### 5.3 REFERENCES CITED

---

- 1 G. N. Walker, *J. Am. Chem. Soc.*, 1955, **77**, 3664.
- 2 J. F. D. Kelly, Ph.D. Thesis, University of Dublin 1998.
- 3 W. C. Still, M. Kahn and A. Mitra, *J. Org. Chem.*, 1978, **43**, 2923.
- 4 X. Z. Sun, S. M. Nikoiforov, X. Y. Yang, C. S. Colley and M. W. George, *Appl. Spec.*, 2002, **56**, 31.
- 5 X. Z. Sun, Ph.D. Thesis, University of Nottingham, 2000.

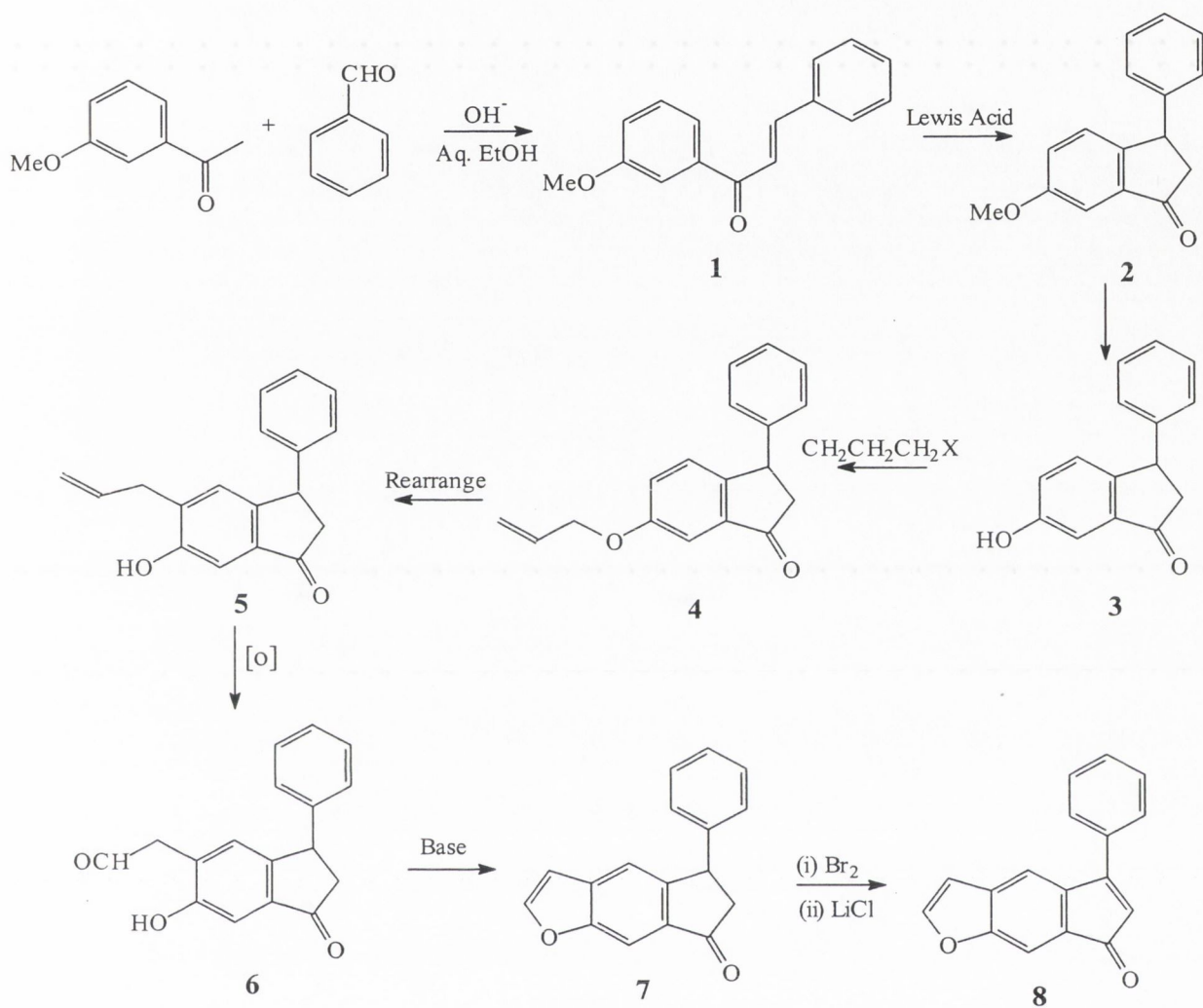
## Future Work

In Chapter Two, the interaction of 3-phenylcyclohexeneone with 1-phenylpropene was examined. The nature of the intermediates in this reaction have been the subject of much debate and time-resolved infrared spectroscopy offers a very powerful tool to examine these intermediates. Further work in this area could concentrate on the following areas:

- (i) The examination of the enone-alkene reaction at lower resolution to obtain a more detailed spectrum and see if a second peak in the product region can be resolved;
- (ii) Kinetics at wavelengths of interest using either diode single frequency IR sources or the step-scan technique;
- (iii) Examination of reaction with different alkenes - those with electron withdrawing and donating substituents and monitor the placement of intermediate peaks;
- (iv) Investigation of the reaction with  $^{18}\text{O}$  labelled enone.

In Chapter Three, the synthesis of 6-methoxy-3-phenylindenone was undertaken. This is a synthetic precursor to a psoralen analogue as mentioned. The full proposed synthetic route to this furanoindenone is shown below. The examination of the interaction of this enone with alkenes and thymine would provide extremely useful information on the potential of this compound as a photoactive DNA binder.





Finally in Chapter Four, the interaction of 6-methoxy-3-phenylindenone with (*E*)-1-phenylpropene was studied. This showed strong bias towards dimerisation. Similar reactions with the other substituted indenones could be carried out to examine the effect of substituents on the rate of reactivity with alkenes.

## **Appendices**

**Appendix 1:** X-ray Crystal Structure Data for 2-bromo-6-methoxy-3-phenylindanone

**Appendix 2:** X-ray Crystal Structure Data for 2-bromo-6-methoxy-3-phenylindenone

## Appendix 1

### X-ray Crystal Structure Data for 2-bromo-6-methoxy-3-phenylindanone

Identification code	mich213m	
Empirical formula	C <sub>16</sub> H <sub>13</sub> Br O <sub>2</sub>	
Formula weight	317.17	
Temperature	568(2) K	
Wavelength	0.71073 Å	
Crystal system	Monoclinic	
Space group	Cc	
Unit cell dimensions	a = 9.3532(16) Å	α = 90°.
	b = 27.521(5) Å	β = 126.210(2)°.
	c = 6.4138(11) Å	γ = 90°.
Volume	1332.1(4) Å <sup>3</sup>	
Z	4	
Density (calculated)	1.582 g/cm <sup>3</sup>	
Absorption coefficient	3.080 mm <sup>-1</sup>	
F(000)	640	
Crystal size	0.2 x 0.2 x 0.3 mm <sup>3</sup>	
Theta range for data collection	2.80 to 23.28°.	
Index ranges	-10 ≤ h ≤ 10, -30 ≤ k ≤ 30, -7 ≤ l ≤ 7	
Reflections collected	4034	
Independent reflections	1885 [R(int) = 0.1021]	
Completeness to theta = 23.28°	99.9 %	
Refinement method	Full-matrix least-squares on F <sup>2</sup>	
Data / restraints / parameters	1885 / 2 / 173	
Goodness-of-fit on F <sup>2</sup>	1.007	
Final R indices [I > 2σ(I)]	R1 = 0.0404, wR2 = 0.0981	
R indices (all data)	R1 = 0.0416, wR2 = 0.0989	
Absolute structure parameter	0.001(13)	
Largest diff. peak and hole	0.543 and -0.542 e.Å <sup>-3</sup>	



Atomic coordinates ( $\times 10^4$ ) and equivalent isotropic displacement parameters ( $\text{\AA}^2 \times 10^3$ )

for mich213m.  $U(\text{eq})$  is defined as one third of the trace of the orthogonalized  $U_{ij}$  tensor.

	x	y	z	U(eq)
C(17)	5398(7)	6581(2)	10491(11)	59(1)
Br(1)	3786(1)	9446(1)	7565(1)	63(1)
O(2)	6370(5)	6751(1)	9551(7)	51(1)
O(1)	4262(4)	8491(1)	10863(6)	53(1)
C(9)	6232(5)	8206(2)	7753(7)	38(1)
C(10)	6818(8)	9372(2)	5269(10)	45(1)
C(8)	5626(5)	8064(2)	9181(8)	38(1)
C(5)	6969(6)	7376(2)	7697(9)	44(1)
C(3)	5872(5)	8735(2)	7045(7)	40(1)
C(6)	6296(6)	7236(2)	9055(8)	41(1)
C(4)	6931(6)	7851(2)	7026(8)	44(1)
C(15)	7282(5)	9026(2)	7127(7)	39(1)
C(13)	10329(7)	9272(3)	9371(12)	58(2)
C(7)	5650(5)	7583(2)	9867(8)	42(1)
C(1)	4988(6)	8481(2)	9808(8)	42(1)
C(12)	9832(7)	9624(2)	7500(12)	57(1)
C(2)	5504(6)	8924(2)	8931(8)	43(1)
C(14)	9078(6)	8978(2)	9195(9)	50(1)
C(11)	8072(7)	9666(2)	5436(10)	54(1)

Bond lengths [Å] and angles [°] for mich213m.

---

C(17)-O(2)	1.435(7)
Br(1)-C(2)	1.936(4)
O(2)-C(6)	1.363(6)
O(1)-C(1)	1.210(6)
C(9)-C(8)	1.388(7)
C(9)-C(4)	1.399(7)
C(9)-C(3)	1.504(7)
C(10)-C(11)	1.376(9)
C(10)-C(15)	1.380(7)
C(8)-C(7)	1.392(7)
C(8)-C(1)	1.456(7)
C(5)-C(4)	1.370(7)
C(5)-C(6)	1.397(7)
C(3)-C(15)	1.517(6)
C(3)-C(2)	1.531(7)
C(6)-C(7)	1.386(7)
C(15)-C(14)	1.402(7)
C(13)-C(14)	1.372(9)
C(13)-C(12)	1.390(10)
C(1)-C(2)	1.535(7)
C(12)-C(11)	1.379(8)
C(6)-O(2)-C(17)	117.5(4)
C(8)-C(9)-C(4)	118.4(4)
C(8)-C(9)-C(3)	111.5(4)
C(4)-C(9)-C(3)	129.9(4)
C(11)-C(10)-C(15)	121.3(5)
C(9)-C(8)-C(7)	122.8(4)
C(9)-C(8)-C(1)	110.7(4)
C(7)-C(8)-C(1)	126.5(4)
C(4)-C(5)-C(6)	121.4(4)
C(9)-C(3)-C(15)	117.7(4)

C(9)-C(3)-C(2)	101.8(4)
C(15)-C(3)-C(2)	113.0(4)
O(2)-C(6)-C(7)	124.0(4)
O(2)-C(6)-C(5)	115.9(4)
C(7)-C(6)-C(5)	120.1(5)
C(5)-C(4)-C(9)	119.5(4)
C(10)-C(15)-C(14)	118.1(5)
C(10)-C(15)-C(3)	120.7(4)
C(14)-C(15)-C(3)	121.0(4)
C(14)-C(13)-C(12)	120.4(5)
C(6)-C(7)-C(8)	117.7(4)
O(1)-C(1)-C(8)	129.0(5)
O(1)-C(1)-C(2)	126.1(4)
C(8)-C(1)-C(2)	104.8(4)
C(11)-C(12)-C(13)	119.2(5)
C(1)-C(2)-C(3)	106.6(4)
C(1)-C(2)-Br(1)	113.5(3)
C(3)-C(2)-Br(1)	114.1(3)
C(13)-C(14)-C(15)	120.6(5)
C(12)-C(11)-C(10)	120.3(5)

---



Anisotropic displacement parameters ( $\text{\AA}^2 \times 10^3$ ) for mich213m. The anisotropic displacement factor exponent takes the form:  $-2\pi^2 [ h^2 a^{*2} U^{11} + \dots + 2 h k a^* b^* U^{12} ]$

	U <sup>11</sup>	U <sup>22</sup>	U <sup>33</sup>	U <sup>23</sup>	U <sup>13</sup>	U <sup>12</sup>
C(17)	55(3)	58(3)	61(3)	14(3)	33(3)	2(2)
Br(1)	67(1)	53(1)	84(1)	8(1)	53(1)	13(1)
O(2)	55(2)	42(2)	56(2)	5(2)	33(2)	-2(2)
O(1)	62(2)	63(2)	52(2)	-2(2)	44(2)	-1(2)
C(9)	38(2)	44(3)	31(2)	-2(2)	21(2)	-3(2)
C(10)	58(3)	43(3)	46(3)	3(2)	37(2)	5(2)
C(8)	36(2)	43(3)	35(2)	-1(2)	21(2)	-1(2)
C(5)	43(2)	45(3)	43(2)	-1(2)	24(2)	4(2)
C(3)	41(2)	46(3)	36(2)	-1(2)	24(2)	-2(2)
C(6)	37(2)	46(3)	34(2)	2(2)	17(2)	-2(2)
C(4)	50(2)	50(3)	43(2)	-1(2)	34(2)	-1(2)
C(15)	45(2)	40(3)	41(2)	-1(2)	30(2)	1(2)
C(13)	47(3)	64(4)	67(3)	-6(3)	37(3)	-1(3)
C(7)	41(2)	54(3)	34(2)	3(2)	24(2)	-6(2)
C(1)	41(2)	51(3)	33(2)	-1(2)	23(2)	0(2)
C(12)	64(3)	52(3)	81(4)	-8(3)	57(3)	-9(2)
C(2)	40(2)	41(3)	44(2)	-2(2)	23(2)	3(2)
C(14)	45(2)	55(3)	50(2)	7(2)	28(2)	4(2)
C(11)	79(4)	43(3)	66(3)	10(2)	57(3)	5(2)

Hydrogen coordinates ( $\times 10^4$ ) and isotropic displacement parameters ( $\text{\AA}^2 \times 10^3$ )  
for mich213m.

	x	y	z	U(eq)
H(17A)	5914	6711	12184	88
H(17B)	5442	6232	10573	88
H(17C)	4187	6685	9343	88
H(10)	5634	9408	3877	54
H(5)	7453	7142	7238	53
H(3)	4770	8759	5293	48
H(4)	7365	7937	6095	52
H(13)	11517	9237	10751	69
H(7)	5245	7497	10838	51
H(12)	10677	9828	7638	69
H(2)	6623	9050	10450	51
H(14)	9424	8745	10460	60
H(11)	7731	9894	4150	65

## Appendix 2

### X-ray Crystal Structure Data for 2-bromo-6-methoxy-3-phenylindenone

Identification code	michsm	
Empirical formula	C <sub>16</sub> H <sub>11</sub> Br O <sub>2</sub>	
Formula weight	315.16	
Temperature	568(2) K	
Wavelength	0.71073 Å	
Crystal system	Triclinic	
Space group	P1	
Unit cell dimensions	a = 7.6222(11) Å	α = 104.204(2)°
	b = 8.1632(12) Å	β = 92.342(3)°
	c = 10.8258(16) Å	γ = 94.563(2)°
Volume	649.66(16) Å <sup>3</sup>	
Z	2	
Density (calculated)	1.611 Mg/m <sup>3</sup>	
Absorption coefficient	3.157 mm <sup>-1</sup>	
F(000)	316	
Crystal size	0.2 x 0.2 x 0.3 mm <sup>3</sup>	
Theta range for data collection	1.94 to 26.39°.	
Index ranges	-9 ≤ h ≤ 9, -10 ≤ k ≤ 10, -13 ≤ l ≤ 13	
Reflections collected	6924	
Independent reflections	4643 [R(int) = 0.0162]	
Completeness to theta = 26.39°	98.5 %	
Absorption correction	None	
Refinement method	Full-matrix least-squares on F <sup>2</sup>	
Data / restraints / parameters	4643 / 3 / 345	
Goodness-of-fit on F <sup>2</sup>	1.013	
Final R indices [I > 2σ(I)]	R1 = 0.0398, wR2 = 0.1011	
R indices (all data)	R1 = 0.0513, wR2 = 0.1086	
Absolute structure parameter	0.28(3)	
Largest diff. peak and hole	0.648 and -0.243 e.Å <sup>-3</sup>	



Atomic coordinates ( $\times 10^4$ ) and equivalent isotropic displacement parameters ( $\text{\AA}^2 \times 10^3$ )

for michsm.  $U(\text{eq})$  is defined as one third of the trace of the orthogonalized  $U_{ij}$  tensor.

	x	y	z	U(eq)
Br(1)	5046(1)	2210(1)	2018(1)	60(1)
Br(2)	8071(1)	7961(1)	6342(1)	60(1)
O(5)	10694(11)	760(11)	830(6)	55(2)
O(6)	2456(11)	9360(10)	7519(8)	61(2)
C(23)	9986(13)	3225(14)	2333(10)	53(3)
C(8)	3634(14)	6160(12)	4960(10)	39(2)
C(24)	9449(13)	4025(13)	3517(10)	38(2)
C(7)	3118(12)	6918(10)	6107(7)	35(2)
C(1)	4005(14)	4316(11)	4352(10)	48(3)
O(3)	3923(11)	3210(9)	4913(8)	59(2)
O(4)	9223(12)	6942(9)	3435(9)	66(2)
C(17)	9142(12)	5802(13)	3955(10)	43(2)
C(18)	8675(12)	5903(10)	5310(8)	39(2)
C(2)	4507(13)	4227(13)	3038(11)	52(3)
C(19)	8678(12)	4379(11)	5599(10)	42(2)
C(3)	4473(12)	5783(12)	2805(8)	39(2)
C(6)	2937(12)	8689(10)	6299(8)	39(2)
C(22)	10240(13)	1522(12)	2009(9)	49(3)
C(25)	9148(12)	3226(12)	4413(9)	38(2)
C(9)	3936(13)	7074(12)	3947(9)	39(2)
C(15)	4780(12)	6245(10)	1609(9)	39(2)
C(31)	8315(14)	3909(13)	6798(9)	44(2)
C(10)	5869(14)	7679(13)	1588(9)	54(3)
C(30)	7226(11)	2480(10)	6793(9)	42(2)
C(5)	3181(14)	9514(11)	5410(9)	49(2)
C(21)	9934(12)	628(12)	2984(10)	46(2)
C(32)	11076(19)	-944(15)	592(12)	76(4)
C(4)	3681(14)	8655(13)	4182(9)	46(2)

C(14)	3968(14)	5273(11)	413(10)	53(3)
C(20)	9395(14)	1435(11)	4162(9)	43(2)
C(26)	9126(13)	4876(12)	7907(9)	51(2)
C(11)	6164(15)	8154(14)	423(11)	55(3)
C(29)	6965(15)	2048(12)	7890(10)	53(3)
C(28)	7840(16)	3023(15)	9018(10)	58(3)
C(12)	5374(16)	7200(15)	-696(12)	60(3)
C(27)	8867(16)	4441(14)	9043(10)	60(3)
C(13)	4237(17)	5770(15)	-683(11)	63(3)
C(16)	1968(15)	11074(14)	7818(10)	57(3)

---

Table 3. Bond lengths [Å] and angles [°] for michsm.

---

Br(1)-C(2)	1.830(11)
Br(2)-C(18)	1.877(8)
O(5)-C(22)	1.347(13)
O(5)-C(32)	1.408(13)
O(6)-C(6)	1.377(12)
O(6)-C(16)	1.440(13)
C(23)-C(22)	1.379(14)
C(23)-C(24)	1.383(15)
C(8)-C(7)	1.335(14)
C(8)-C(9)	1.486(12)
C(8)-C(1)	1.541(14)
C(24)-C(25)	1.313(13)
C(24)-C(17)	1.452(14)
C(7)-C(6)	1.428(11)
C(1)-O(3)	1.205(12)
C(1)-C(2)	1.474(16)
O(4)-C(17)	1.199(12)
C(17)-C(18)	1.508(13)
C(18)-C(19)	1.355(12)
C(2)-C(3)	1.356(13)
C(19)-C(25)	1.470(13)
C(19)-C(31)	1.472(14)
C(3)-C(15)	1.458(12)
C(3)-C(9)	1.509(13)
C(6)-C(5)	1.314(13)
C(22)-C(21)	1.439(12)
C(25)-C(20)	1.449(13)
C(9)-C(4)	1.285(14)
C(15)-C(10)	1.385(14)
C(15)-C(14)	1.428(13)
C(31)-C(30)	1.376(13)
C(31)-C(26)	1.357(14)



C(10)-C(11)	1.428(14)
C(30)-C(29)	1.337(15)
C(5)-C(4)	1.425(13)
C(21)-C(20)	1.380(14)
C(14)-C(13)	1.363(16)
C(26)-C(27)	1.379(15)
C(11)-C(12)	1.356(16)
C(29)-C(28)	1.394(16)
C(28)-C(27)	1.339(16)
C(12)-C(13)	1.401(16)

C(22)-O(5)-C(32)	118.0(8)
C(6)-O(6)-C(16)	117.5(8)
C(22)-C(23)-C(24)	122.1(8)
C(7)-C(8)-C(9)	122.6(9)
C(7)-C(8)-C(1)	132.4(8)
C(9)-C(8)-C(1)	105.0(9)
C(25)-C(24)-C(23)	122.7(10)
C(25)-C(24)-C(17)	110.7(9)
C(23)-C(24)-C(17)	126.6(9)
C(8)-C(7)-C(6)	114.7(7)
O(3)-C(1)-C(2)	128.8(10)
O(3)-C(1)-C(8)	123.5(10)
C(2)-C(1)-C(8)	107.7(7)
O(4)-C(17)-C(24)	131.9(10)
O(4)-C(17)-C(18)	126.7(10)
C(24)-C(17)-C(18)	101.3(7)
C(19)-C(18)-C(17)	112.0(7)
C(19)-C(18)-Br(2)	128.1(7)
C(17)-C(18)-Br(2)	119.8(6)
C(3)-C(2)-C(1)	109.2(9)
C(3)-C(2)-Br(1)	130.8(8)
C(1)-C(2)-Br(1)	119.9(7)
C(18)-C(19)-C(25)	104.0(8)

C(18)-C(19)-C(31)	130.1(9)
C(25)-C(19)-C(31)	125.9(8)
C(2)-C(3)-C(15)	127.5(9)
C(2)-C(3)-C(9)	111.8(8)
C(15)-C(3)-C(9)	120.6(8)
C(5)-C(6)-O(6)	126.3(8)
C(5)-C(6)-C(7)	123.4(8)
O(6)-C(6)-C(7)	110.2(8)
C(23)-C(22)-O(5)	120.8(8)
C(23)-C(22)-C(21)	116.0(9)
O(5)-C(22)-C(21)	123.1(9)
C(24)-C(25)-C(20)	119.1(9)
C(24)-C(25)-C(19)	111.9(9)
C(20)-C(25)-C(19)	129.0(9)
C(4)-C(9)-C(8)	118.7(10)
C(4)-C(9)-C(3)	135.0(8)
C(8)-C(9)-C(3)	106.3(8)
C(10)-C(15)-C(14)	116.8(9)
C(10)-C(15)-C(3)	120.9(9)
C(14)-C(15)-C(3)	122.3(8)
C(30)-C(31)-C(26)	120.4(9)
C(30)-C(31)-C(19)	120.7(9)
C(26)-C(31)-C(19)	118.8(9)
C(11)-C(10)-C(15)	121.4(10)
C(31)-C(30)-C(29)	119.6(9)
C(6)-C(5)-C(4)	120.4(9)
C(20)-C(21)-C(22)	121.5(9)
C(9)-C(4)-C(5)	120.0(9)
C(13)-C(14)-C(15)	120.9(9)
C(21)-C(20)-C(25)	118.6(8)
C(31)-C(26)-C(27)	120.5(9)
C(12)-C(11)-C(10)	120.3(10)
C(28)-C(29)-C(30)	119.6(10)
C(27)-C(28)-C(29)	121.4(10)

C(11)-C(12)-C(13)	118.9(10)
C(28)-C(27)-C(26)	118.4(10)
C(14)-C(13)-C(12)	121.7(11)

---



Anisotropic displacement parameters ( $\text{\AA}^2 \times 10^3$ ) for michsm. The anisotropic displacement factor exponent takes the form:  $-2\pi^2 [ h^2 a^{*2} U^{11} + \dots + 2 h k a^* b^* U^{12} ]$

	U <sup>11</sup>	U <sup>22</sup>	U <sup>33</sup>	U <sup>23</sup>	U <sup>13</sup>	U <sup>12</sup>
Br(1)	60(1)	37(1)	83(1)	11(1)	12(1)	7(1)
Br(2)	62(1)	38(1)	80(1)	11(1)	9(1)	6(1)
O(5)	72(5)	60(5)	33(4)	11(3)	13(3)	8(4)
O(6)	72(6)	51(5)	63(5)	18(4)	5(4)	11(4)
C(23)	38(5)	65(6)	69(6)	46(5)	-8(4)	-8(4)
C(8)	48(5)	30(4)	44(4)	26(4)	-5(4)	-4(4)
C(24)	34(4)	38(5)	44(4)	12(4)	-1(3)	2(3)
C(7)	51(5)	32(4)	25(4)	13(3)	4(3)	2(3)
C(1)	48(6)	23(4)	72(6)	18(4)	-15(5)	3(4)
O(3)	77(6)	37(4)	69(5)	25(4)	6(4)	2(4)
O(4)	79(6)	45(4)	89(6)	44(4)	6(4)	10(4)
C(17)	29(4)	53(6)	51(5)	23(4)	5(4)	-4(4)
C(18)	46(5)	18(4)	47(5)	-3(3)	3(4)	4(3)
C(2)	39(5)	54(6)	70(6)	32(5)	-2(4)	-4(4)
C(19)	39(5)	25(4)	60(6)	6(4)	-8(4)	2(3)
C(3)	41(5)	44(5)	38(4)	21(4)	0(4)	-3(4)
C(6)	42(5)	33(4)	35(4)	-5(3)	2(3)	-3(4)
C(22)	45(5)	60(6)	53(5)	38(5)	-2(4)	5(4)
C(25)	41(5)	32(4)	44(5)	13(3)	1(4)	4(4)
C(9)	43(5)	37(5)	41(4)	22(4)	-6(4)	-5(4)
C(15)	40(5)	26(4)	53(5)	12(3)	8(4)	3(3)
C(31)	48(5)	50(6)	38(4)	17(4)	0(4)	12(4)
C(10)	65(7)	68(6)	34(5)	14(4)	8(4)	21(5)
C(30)	35(5)	27(4)	63(5)	15(4)	-1(4)	-9(3)
C(5)	68(7)	26(4)	47(5)	0(3)	7(4)	3(4)
C(21)	43(5)	42(5)	65(6)	35(4)	4(4)	6(4)
C(32)	94(9)	57(7)	73(8)	-3(6)	25(7)	24(6)
C(4)	55(6)	47(6)	43(5)	22(4)	9(4)	1(4)

C(14)	61(6)	33(4)	54(5)	-2(4)	-14(4)	2(4)
C(20)	59(6)	26(4)	45(5)	16(3)	-8(4)	-1(4)
C(26)	51(6)	55(6)	53(5)	23(4)	7(4)	6(4)
C(11)	49(6)	57(7)	74(7)	41(6)	15(6)	13(5)
C(29)	57(7)	42(5)	58(6)	11(4)	15(5)	1(5)
C(28)	70(7)	72(7)	42(5)	23(5)	11(5)	26(6)
C(12)	70(7)	60(7)	59(6)	31(5)	17(5)	14(6)
C(27)	75(7)	58(6)	39(5)	-2(4)	2(5)	1(5)
C(13)	79(8)	65(7)	51(6)	22(5)	-11(5)	19(6)
C(16)	63(6)	57(6)	52(6)	17(5)	4(5)	1(4)

---

Hydrogen coordinates ( $\times 10^4$ ) and isotropic displacement parameters ( $\text{\AA}^2 \times 10^{-3}$ )  
for michsm.

	x	y	z	U(eq)
H(23)	10182	3855	1735	64
H(7)	2894	6339	6732	42
H(10)	6419	8345	2348	65
H(30)	6675	1819	6031	50
H(5)	3026	10665	5583	58
H(21)	10104	-520	2816	55
H(32A)	12130	-1017	1085	114
H(32B)	11248	-1366	-300	114
H(32C)	10112	-1611	827	114
H(4)	3823	9240	3551	56
H(14)	3247	4288	382	63
H(20)	9193	842	4782	52
H(26)	9861	5839	7900	61
H(11)	6900	9122	432	66
H(29)	6204	1103	7899	63
H(28)	7708	2680	9770	70
H(12)	5584	7491	-1459	72
H(27)	9392	5117	9809	72
H(13)	3650	5142	-1442	76
H(16A)	2986	11842	7807	86
H(16B)	1512	11340	8650	86
H(16C)	1081	11185	7195	86